Supporting Information

Tungsten Promoted Decarboxylative Oxygenation and Ring-Opening *via* Ligand-to-Metal Charge Transfer

Heng Song,* † Li Fang,† Jiahao Wang,† Xingwei Cai,† Yougen Cai,† Ying Li,† Jia-Jia Zhao,† Lei Chen,† Hongxian Sun,* ‡ Chen Xu*†

†School of Environmental and Chemical Engineering, Jiangsu University of Science and Technology, Zhenjiang 212003, Jiangsu, P. R. China

‡College of Chemistry and Pharmaceutical Engineering, Nanyang Normal University, Nan yang 473061, P. R. China.

*Corresponding author. hengsong@just.edu.cn

Table of content

1. General Procedure

All operations were performed under a N_2 atmosphere using standard Schlenk techniques or in a glove box, unless otherwise specified. Reagents and other chemical materials were purchased from Energy Chemical and Bide Pharmatech, and were used without further purification unless noted. Dichloromethane, n-hexane, tetrahydrofuran, and toluene were dried and degassed using a solvent purification system (Innovative Technology).

Flash chromatography was carried out utilizing silica gel (100-300 mesh). ^{1}H NMR, ^{13}C NMR and ^{19}F NMR spectra were recorded at room temperature on a JEOL 400 MHz spectrometer. The chemical shifts are reported in ppm relative to either the residual solvent peak or tetraethylsilane as an internal standard. Coupling constants (*J*) were reported in Hz. Attribution of peaks were performed by using the multiplicities and integrals of the peaks. Coupling patterns are indicated as s (singlet), d (doublet), t (triplet), dd (doublet of doublet), td (triplet of doublet), or m (multiplet). Mass spectral analyses were done in Bruker micrOTOF-Q II Spectrometer. For thin-layer chromatography (TLC) analysis, Merck precoated TLC plates (silica gel 60 F254/ 0.25 mm) were used. Visualization was accomplished by UV light (254 and 365 nm).

2. General Procedures for Synthesis of W-1 and W-2

Synthesis of W-1: Compound **W-1** was prepared by a modification of the published procedure.[1] A solution of hexamethyldisiloxane (21.49 g, 132 mmol, 2.1 equiv.) was added dropwise to the solution of tungsten hexachloride (25.00 g, 63.0 mmol) in 250 mL of dichloromethane. A solution of dimethoxyethane (13.06 g, 145 mmol, 2.3 equiv.) was added. The mixture was stirred for 2 h at room temperature, during which time it became dark blue and contained a suspended precipitate. A pale blue solution was obtained after filtration of the mixture through Celite. A solution of 4,4'-di-tert-butyl-2,2'-bipyridyl (17.75 g, 66.1 mmol, 1.05 equiv.) in 30 mL of dichloromethane was added, and the mixture was stirred for 30 min. The precipitate was isolated by filtration, washed twice with 50 mL of dichloromethane, and dried under vacuum. The white powder **W-1** was collected, in 90% yield. ^{1}H NMR (400 MHz,

Chloroform-d) δ 9.45 (d, J = 5.4 Hz, 2H), 8.11 (s, 2H), 7.68 (d, J = 5.5 Hz, 2H), 1.42 (s, 18H). ^{13}C {^{1}H} NMR (101 MHz, Chloroform-d) δ 166.50, 152.41, 150.66, 124.87, 119.52, 36.07, 30.57.

Synthesis of W-2: 4,4'-di-tert-butyl-2,2'-bipyridyl (86 mg, 0.32 mmol, 1 eq.), norbornene (61 mg, 0.64 mmol, 2 eq.) were added to WCl_6 (127 mg, 0.32 mmol, 1.0 eq.) in a dry toluene (15 mL) solution. The mixture was stirred at room temperature for 1 hour. After the reaction, the yellow supernatant was removed. The system was washed with n-hexane until the supernatant became colorless, and the residue was dried under reduced pressure. The residue was dissolved in methanol, and a small amount of diethyl ether was added as a poor solvent. After volatilization in air overnight until it turned blue-black, the mixture was concentrated under reduced pressure. It was then dissolved in acetonitrile and reacted with 30% H_2O_2 (5.0 eq.) at 60 °C until it turned colorless. Diethyl ether was slowly diffused into the saturated acetonitrile solution at -25 ℃ to afford a white solid, **W-2**, in 65% yield. ^{1}H NMR (400 MHz, DMSO-d_6) δ 8.79 (d, J = 5.2 Hz, 2H), 8.72 (s, 2H), 7.88 (d, J = 5.3 Hz, 2H), 1.42 (s, 18H). ^{13}C {^{1}H} NMR (101 MHz, DMSO-d_6) δ 167.1, 148.6, 146.8, 124.2, 121.5, 36.4, 30.5. HRMS [ESI-TOF] m/z: $[M+H]^+$ calcd for $C_{18}H_{24}N_2O_5W$ 533.1273; found, 533.1270.

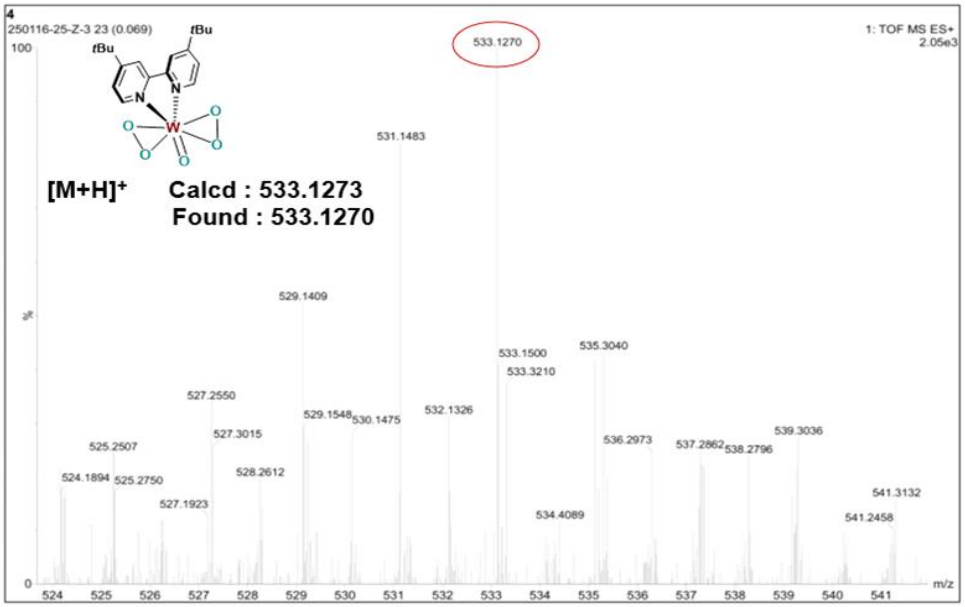

Figure S1. HRMS analysis of **W-2**.

3. Experimental Procedures

3.1 Experimental Procedures for 1°, 2° carboxylic acids and Drug molecules Decarboxylative Oxygenation

A 10 mL crimp cap vial equipped with a magnetic stir bar was charged with **W-1** (5 mol% relative to 0.2 mmol substrate), Na_2CO_3 (0.24 mmol, 25.4 mg, 1.2 equiv.), the corresponding carboxylic acid (0.2 mmol, 1.0 equiv.), and acetonitrile (2 mL, 0.1 M). All solid reagents were added prior to sealing the vial, while liquid reagents were introduced via syringe after placing the sealed vial under an O_2 atmosphere (highly viscous liquids were also added before capping). The reaction mixture was stirred under 1 bar of O_2 (supplied by an O_2-filled balloon) with irradiation from a 365 nm 15W blue LED and fan cooling at room temperature for 12 hours. The crude product was either analyzed by ^1H NMR spectroscopy using tetramethylsilane as an internal standard for yield determination, or purified by automated flash column chromatography using a petroleum ether/ethyl acetate gradient.

3.2 Experimental Procedures for 3°(cyclic) carboxylic acids Decarboxylative Oxygenation

A 10 mL crimp cap vial equipped with a magnetic stir bar was charged with **W-1** (5 mol% relative to 0.2 mmol substrate), Na_2CO_3 (0.24 mmol, 25.4 mg, 1.2 equiv.), the corresponding carboxylic acid (0.2 mmol, 1.0 equiv.), and acetonitrile (2 mL, 0.1 M). All solid reagents were added prior to sealing the vial, while liquid reagents were introduced via syringe after placing the sealed vial under an air atmosphere (highly viscous liquids were also added before capping). The reaction mixture was stirred under 1 bar of air (supplied by an air-filled balloon) with irradiation from a blue 410 nm or 365 nm 15W LED and fan cooling at room temperature for 12 hours. The crude product was either analyzed by ^1H NMR spectroscopy using tetramethylsilane as an internal standard for yield determination, or purified by automated flash column chromatography using a petroleum ether/ethyl acetate gradient.

4. Optimization of Reaction Conditions

Table S1. Screening of Reaction Conditions. [a]

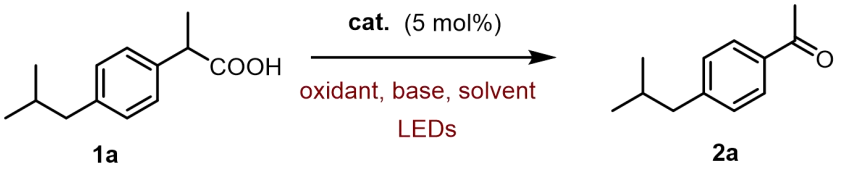

1a **2a**

entry	**cat.** (x mol%)	solvent	oxidant	LEDs(nm)	Na_2CO_3(x eq)	**2a** yield(%)[b]
1	**W-1**	CH_3CN	O_2	365	1	65
2	**W-2**	CH_3CN	O_2	365	1	53
3	**W-1**(10 mol%)	CH_3CN	O_2	365	1	68
4	**W-1**	CH_3CN	O_2	365	1.2	91
5	**W-1**	CH_3CN	O_2	390	1.2	27
6	**W-1**	CH_3CN	Air	365	1.2	50
7	**W-1**	CH_3COCH_3	O_2	365	1.2	86
8	--	CH_3CN	O_2	365	1.2	N.D.
9	**W-1**	CH_3CN	O_2	365	0	17
10	**W-1**(10 mol%)	CH_3CN	O_2	365	1.2	87
11	**W-1**	THF	O_2	365	1.2	57
12	**W-2**	CH_3CN	O_2	365	1.2	77
13	**W-1**	CH_3CN	O_2	no	1.2	N.D.
14	**W-1**	CH_3CN	N_2	365	1.2	N.D.
15	**W-2**	CH_3CN	O_2	--	1.2	N.D.
16	**W-2**	CH_3CN	N_2	365	1.2	N.D.

[a] Reaction condition: **1a** (0.2 mmol), **cat.** (5 mol%), Na_2CO_3 (1.2 eq), 1 bar O_2, solvent (2 mL), 12 h under 365 nm, 15 W, isolated yield. [b] Yields were determined by ^1H NMR using tetraethylsilane as an internal standard. N.D. = not detected.

Table S2. Screening of Reaction Conditions. [a]

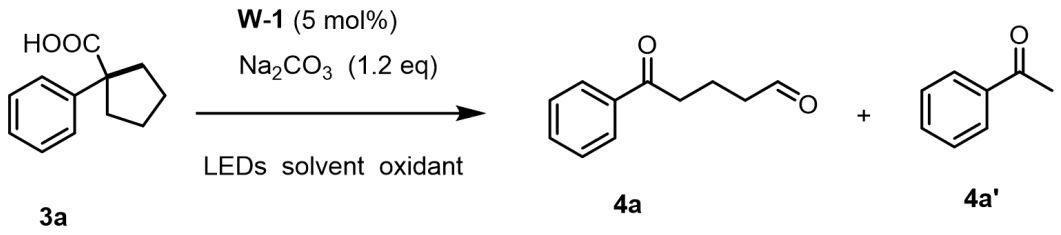

3a **4a** **4a'**

entry	LEDs	time/h	solvent	oxidant	Yield(**4a**)%[b]	Yield(**4a'**)%[b]
1	470nm/15W	16	CH_3CN/4mL	Air	N.D.	N.D.
2	450nm/15W	16	CH_3CN/4mL	Air	26	N.D.
3	430nm/15W	16	CH_3CN/4mL	Air	37	N.D.
4	410nm/15W	16	CH_3CN/4mL	Air	48	N.D.
5	410nm/15W	16	CH_3CN/4mL	O_2	43	15
6	410nm/15W	16	CH_3CN/2mL	Air	47	19
7	390nm/10W	16	CH_3CN/4mL	Air	45	44
8	390nm/10W	16	CH_3CN/2mL	Air	34	22
9	365nm/15W	12	CH_3CN/2mL	Air	5	28
10	410nm/15W	12	THF/2mL	Air	4	34
11	410nm/15W	12	CH_3COCH_3/2mL	Air	43	N.D.
12	410nm/15W	24	CH_3CN/4mL	Air	47	9
13	--	16	CH_3CN/4mL	Air	N.D.	N.D.
14	410nm/15W	16	CH_3CN/4mL	N_2	N.D.	N.D.

[a] Reaction condition: **3a** (0.2 mmol), **W-1** (5 mol%), 1.2 eq Na_2CO_3, solvent, under The LEDs. N.D. = not detected. [b] Yields were determined by ^1H NMR using tetraethylsilane as an internal standard.

5. Mechanistic Experiments

5.1 General Procedures for Synthesis of Int1

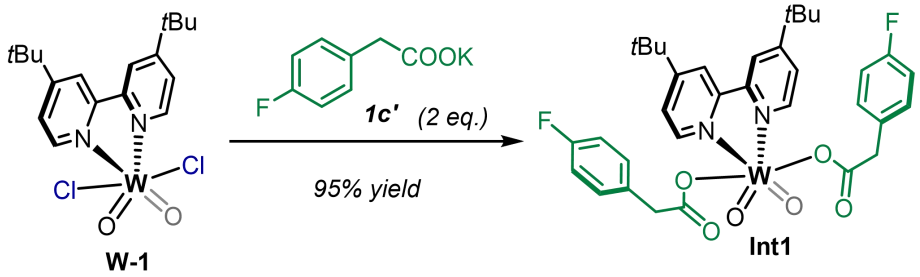

Inside a N_2-filled glovebox, to an oven-dried reaction vial equipped with a magnetic stir bar was added **W-1** (55.4 mg, 0.10 mmol, 1.0 equiv.), 2-(4-fluorophenyl)acetic acid (32 mg, 0.20 mmol, 2.0 equiv.), K_2CO_3 (26 mg, 0.20 mmol, 2.0 equiv.), and MeOH (1.0 mL, 0.1 M). The reaction mixture was stirred for 12 h at 60 ℃ and 1-fluoro-4-methylbenzene (22 μL, 0.2 mmol, 2.0 equiv.) was added as an internal standard (**Figure S2**). The resulting white mixture was filtered through a packed pad of oven-dried Celite (ca. 20 mg). The white solid **Int1** (75 mg, 95%) was obtained by separation. ^{1}H NMR (400 MHz, Methanol-d_4) δ 8.53 (dd, J = 5.3, 0.8 Hz, 2H), 8.32 (dd, J = 2.0, 0.7 Hz, 2H), 7.47 (dd, J = 5.3, 2.0 Hz, 2H), 7.26 (dd, J = 8.8, 5.4 Hz, 4H), 6.97 (t, J = 8.8 Hz, 4H), 3.49 (s, 4H), 1.38 (s, 18H). ^{13}C NMR (101 MHz, Methanol-d_4) δ 176.51, 162.95, 162.06, 160.54, 155.90, 148.75, 132.52, 132.48, 130.69, 130.61, 121.14, 118.66, 114.59, 114.37, 41.98, 34.74, 29.54. ^{19}F NMR (376 MHz, Methanol-d_4) δ -118.48. HRMS (ESI-MS): m/z: $[M+Na]^+$ calcd for $C_{34}H_{36}F_2N_2O_6W$: 813.1951; Found: 813.1951.

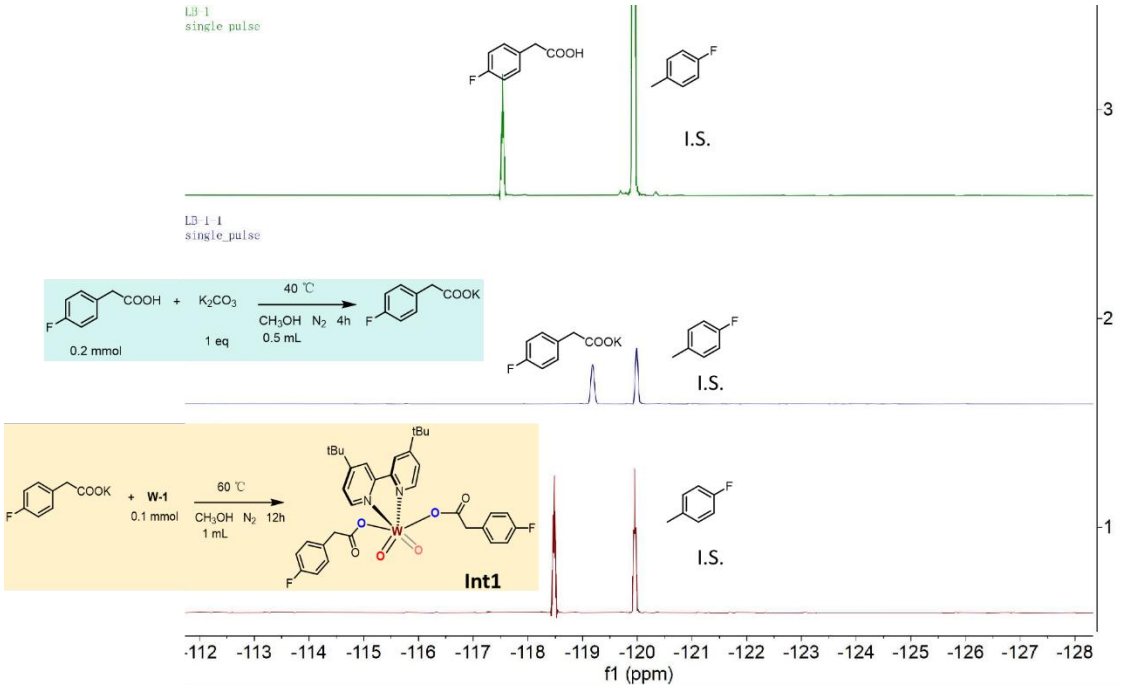

Figure S2: ^{19}F NMR of representative compounds in MeOH.

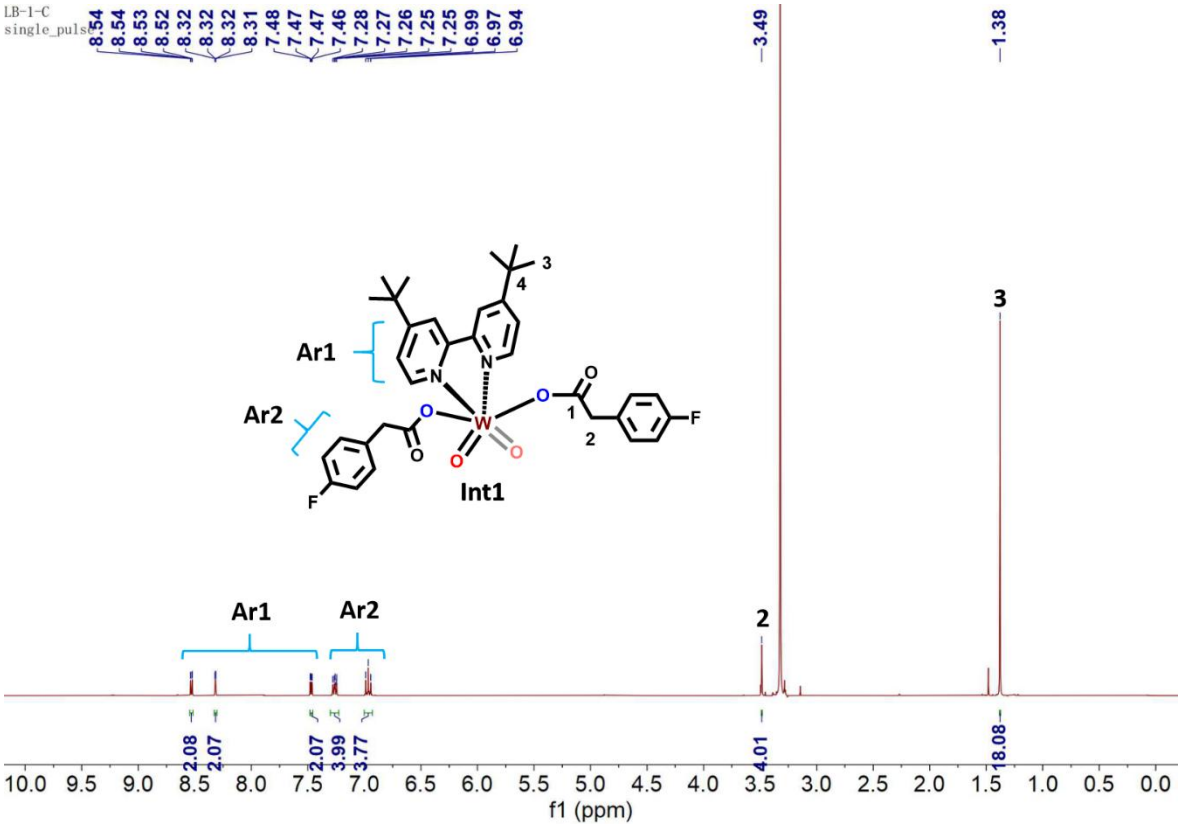

Figure S3. ^{1}H NMR spectrum of **Int1** (400 MHz, Methanol-d_4).

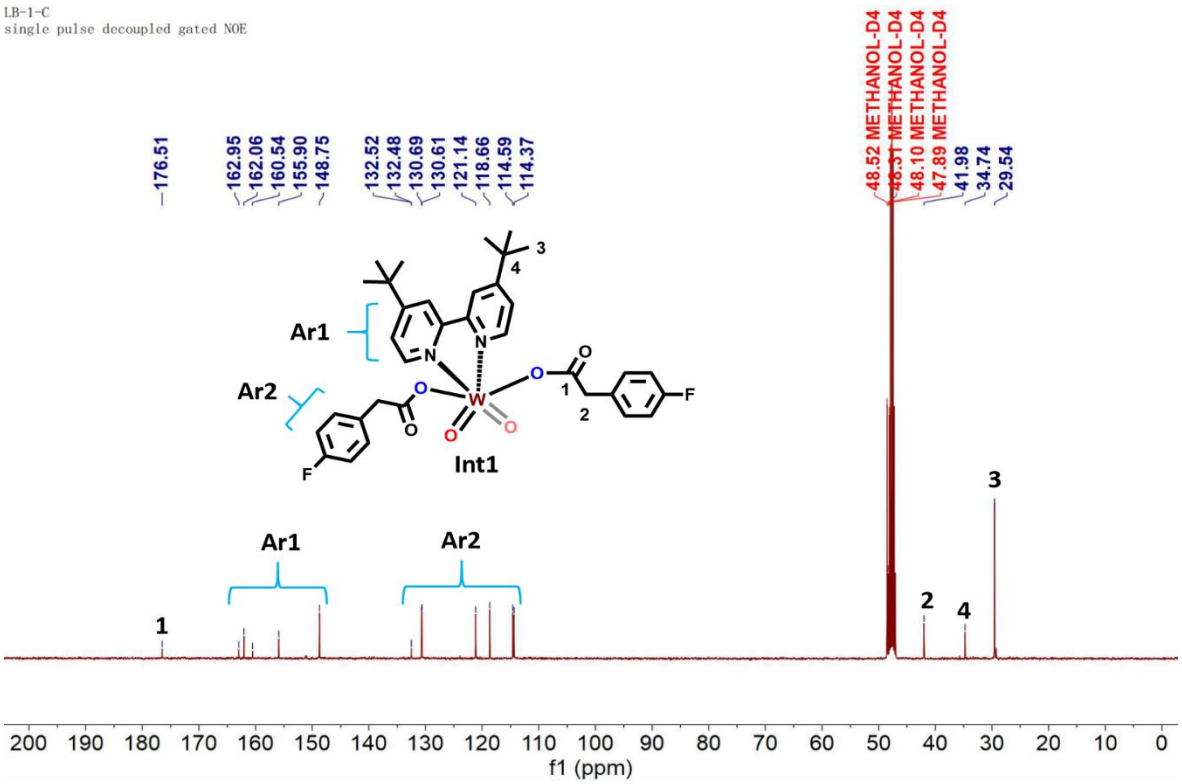

Figure S4. ^{13}C NMR spectrum of **Int1** (400 MHz, Methanol-d$_4$).

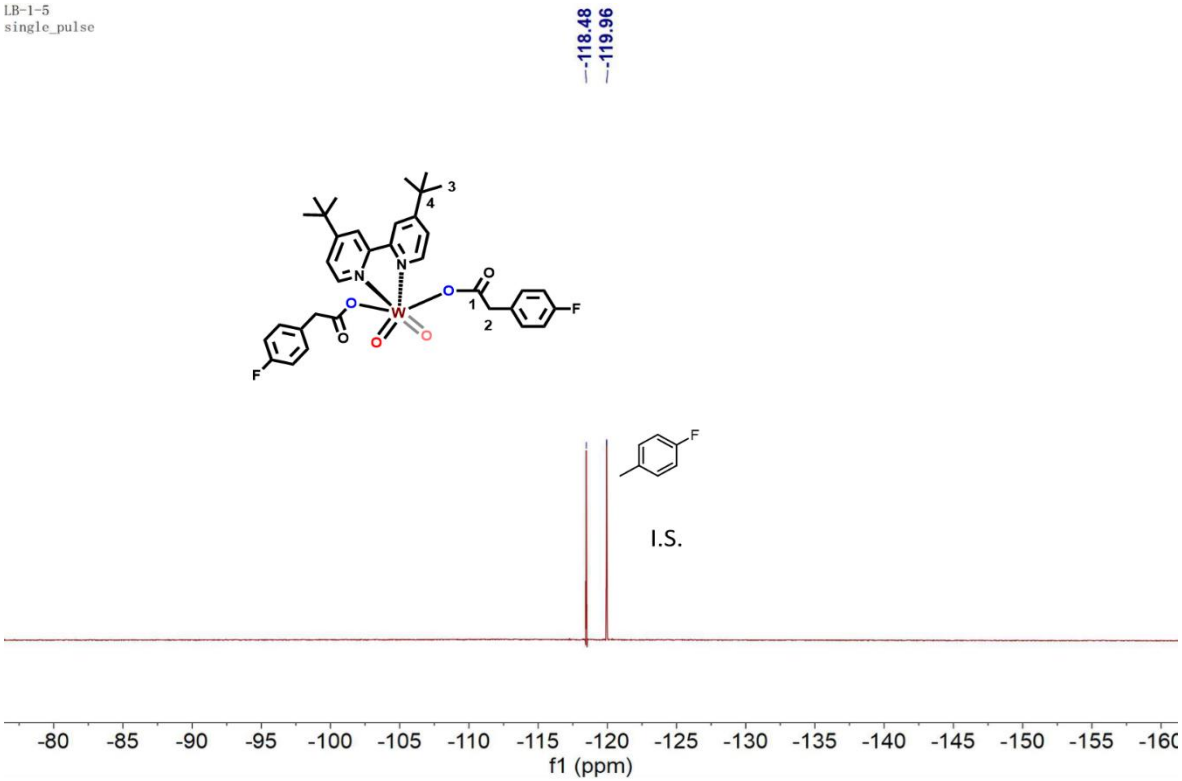

Figure S5. ^{19}F NMR spectrum of **Int1** (376 MHz, Methanol-d$_4$).

5.2 Decarboxylative LMCT Experiments with Int1.

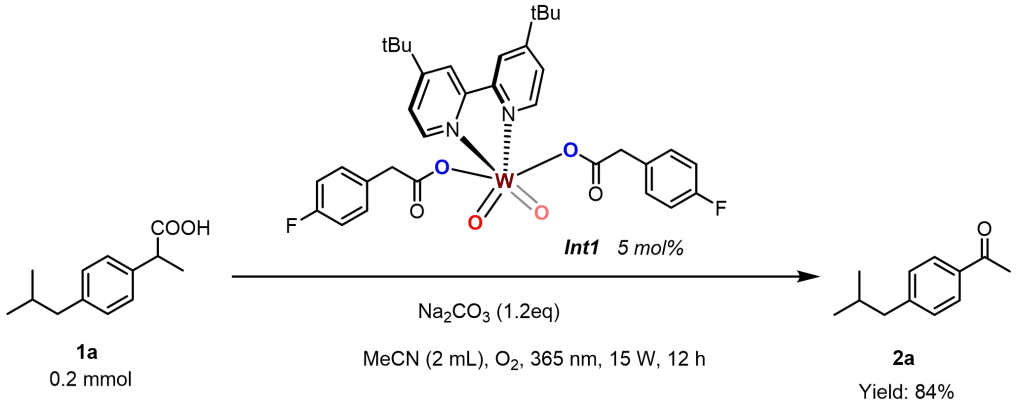

Reactions were performed 2-(4-isobutylphenyl) propanoic acid (**1a**) (41 mg, 0.2 mmol, 1.0 equiv.) and Na_2CO_3 (25 mg, 0.24 mmol, 1.2 equiv.), with **Int1** (5 mol% based on **1a**) as the catalyst and MeCN (2 mL, 0.1 M) as the solvent. The reaction mixture was stirred under 1 bar of air (supplied by an air-filled balloon) with irradiation from a blue 365 nm 15 W LED and fan cooling at room temperature for 12 hours. NMR yields of **2a (Figure S6)** were determined by ^{1}H NMR spectroscopy of the crude reaction mixture using tetraethylsilane as the internal standard.

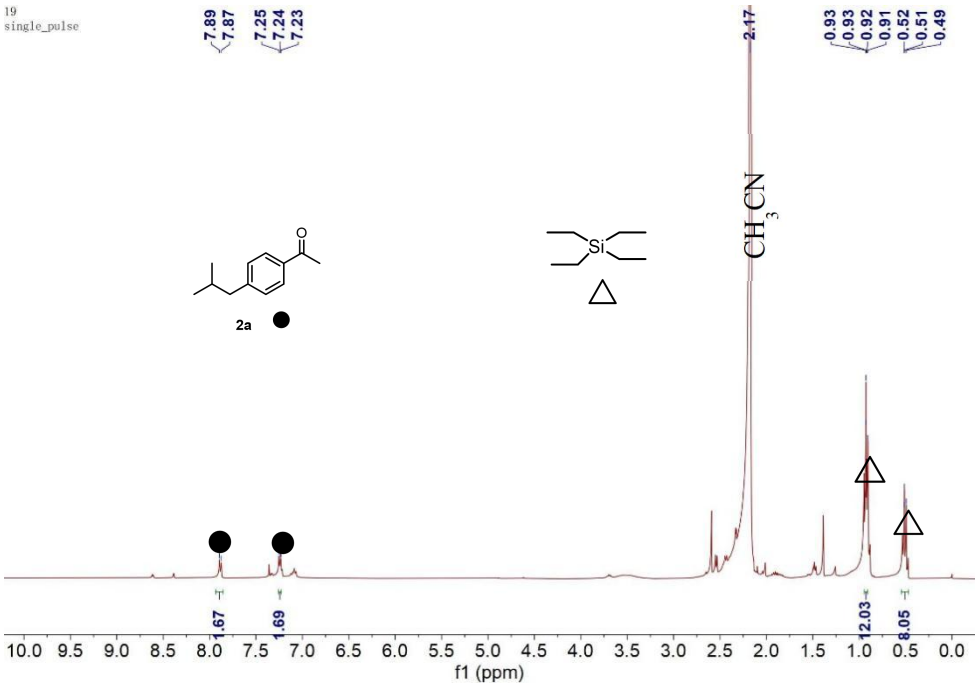

Figure S6. ^{1}H NMR spectroscopy of **2a** crude reaction mixture. (400 MHz, MeCN).

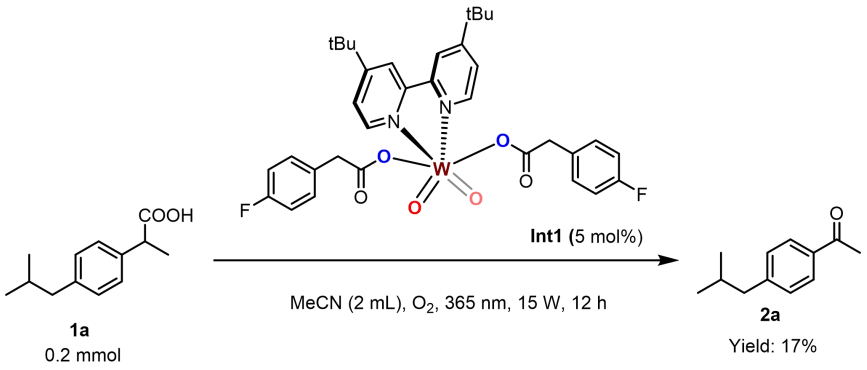

Reactions were performed 2-(4-isobutylphenyl) propanoic acid (**1a**) (41 mg, 0.2 mmol, 1.0 equiv.), with **Int1** (5 mol% based on **1a**) as the catalyst and MeCN (2 mL, 0.1 M) as the solvent. The reaction mixture was stirred under 1 bar of air (supplied by an air-filled balloon) with irradiation from a blue 365 nm 15 W LED and fan cooling at room temperature for 12 hours. NMR yields of **2a (Figure S7)** were determined by ^{1}H NMR spectroscopy of the crude reaction mixture using tetraethylsilane as the internal standard.

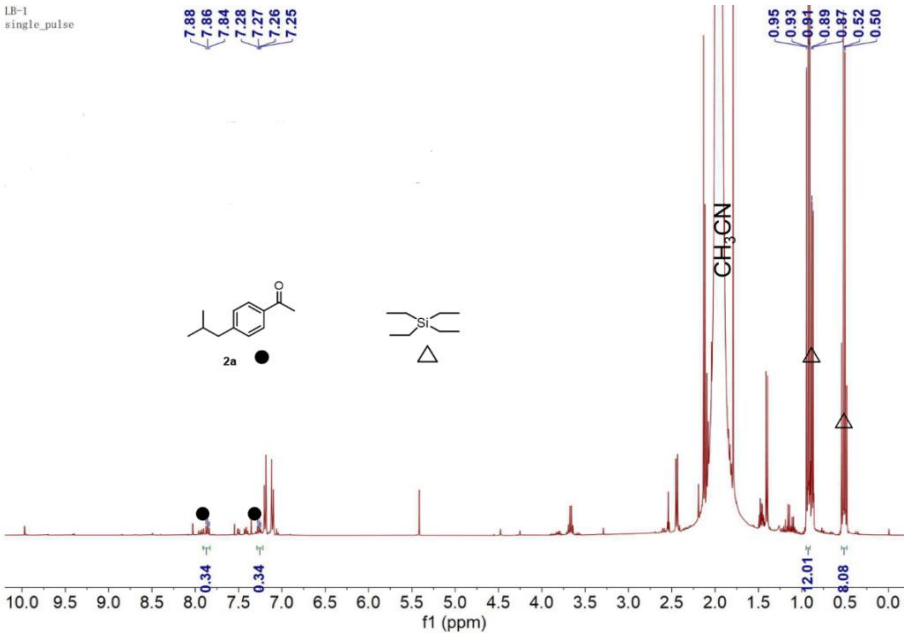

Figure S7. ^{1}H NMR spectroscopy of **2a** crude reaction mixture. (400 MHz, MeCN).

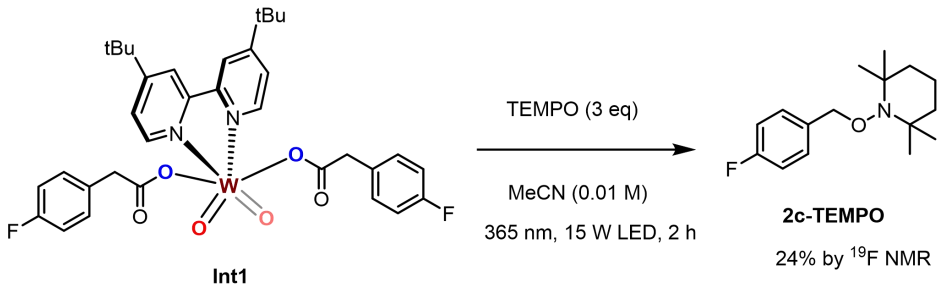

In a N_2-filled glovebox, a 10 mL crimp cap vial equipped with a magnetic stir bar was charged TEMPO (4.7 mg, 30 μmol, 3.0 equiv.) and a solution of dicarboxylate complex **Int1** in MeCN (0.01 M, 1.0 mL, 10 μmol, 1.0 equiv.). The reaction mixture irradiation from a blue 365 nm 15 W LED and fan cooling at room temperature. After 2 hours, the vial was removed from the photoreactor, the resulting mixture was filtered through a packed pad of oven-dried Celite (ca. 20 mg), and concentrated *in vacuo* with the aid of a rotary evaporator. **2c-TEMPO (Figure S8)** was detected by ^{19}F NMR spectroscopy using $CDCl_3$ as the solvent.

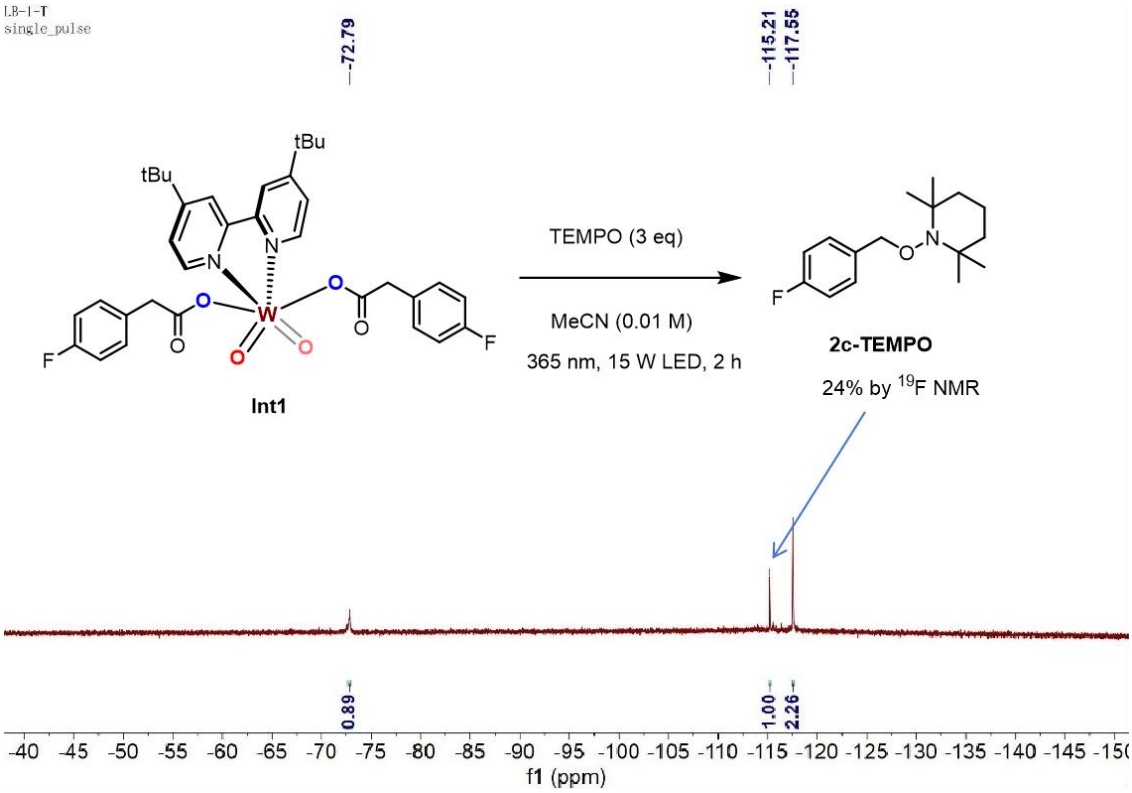

Figure S8. ^{19}F NMR spectroscopy of **2c-TEMPO** crude reaction mixture. (376 MHz, $CDCl_3$).

An analytically pure sample of **2c-TEMPO** was purified by preparatory thin-layer chromatography (10% EtOAc in hexanes) to yield **2c-TEMPO** as a colorless solid.

1-((4-fluorobenzyl) oxy)-2,2,6,6-tetramethylpiperidine (**2c-TEMPO**)

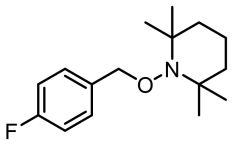

2c-TEMPO

^{1}H NMR (400 MHz, $CDCl_3$) δ 7.33 - 7.30 (m, 2H), 7.03 - 6.99 (m, 2H), 4.76 (s, 2H), 1.59 - 1.49 (m, 6H), 1.24 (s, 6H), 1.13 (s, 6H). ^{13}C NMR (101 MHz, $CDCl_3$) δ 163.45, 161.01, 134.07, 134.04, 129.35, 129.27, 115.27, 115.05, 78.09, 60.10, 39.76, 33.18, 20.37, 17.18. ^{19}F NMR (376 MHz,$CDCl_3$) δ - 115.17.

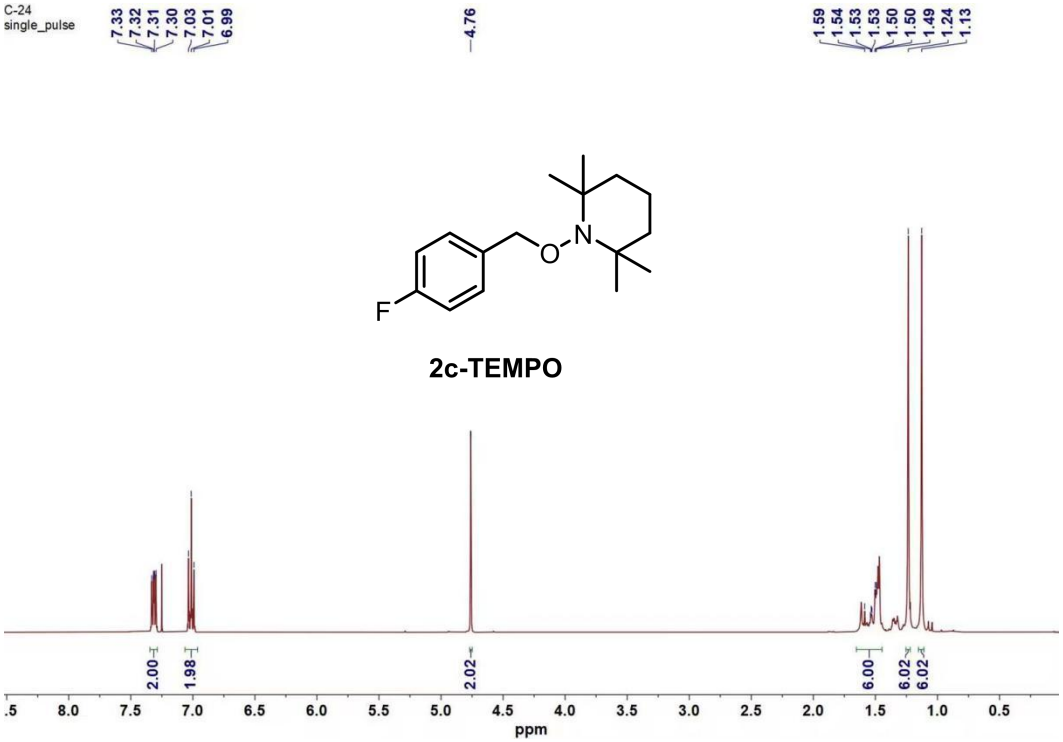

Figure S9. ^{1}H NMR spectrum of **2c-TEMPO** (400 MHz, Chloroform-d).

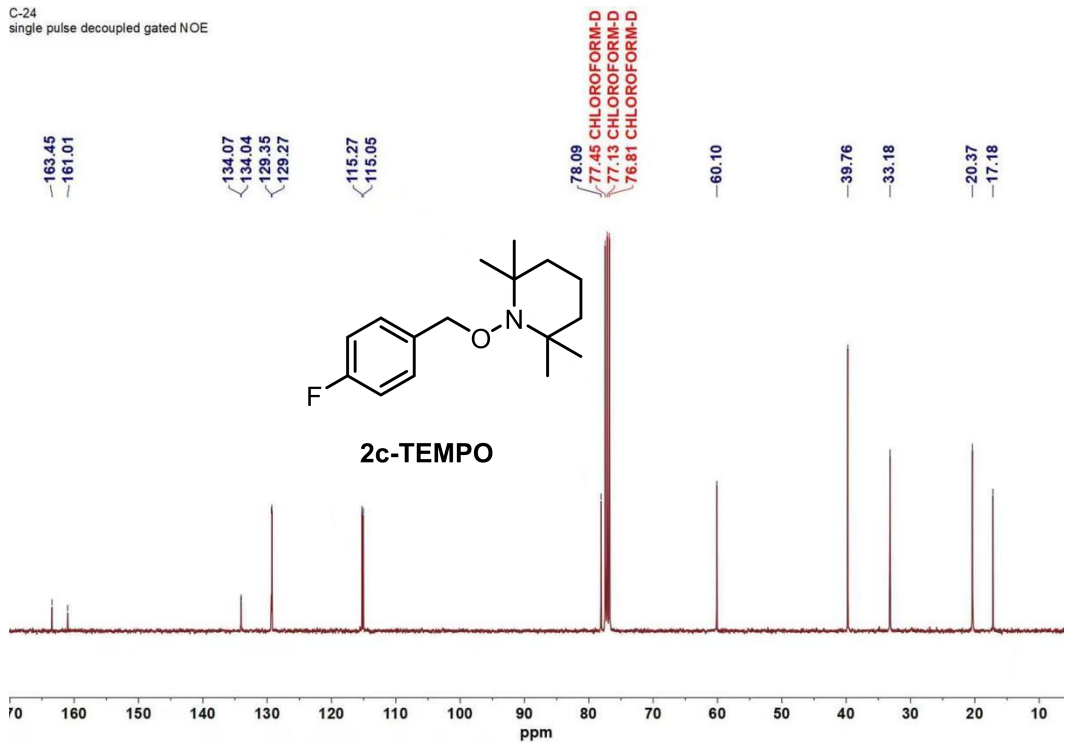

Figure S10. ^{13}C NMR spectrum of **2c-TEMPO** (101 MHz, Chloroform-d).

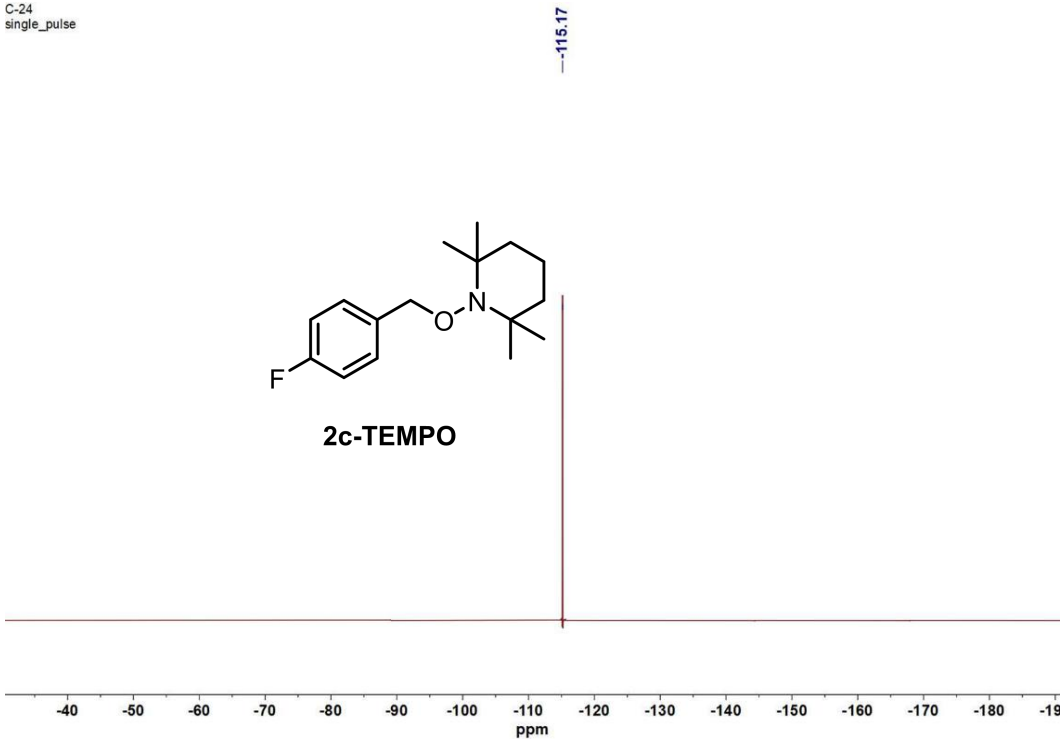

Figure S11. ^{19}F NMR spectrum of **2c-TEMPO** (376 MHz, Chloroform-d).

6. UV-vis experiments

The UV-Vis measurements were carried out using a UV-Vis spectrophotometer (ULN 2209003, MAPADA P6).

The spectra were aquired from 250 to 500 nm using 1.0 nm steps. All measurements were performed in MeCN at the following concentrations: pure **W-1** (0.1 mM).

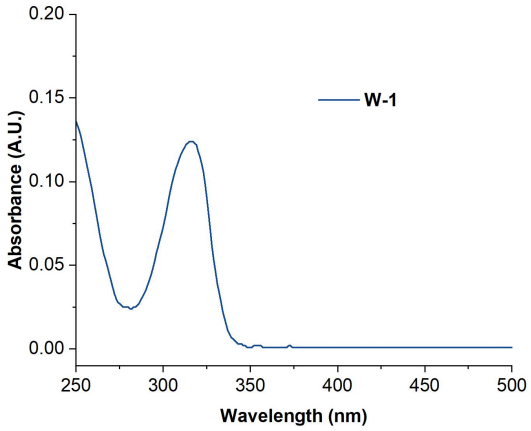

Figure S12. UV-Visible spectra of a solution of pure **W-1**

Preparation of a stock solution (solution A): In a glass vial equipped with a teflon-coated stirring bar and a septum, **W-1** (5.5 mg, 0.01 mmol) and Na_2CO_3 (25 mg, 0.24 mmol) were dissolved in MeCN (3 mL). Dilute 66 µL of the above solution to 6 mL to obtain solution A.

UV-vis spectra were recorded after irradiation the cuvette solution with 15 W 365 nm LED light.

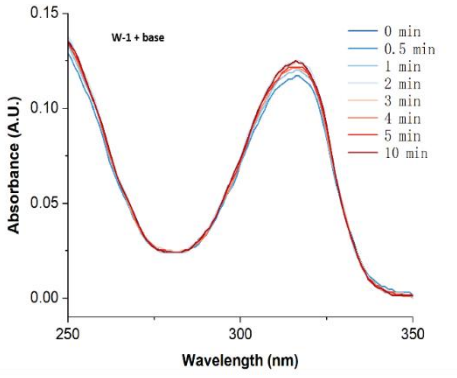

Figure S13. UV-Visible spectra contain a solution of **W-1** with base after 365 nm LED irradiation

Preparation of a stock solution (solution B): In a glass vial equipped with a teflon-coated stirring bar and a septum, **W-1** (5.5 mg, 0.01 mmol) and 4-fluorophenylacetic acid (**1c**) (32 mg, 0.2 mmol) were dissolved in MeCN (3 mL). Dilute 66 μL of the above solution to 6 mL to obtain solution B.

UV-vis spectra were recorded after irradiation the cuvette solution with 15 W 365 nm LED light.

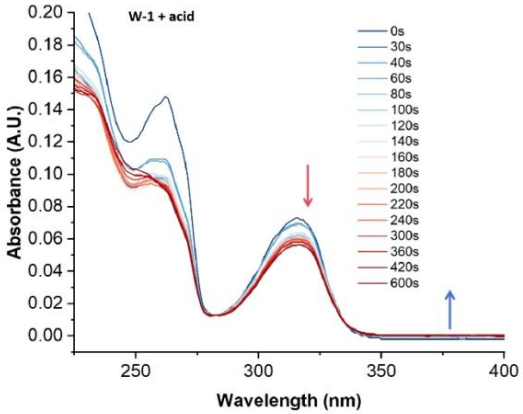

Figure S14. UV-Visible spectra contain a solution of **W-1** with acid after 365 nm LED irradiation

Preparation of a stock solution (solution C): In a glass vial equipped with a teflon-coated stirring bar and a septum, **W-1** (5.5 mg, 0.01 mmol), 4-fluorophenylacetic acid (**1c**) (32 mg, 0.2 mmol) and Na_2CO_3 (25 mg, 0.24 mmol) were dissolved in MeCN (3 mL). Dilute 66 μL of the above solution to 6 mL to obtain solution C.

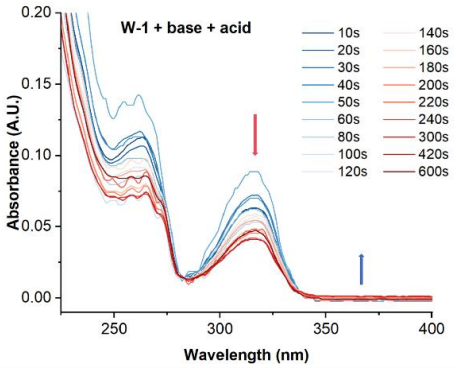

Figure S15. UV-Visible spectra contain a solution of **W-1** + acid + base after 365 nm LED irradiation

7.Kinetic Studies

7.1 Monitoring the Reaction Progress over Time

To a 10 mL screw-cap vial fitted with a magneton was added **1y** (0.2 mmol), **W-1** (5 mol% based on the substrate), MeCN (2 mL), Na_2CO_3 (0.24 mmol,1.2 equiv.). The reaction tube is charged with pure oxygen via a double-manifold operation and subjected to reaction under 365 nm, 15 W light irradiation. At 0 min, 10 min, 20 min, 30 min, 40 min, 50 min, 60 min, 70 min, 90 min, 120 min, 150 min, and so on, a 25 μL aliquot of the reaction mixture was removed under N_2 atmosphere, transferred into nuclear magnetic tube and add MeCN (0.8 mL). Yields were determined by ^{19}F NMR integration.

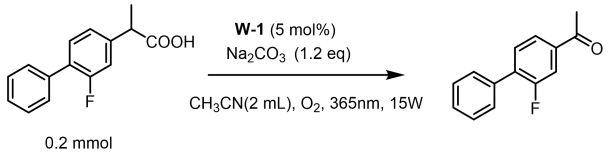

Table S3. Reaction Profile.

Entry	Time (min)	Yield 2y (%)
1	0	0
2	10	8
3	20	20
4	30	28
5	40	32
6	50	39
7	60	44
8	70	46
9	80	52
10	90	54
11	120	57
12	150	60
13	180	62
14	240	64
15	300	66
16	360	67
17	420	69
18	480	70
19	540	71
20	600	72
21	660	72
22	720	72

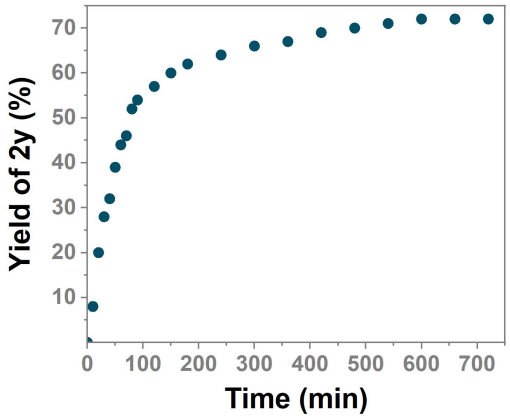

Figure S16. Reaction profiles for synthesis of **2y**.

7.2 Kinetic Experiments for the Decarboxylative Oxidation of 1y

We started the kinetic experiments to determine the overall order and the rate equation of the decarboxylative C-O bond-forming reaction of 2-(2-fluoro-[1,1'-biphenyl]-4-yl) propanoic acid (**1y**) with Na_2CO_3 using **W-1** as a catalyst under 1 bar O_2. Yields were determined by ^{19}F NMR integration. We started the investigation one by one: (i) the order of the oxidation reaction with respect to **1y**, (ii) the order of the oxidation reaction with respect to the catalyst **W-1**, and (iii) the order of the oxidation reaction with respect to O_2.

7.2.1 Representative procedure for the 2-(2-fluoro-[1,1'-biphenyl]-4-yl) propanoic acid (1y) decarboxylative oxidation reaction carried out with various concentrations of 2-(2-fluoro-[1,1'-biphenyl]-4-yl) propanoic acid (1y)

Initial rates (k_{obs}) were determined using various concentrations of 2-(2-fluoro-[1,1'-biphenyl]-4-yl) propanoic acid (**1y**) (0.1 M, 0.2 M, 0.3 M, and 0.4 M) by keeping the concentration of **W-1** (0.005 M) and O_2 (40.95×10^{-3} M) constant. We observed k_{obs} values of the reaction from [product] *vs* time plot, which was equal to the slope of the linear fit lines (**Table S4**). The experimental procedure that has been used is described below.

To a 10 mL Schlenk tube fitted with a stir bar was added **W-1** (0.005 M), 2-(2-fluoro-[1,1'-biphenyl]-4-yl) propanoic acid (**1y**) (in different concentrations, 0.1 M, 0.2 M, 0.3 M, and 0.4 M), O_2(40.95×10^{-3} M) and MeCN (2 mL) inside the glove box. The tube was sealed and the mixture was under the 365 nm, 15 W light irradiation. After that, the ^{19}F NMR

spectra were recorded at various time intervals. The varying 2-(2-fluoro-[1,1'-biphenyl]-4-yl) propanoic acid (**1y**) concentration and the constant concentration of **W-1** and O_2 for each set of experiments are given in Table S4 and represent the data graphically.

Table S4. Initial rates (k_{obs}) for the decarboxylative oxidation reaction of 2-(2-fluoro-[1,1'-biphenyl]-4-yl) propanoic acid (1y) were carried out under varying concentrations of 2-(2-fluoro-[1,1'-biphenyl]-4-yl) propanoic acid (1y).

1y(M)	W-1(M)	O_2(M)	Initial rates(M/min)	R^2
0.1	0.005	40.95×10^{-3}	$(0.64\pm0.0462)\times10^{-3}$	0.9643
0.2	0.005	40.95×10^{-3}	$(1.27\pm0.0778)\times10^{-3}$	0.9646
0.3	0.005	40.95×10^{-3}	$(1.74\pm0.1223)\times10^{-3}$	0.9254
0.4	0.005	40.95×10^{-3}	$(2.36\pm0.0729)\times10^{-3}$	0.9803

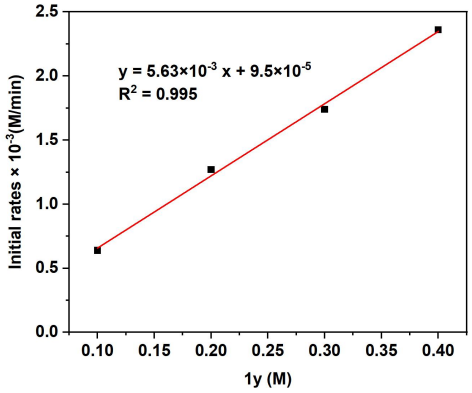

Figure S17. Plot of reaction initial rates (M/min) *vs* **1y**(M).

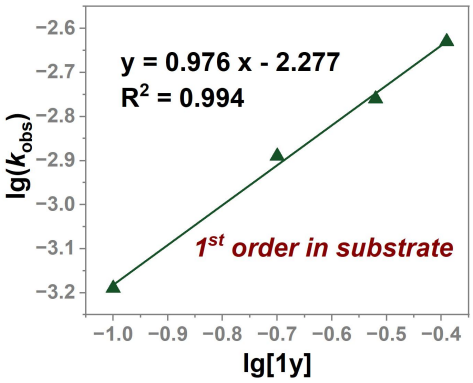

Figure S18. Plot of lg(k_{obs}) *vs* lg (concn of **1y**).

7.2.2 Representative procedure for the 2-(2-fluoro-[1,1'-biphenyl]-4-yl) propanoic acid (1y) decarboxylative oxidation reaction carried out with various concentrations of W-1.

Initial rates (k_{obs}) were determined using various concentrations of **W-1** (0.005 M, 0.01 M, 0.02 M, 0.03 M, and 0.04 M) by keeping the concentration of 2-(2-fluoro-[1,1'-biphenyl]-4-yl) propanoic acid (**1y**) (0.1 M) and O_2 (40.95×10^{-3} M) constant. We observed k_{obs} values of the reaction from [product] *vs* time plot, which was equal to the slope of the linear fit lines (**Table S5**). The experimental procedure that has been used is described below.

To a 10 mL Schlenk tube fitted with a stir bar was added 2-(2-fluoro-[1,1'-biphenyl]-4-yl) propanoic acid (**1y**) (0.1M), **W-1** (in different concentrations, 0.005 M, 0.01 M, 0.02 M, 0.03 M, and 0.04 M), O_2(40.95×10^{-3} M) and MeCN (2 mL) inside the glove box. The tube was sealed and the mixture was under the 365 nm, 15 W light irradiation. After that, the ^{19}F NMR spectra were recorded at various time intervals. The varying catalyst concentration and the concentration of O_2 and 2-(2-fluoro-[1,1'-biphenyl]-4-yl) propanoic acid (**1y**) for each set of experiments are given in Table S5 and represent the data graphically.

Table S5. Initial rates (k_{obs}) for the decarboxylative oxidation reaction of 2-(2-fluoro-[1,1'-biphenyl]-4-yl) propanoic acid (1y) with O_2 carried out under varying concentrations of W-1.

1y(M)	W-1(M)	O_2(M)	Initial rates(M/min)	R^2
0.1	0.005	40.95×10^{-3}	$(0.635\pm0.0462)\times10^{-3}$	0.9643
0.1	0.01	40.95×10^{-3}	$(0.637\pm0.0402)\times10^{-3}$	0.9721
0.1	0.02	40.95×10^{-3}	$(0.643\pm0.0482)\times10^{-3}$	0.9622
0.1	0.03	40.95×10^{-3}	$(0.644\pm0.0447)\times10^{-3}$	0.9661
0.1	0.04	40.95×10^{-3}	$(0.645\pm0.0411)\times10^{-3}$	0.9714

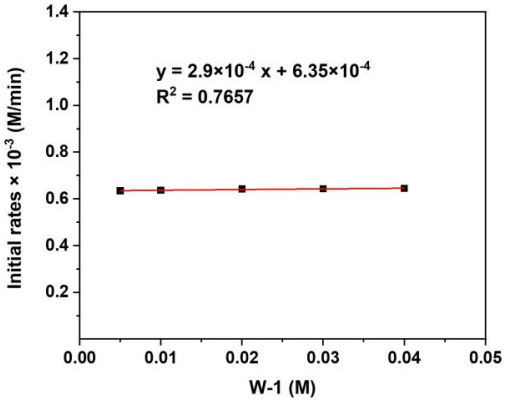

Figure S19. Plot of reaction initial rates (M/min) *vs* **W-1**(M).

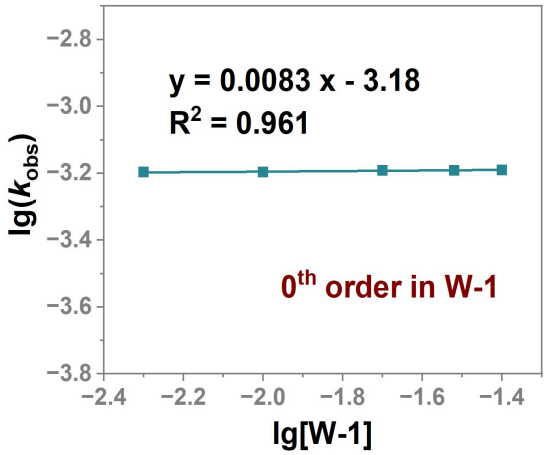

Figure S20. Plot of lg(k_{obs}) *vs* lg (concn of **W-1**).

7.2.3 Representative procedure for the 2-(2-fluoro-[1,1'-biphenyl]-4-yl) propanoic acid (1y) decarboxylative oxidation reaction carried out with various concentrations of O_2

Initial rates (k_{obs}) were determined using various concentrations of O_2 (8.6×10^{-3} M, 20.48×10^{-3} M, 30.71×10^{-3} M, 40.95×10^{-3} M) by keeping the concentration of 2-(2-fluoro-[1,1'-biphenyl]-4-yl) propanoic acid (**1y**) (0.1 M) and **W-1** (0.005 M) constant. We observed k_{obs} values of the reaction from [product] *vs* time plot, which was equal to the slope of the linear fit lines (**Table S6**). The experimental procedure that has been used is described below.

To a 10 mL Schlenk tube fitted with a stir bar was added 2-(2-fluoro-[1,1'-biphenyl]-4-yl) propanoic acid (**1y**) (0.1 M), O_2 (in different concentrations, 8.6×10^{-3} M, 20.48×10^{-3} M, 30.71×10^{-3} M, 40.95×10^{-3} M), **W-1** (0.005 M) and MeCN (2 mL) inside the glove box. The tube was sealed and the mixture was under the 365 nm, 15 W light irradiation. After that, the ^{19}F NMR spectra were recorded at various time intervals. The varying O_2 concentration and the concentration of 2-(2-fluoro-[1,1'-biphenyl]-4-yl) propanoic acid (**1y**) and **W-1** for each set of experiments are given in Table S6 and represent the data graphically.

Table S6. Initial rates (k_{obs}) for the Decarboxylative oxidation reaction of 2-(2-fluoro-[1,1'-biphenyl]-4-yl) propanoic acid (1y) with W-1 carried out under varying concentrations of O_2.

1y(M)	W-1(M)	O_2(M)	Initial rates(M/min)	R^2
0.1	0.005	8.6×10^{-3}	$(0.15\pm0.0462)\times10^{-3}$	0.9859
0.1	0.005	20.48×10^{-3}	$(0.31\pm0.0482)\times10^{-3}$	0.9861
0.1	0.005	30.71×10^{-3}	$(0.47\pm0.0447)\times10^{-3}$	0.9793
0.1	0.005	40.95×10^{-3}	$(0.64\pm0.0462)\times10^{-3}$	0.9643

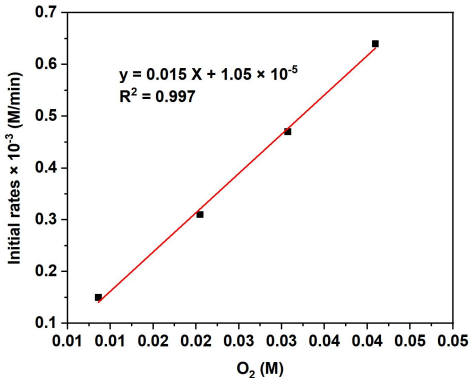

Figure S21. Plot of reaction initial rates (M/min) *vs* **O_2**(M).

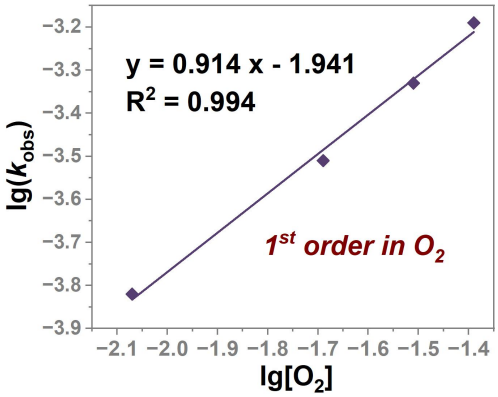

Figure S22. Plot of lg(k_{obs}) *vs* lg (concn of O_2).

8.Control Experiments

8.1 Control Experiments on Light Switch

To a 10 mL screw-cap vial fitted with a magneton was added **1y** (0.2 mmol), **W-1** (5 mol% based on the substrate), Na_2CO_3 (0.24 mmol, 1.2 equiv.), MeCN (2 mL). The reaction tube is charged with pure oxygen via a double-manifold operation and subjected to reaction under 365 nm, 15 W light irradiation, as the time period indicated in **Figure S23**. At the end of each period, a small portion (25 μL) of the reacting solution was taken by a syringe, transferred into nuclear magnetic tube and add MeCN (0.8 mL). Yields were determined by ^{19}F NMR integration.

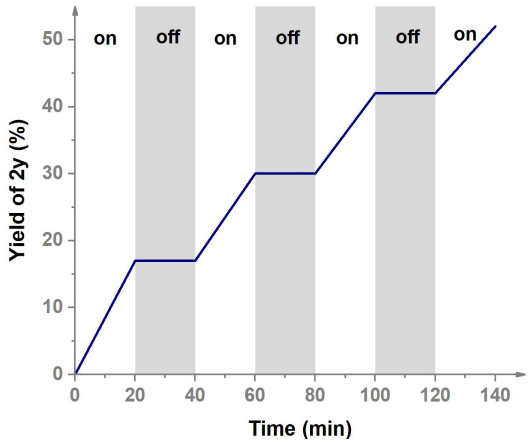

Figure S23. Light on/off experiments over time. Time frame for the conversion of **1y** to **2y**.

8.2 Radical Quenching Experiment

To a 10 mL screw-cap vial fitted with a magneton was added **1a** (0.2 mmol), **W-1** (5 mol% based on the substrate), MeCN (2 mL), Na_2CO_3 (0.24 mmol, 1.2 equiv.) and radical quencher (TEMPO or DABCO etc, 0.4 mmol).The reaction tube is charged with pure oxygen via a double-manifold operation and subjected to reaction under 365 nm, 15 W light irradiation. After 12 hours, the reaction mixture was removed from light and added tetraethylsilane (1eq based on the substrate). Yield was determined by ^{1}H NMR integration (**Figure S24**). For TEMPO trapping experiments, 4-methoxyphenylacetic acid (**1b**) (33.2 mg, 0.2 mmol, 1.0 equiv.) and **W-1** (5.5 mg, 5 mol%) and Na_2CO_3 (0.24 mmol, 1.2 equiv.) and (2,2,6,6-tetramethylpiperidin-1-yl) oxyl (TEMPO) (31.3 mg, 0.40 mmol, 2 equiv.) were dissolved in MeCN (2.0 mL, 0.1 M). The mixture was irradiated at 365 nm 15W under O_2 atmosphere for 12 h at room temperature (30°C). The decarboxylation reaction is completely suppressed and the **2b-TEMPO** (**Figure S96, S97**) was observed by ^{1}H NMR and purified by automated flash column chromatography using a petroleum ether/ethyl acetate gradient. The result indicates the formation of alkyl radicals in the mechanistic pathway.

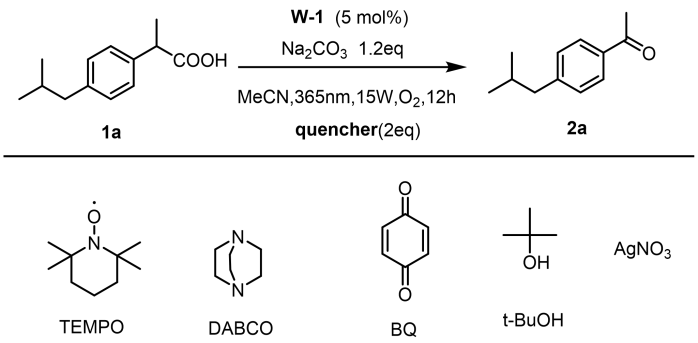

Table S7. Quencher experiments

entry	quencher(2eq)	Yield of 2a
1	TEMPO	6
2	BQ	14
3	$AgNO_3$	20
4	DABCO	33
5	t-BuOH	84
6	none	87

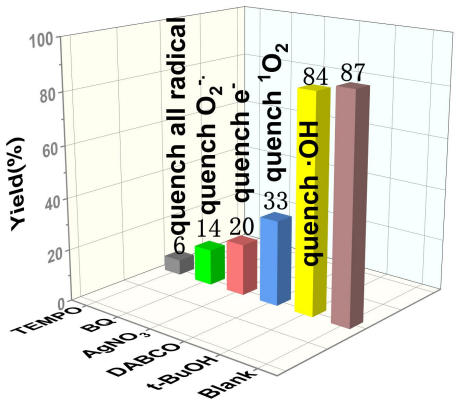

Figure S24. Ridical trapping experiment.

9. NMR date

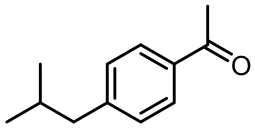

1-(4-isobutylphenyl)ethan-1-one[2](2a) ^{1}H NMR (400 MHz, Chloroform-d) δ 7.86 (d, J = 8.3 Hz, 2H), 7.22 (d, J = 8.6 Hz, 2H), 2.57 (s, 3H), 2.52 (d, J = 7.2 Hz, 2H), 1.94 – 1.83 (m, 1H), 0.89 (d, J = 6.6 Hz, 6H). ^{13}C NMR (101 MHz, Chloroform-d) δ 198.10, 147.73, 135.03, 129.39, 128.41, 45.47, 30.22, 26.66, 22.42. **Colorless oil.**

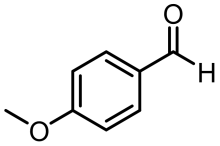

4-methoxybenzaldehyde(2b) ^{1}H NMR (400 MHz, Chloroform-d) δ 9.85 (s, 1H), 7.81 (d, J = 8.8 Hz, 2H), 6.97 (d, J = 8.7 Hz, 2H), 3.86 (s, 3H). ^{13}C NMR (101 MHz, Chloroform-d) δ 190.97, 164.70, 132.09, 130.01, 114.40, 55.68. **Colorless oil.**

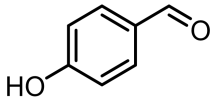

4-hydroxybenzaldehyde[3](2e) ^{1}H NMR (400 MHz, Chloroform-d) δ 9.85 (s, 1H), 7.80 (d, J = 8.7 Hz, 2H), 6.95 (d, J = 8.6 Hz, 2H), 6.30 (s, 1H). ^{13}C NMR (101 MHz, Chloroform-d) δ 191.23, 161.58, 132.58, 129.98, 116.07. **White solid.**

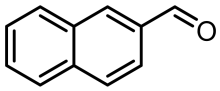

2-naphthaldehyde(2h)[4] ^{1}H NMR (400 MHz, Chloroform-d) δ 10.16 (s, 1H), 8.34 (s, 1H), 8.01 - 7.89 (m, 4H), 7.61 (dd, J = 15.6, 7.7 Hz, 2H). ^{13}C NMR (101 MHz, Chloroform-d) δ 192.40, 136.56, 134.69, 134.21, 132.74, 129.64, 129.22, 128.19, 127.20, 122.87. **Off white solid.**

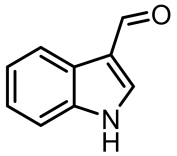

1*H*-indole-3-carbaldehyde[5](2j) ^{1}H NMR (400 MHz, DMSO-d_6) δ 9.89 (s, 1H), 8.25 (d, J = 0.9 Hz, 1H), 8.05 (d, J = 7.8 Hz, 1H), 7.47 (dd, J = 7.9, 1.1 Hz, 1H), 7.20 (dtt, J = 17.9, 7.2, 1.2 Hz, 2H). ^{13}C NMR (101 MHz, DMSO-d_6) δ 185.66, 139.25, 137.57, 124.62, 123.89, 122.52, 121.42, 118.67, 112.96. **Brown solid.**

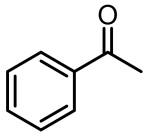

acetophenone(2k) ^{1}H NMR (400 MHz, Chloroform-d) δ 7.90 (d, J = 8.5 Hz, 2H), 7.53 -7.46 (m, 1H), 7.43 -7.35 (m, 2H), 2.53 (s, 3H). ^{13}C NMR (101 MHz, Chloroform-d) δ 198.23, 137.14, 133.20, 128.65, 128.37, 26.67. **Colorless liquid.**

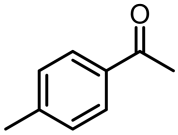

1-(*p*-tolyl) ethan-1-one(2l) ^{1}H NMR (400 MHz, Chloroform-d) δ 7.85 (d, J = 8.2 Hz, 2H), 7.24 (d, J = 8.1 Hz, 2H), 2.57 (s, 3H), 2.40 (s, 3H). ^{13}C NMR (101 MHz, Chloroform-d) δ 198.00, 143.99, 134.80, 129.34, 128.54, 26.64, 21.74. **Colorless liquid.**

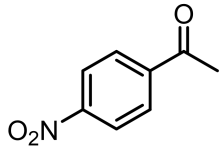

1-(4-nitrophenyl) ethan-1-one[6](2m) ^{1}H NMR (400 MHz, Chloroform-d) δ 8.29 (d, J = 8.7 Hz, 2H), 8.09 (d, J = 8.8 Hz, 2H), 2.66 (s, 3H). ^{13}C NMR (101 MHz, Chloroform-d) δ 196.50, 150.43, 141.44, 129.44, 123.98, 27.14. **White solid.**

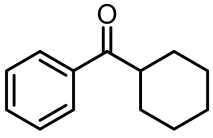

cyclohexyl(phenyl)methanone(2n) ^{1}H NMR (400 MHz, Chloroform-d) δ 7.93 (d, J = 7.0 Hz, 2H), 7.52 (d, J = 7.4 Hz, 1H), 7.44 (dd, J = 8.2, 6.8 Hz, 2H), 3.25 (tt, J = 11.4, 3.2 Hz, 1H), 1.91 - 1.80 (m, 4H), 1.75 - 1.71 (m, 1H), 1.51 - 1.22 (m, 5H). ^{13}C NMR (101 MHz, Chloroform-d) δ 204.05, 136.41, 132.84, 128.68, 128.36, 45.71, 29.51, 26.05, 25.95. **Colorless liquid.**

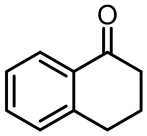

3,4-dihydronaphthalen-1(2*H*)-one[7](2o) ^{1}H NMR (400 MHz, Chloroform-d) δ 8.02 (dd, J = 7.8, 1.5 Hz, 1H), 7.46 (td, J = 7.5, 1.5 Hz, 1H), 7.32-7.25 (m, 2H), 2.96 (t, J = 6.1 Hz, 2H), 2.67-2.63 (m, 2H), 2.14 (dt, J = 8.3, 5.8 Hz, 2H). ^{13}C NMR (101 MHz, Chloroform-d) δ 198.63, 144.62, 133.53, 132.69, 128.89, 127.27, 126.74, 39.28, 29.80, 23.37. **Yellow oil.**

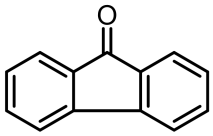

9*H*-fluoren-9-one(2p) ^{1}H NMR (400 MHz, Chloroform-d) δ 7.65 (dt, J = 7.3, 1.0 Hz, 2H), 7.53 -7.45 (m, 4H), 7.28 (td, J = 7.2, 1.4 Hz, 2H). ^{13}C NMR (101 MHz, Chloroform-d) δ 194.11, 144.53, 134.82, 134.23, 129.19, 124.44, 120.43. **Yellow solid**.

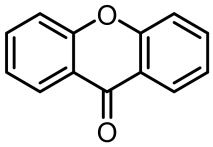

9*H*-xanthen-9-one(2q) ^{1}H NMR (400 MHz, Chloroform-d) δ 8.32 (d, J = 7.0 Hz, 2H), 7.70 (t, J = 7.8 Hz, 2H), 7.49 - 7.44 (m, 2H), 7.38 - 7.34 (m, 2H). ^{13}C NMR (101 MHz, Chloroform-d) δ 177.33, 156.26, 134.92, 126.82, 124.00, 121.93, 118.07. **White solid.**

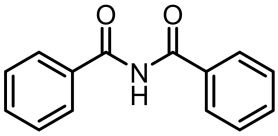

N-benzoylbenzamide(2r) ^{1}H NMR (400 MHz, Chloroform-d) δ 9.00 (s, 1H), 7.86 (d, J = 7.1 Hz, 4H), 7.60 (t, J = 7.4 Hz, 2H), 7.50 (dd, J = 8.3, 6.9 Hz, 4H). ^{13}C NMR (101 MHz, Chloroform-d) δ 166.49, 133.42, 133.26, 129.06, 128.03. **White solid.**

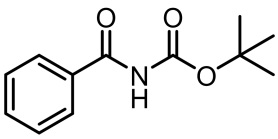

tert-butyl benzoylcarbamate(2s) ^{1}H NMR (400 MHz, Chloroform-d) δ 7.94 (s, 1H), 7.82 - 7.78

(m, 2H), 7.58 - 7.53 (m, 1H), 7.50 - 7.44 (m, 2H), 1.52 (s, 9H). ^{13}C NMR (101 MHz, Chloroform-d) δ 165.33, 149.63, 133.48, 132.90, 128.93, 127.59, 82.93, 28.12. **White solid.**

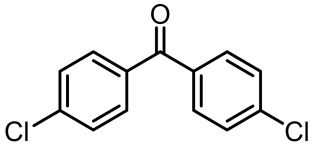

bis(4-chlorophenyl) methanone[8](2t) ^{1}H NMR (400 MHz, Chloroform-d) δ 7.72 (d, J = 8.7 Hz, 4H), 7.46 (d, J = 8.7 Hz, 4H). ^{13}C NMR (101 MHz, Chloroform-d) δ 194.43, 139.28, 135.58, 131.50, 128.82. **White solid.**

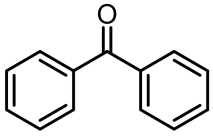

benzophenone(2u) ^{1}H NMR (400 MHz, Chloroform-d) δ 7.80 (d, J = 7.8 Hz, 4H), 7.58 (t, J = 7.4 Hz, 2H), 7.47 (t, J = 7.6 Hz, 4H). ^{13}C NMR (101 MHz, Chloroform-d) δ 196.88, 137.69, 132.54, 130.17, 128.39. **White solid.**

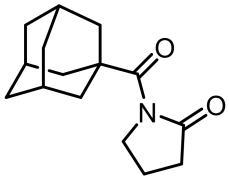

1-((3*r*,5*r*,7*r*)-adamantane-1-carbonyl)pyrrolidin-2-one[9](2v) ^{1}H NMR (400 MHz, Chloroform-d) δ 3.89 - 3.74 (m, 2H), 2.57 (t, J = 8.0 Hz, 2H), 2.10 - 1.99 (m, 11H), 1.73 (t, J = 11.8 Hz, 6H). ^{13}C NMR (101 MHz, Chloroform-d) δ 180.41, 173.65, 48.67, 44.05, 36.56, 36.49, 34.62, 28.31, 18.00. **White solid.**

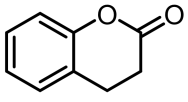

chroman-2-one(2w) ^{1}H NMR (400 MHz, Chloroform-d) δ 7.32 - 7.16 (m, 2H), 7.18 - 6.89 (m, 2H), 3.00 (t, J = 7.3 Hz, 2H), 2.78 (dd, J = 8.3, 6.2 Hz, 2H). ^{13}C NMR (101 MHz, Chloroform-d) δ 168.70, 152.10, 128.38, 128.11, 124.50, 122.72, 117.06, 29.33, 23.80. **Colorless liquid.**

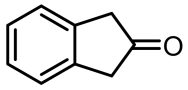

1,3-dihydro-2*H*-inden-2-one(2x) ^{1}H NMR (400 MHz, Chloroform-d) δ 7.31 - 7.25 (m, 4H), 3.56 (s, 4H). ^{13}C NMR (101 MHz, Chloroform-d) δ 215.49, 137.87, 127.51, 125.12, 44.22. **Colorless liquid.**

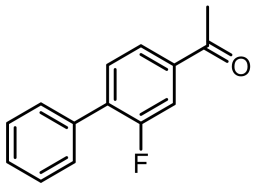

1-(2-fluoro-[1,1'-biphenyl]-4-yl) ethan-1-one(2y) ^{1}H NMR (400 MHz, Chloroform-d) δ 7.80 (dd, J = 8.0, 1.7 Hz, 1H), 7.73 (dd, J = 11.1, 1.7 Hz, 1H), 7.59-7.52 (m, 3H), 7.50-7.39 (m, 3H), 2.62 (s, 3H). ^{13}C NMR (101 MHz, Chloroform-d) δ 196.70, 161.02, 158.53, 137.90, 137.83, 134.76, 133.98, 133.84, 131.07, 131.03, 129.13, 129.10, 128.74, 128.63, 124.49, 124.46, 116.15, 115.91, 26.81. ^{19}F NMR (376 MHz, Chloroform-d) δ -116.65. **White solid.**

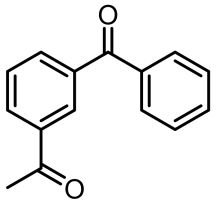

1-(3-benzoylphenyl) ethan-1-one(2z) ^{1}H NMR (400 MHz, Chloroform-d) δ 8.34 (s, 1H), 8.16 (ddd, J = 7.8, 1.8, 1.2 Hz, 1H), 7.98-7.95 (m, 1H), 7.78 (dd, J = 8.3, 1.4 Hz, 2H), 7.63-7.56 (m, 2H), 7.51-7.46 (m, 2H), 2.63 (s, 3H). ^{13}C NMR (101 MHz, Chloroform-d) δ 197.49, 195.93, 138.01, 137.13, 134.33, 132.96, 131.89, 130.12, 129.73, 128.76, 128.55, 26.89. **Yellow gum.**

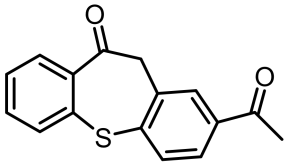

2-acetyldibenzo[*b*,*f*]thiepin-10(11*H*)-one(2aa) ^{1}H NMR (400 MHz, Chloroform-d) 8.19 δ (d, J = 8.0 Hz, 1H), 7.99 (s, 1H), 7.79 - 7.70 (m, 2H), 7.59 (d, J = 7.9 Hz, 1H), 7.44 (t, J = 7.6 Hz, 1H), 7.33 (t, J = 7.6 Hz, 1H), 4.41 (s, 2H), 2.59 (s, 3H). ^{13}C NMR (101 MHz, Chloroform-d) δ 197.09, 190.84, 140.20, 139.16, 138.26, 138.03, 136.11, 132.91, 131.71, 131.58, 131.04, 129.25, 127.29, 127.03, 51.09, 26.87. **White solid.**

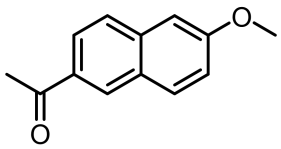

1-(6-methoxynaphthalen-2-yl)ethan-1-one(2ab) ^{1}H NMR (400 MHz, Chloroform-d) δ 8.37 (s, 1H), 7.99 (dd, J = 8.6, 1.8 Hz, 1H), 7.83 (d, J = 9.1 Hz, 1H), 7.75 (d, J = 8.7 Hz, 1H), 7.19 (dd, J = 8.9, 2.5 Hz, 1H), 7.14 (d, J = 2.5 Hz, 1H), 3.93 (s, 3H), 2.68 (s, 3H). ^{13}C NMR (101 MHz, Chloroform-d) δ 198.09, 159.84, 137.38, 132.66, 131.20, 130.09, 127.88, 127.19, 124.74, 119.42, 105.63, 55.53, 26.68. **Brown solid.**

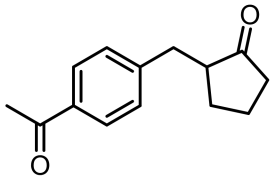

2-(4-acetylbenzyl)cyclopentan-1-one(2ac) ^{1}H NMR (400 MHz, Chloroform-d) δ 7.86 (d, J = 8.3 Hz, 2H), 7.24 (d, J = 8.3 Hz, 2H), 3.17 (dd, J = 13.8, 4.3 Hz, 1H), 2.64 - 2.57 (m, 1H), 2.57 (s, 3H), 2.35 (dddt, J = 12.5, 9.7, 6.9, 1.6 Hz, 2H), 2.14 - 2.01 (m, 2H), 1.95 (dddt, J = 13.6, 8.9, 6.5, 2.4 Hz, 1H), 1.71 (d, J = 3.0 Hz, 1H), 1.51 (dtd, J = 12.5, 11.1, 6.5 Hz, 1H). ^{13}C NMR (101 MHz, Chloroform-d) δ 219.85, 197.99, 145.96, 135.42, 129.23, 128.71, 50.80, 38.17, 35.63, 29.21, 26.71, 20.62. **White solid.**

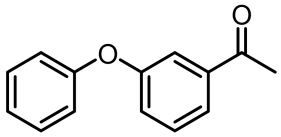

1-(3-phenoxyphenyl)ethan-1-one(2ad) ^{1}H NMR (400 MHz, Chloroform-d) δ 7.67 (d, J = 8.0 Hz, 1H), 7.57 (s, 1H), 7.41 (t, J = 7.9 Hz, 1H), 7.38 - 7.32 (m, 2H), 7.20 (d, J = 8.2 Hz, 1H), 7.16 - 7.11 (m, 1H), 7.01 (d, J = 7.7 Hz, 2H), 2.57 (s, 3H). ^{13}C NMR (101 MHz, Chloroform-d) δ 197.68, 157.84, 156.68, 138.93, 130.08, 123.95, 123.46, 123.23, 119.23, 118.19, 26.89. **Colorless liquid.**

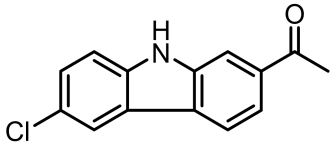

1-(6-chloro-9*H*-carbazol-2-yl)ethan-1-one(2ae) ^{1}H NMR (400 MHz, Chloroform-d) δ 8.27 - 8.20 (m, 2H), 7.99 (dd, J = 8.2, 1.5 Hz, 1H), 7.53 - 7.50 (m, 1H), 7.34 (dd, J = 8.6, 2.0 Hz, 1H), 7.25 (s, 1H), 6.75 (d, J = 8.6 Hz, 1H), 2.57 (s, 3H). ^{13}C NMR (101 MHz, Chloroform-d) δ 197.70, 140.06, 139.33, 136.33, 128.56, 128.00, 125.01, 122.68, 122.53, 121.70, 121.22, 110.23, 108.85, 27.11. **White solid.**

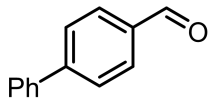

[1,1'-biphenyl]-4-carbaldehyde(2af) ^{1}H NMR (400 MHz, Chloroform-d) δ 10.05 (s, 1H), 7.99-7.92 (m, 2H), 7.78 - 7.72 (m, 2H), 7.66 - 7.62 (m, 2H), 7.51-7.41 (m, 3H). ^{13}C NMR (101 MHz, Chloroform-d) δ 192.14, 147.31, 139.80, 135.25, 130.41, 129.14, 128.59, 127.81, 127.49. **White solid.**

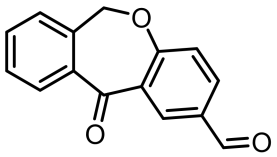

11-oxo-6,11-dihydrodibenzo[*b*,*e*]oxepine-2-carbaldehyde(2ah) ^{1}H NMR (400 MHz, Chloroform-d) δ 9.99 (d, J = 0.7 Hz, 1H), 8.73 (d, J = 2.2 Hz, 1H), 8.02 (dd, J = 8.6, 2.2 Hz, 1H), 7.88 (dd, J = 7.8, 1.4 Hz, 1H), 7.62 - 7.58 (m, 1H), 7.51 (td, J = 7.6, 1.3 Hz, 1H), 7.43 - 7.39 (m, 1H), 7.17 (dd, J = 8.6, 0.7 Hz, 1H), 5.28 (s, 2H). ^{13}C NMR (101 MHz, Chloroform-d) δ 190.60, 190.39, 165.69, 140.43, 137.67, 134.59, 133.53, 133.36, 130.70, 129.88, 129.50, 128.28, 124.90, 122.30, 73.71. **Yellow solid.**

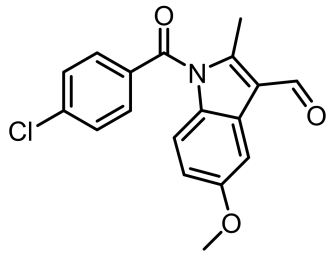

1-(4-chlorobenzoyl)-5-methoxy-2-methyl-1*H*-indole-3-carbaldehyde(2ai) ^{1}H NMR (400 MHz, Chloroform-d) δ 10.31 (s, 1H), 7.80 (s, 1H), 7.69 (d, J = 8.6 Hz, 2H), 7.49 (d, J = 8.5 Hz, 2H), 6.72 (d, J = 1.7 Hz, 2H), 3.86 (s, 3H), 2.75 (s, 3H). ^{13}C NMR (101 MHz, Chloroform-d) δ 185.96,

168.37, 157.26, 148.73, 141.05, 132.11, 131.81, 130.69, 129.61, 127.02, 118.47, 114.42, 114.00, 103.33, 53.57, 12.77. **White solid.**

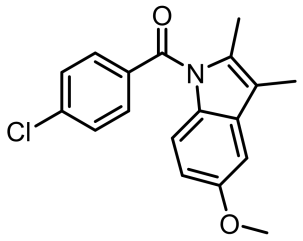

(4-chlorophenyl)(5-methoxy-2,3-dimethyl-1*H*-indol-1-yl)methanone(2ai') ^{1}H NMR (400 MHz, Chloroform-d) δ 7.63 (d, J = 8.5 Hz, 2H), 7.45 (d, J = 8.4 Hz, 2H), 6.92 - 6.87 (m, 2H), 6.65 (dd, J = 8.9, 2.6 Hz, 1H), 3.84 (s, 3H), 2.30 (s, 3H), 2.18 (s, 3H). ^{13}C NMR (101 MHz, Chloroform-d) δ 168.36, 156.00, 138.96, 134.43, 133.88, 132.04, 131.13, 130.91, 129.11, 115.54, 111.24, 55.82, 13.50, 8.91. **Colorless liquid.**

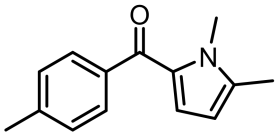

(1,5-dimethyl-1*H*-pyrrol-2-yl)(*p*-tolyl)methanone(2aj') ^{1}H NMR (400 MHz, Chloroform-d) δ 7.68 (d, J = 8.2 Hz, 2H), 7.25 - 7.21 (m, 2H), 6.64 (d, J = 3.9 Hz, 1H), 5.94 (dd, J = 4.0, 0.8 Hz, 1H), 3.91 (s, 3H), 2.40 (s, 3H), 2.29 (s, 3H). ^{13}C NMR (101 MHz, Chloroform-d) δ 185.54, 141.69, 139.35, 137.72, 130.67, 129.98, 129.45, 128.76, 122.86, 108.22, 33.03, 21.66, 12.77. **Colorless liquid.**

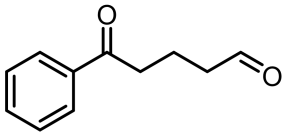

5-oxo-5-phenylpentanal(4a) ^{1}H NMR (400 MHz, Chloroform-d) δ 9.80 (t, J = 1.4 Hz, 1H), 7.98 - 7.93 (m, 2H), 7.55 (d, J = 7.4 Hz, 1H), 7.46 (dt, J = 7.1, 2.0 Hz, 2H), 3.04 (t, J = 7.0 Hz, 2H), 2.59 (t, J = 7.1 Hz, 2H), 2.11 - 2.04 (m, 2H). ^{13}C NMR (101 MHz, Chloroform-d) δ 202.12,199.44,136.76, 133.29, 128.74, 128.18, 128.10, 43.18, 37.36, 16.59. **Colorless liquid.**

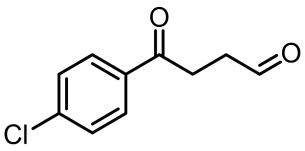

4-(4-chlorophenyl)-4-oxobutanal(4b) ^{1}H NMR (400 MHz, Chloroform-d) δ 9.88 (s, 1H), 7.91 (d, J = 8.6 Hz, 2H), 7.43 (d, J = 8.7 Hz, 2H), 3.31 - 3.23 (m, 2H), 2.93 (t, J = 6.2 Hz, 2H). ^{13}C NMR (101 MHz, Chloroform-d) δ 200.55, 196.72, 139.89, 134.81, 129.59, 129.08, 37.63, 31.01. **Colorless liquid.**

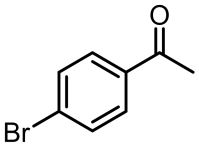

1-(4-bromophenyl)ethan-1-one(6e) ^{1}H NMR (400 MHz, Chloroform-d) δ 7.80 (d, J = 8.6 Hz, 2H), 7.58 (d, J = 8.5 Hz, 2H), 2.57 (s, 3H). ^{13}C NMR (101 MHz, Chloroform-d) δ 197.15, 135.90, 131.99, 129.94, 128.41, 26.64. **Colorless liquid.**

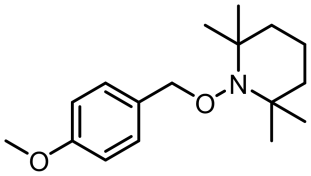

1-((4-methoxybenzyl)oxy)-2,2,6,6-tetramethylpiperidine (2b-TEMPO) ^{1}H NMR (400 MHz, Chloroform-*d*) δ 7.32 - 7.27 (m, 2H), 6.90 - 6.86 (m, 2H), 4.74 (s, 2H), 3.81 (s, 3H), 1.65 - 1.46 (m, 6H), 1.27 (s, 6H), 1.13 (s, 6H). ^{13}C NMR (101 MHz, Chloroform-*d*) δ 159.08, 130.45, 129.32, 113.73, 78.50, 60.06, 55.36, 39.77, 33.24, 20.38, 17.21.

10. NMR spectra

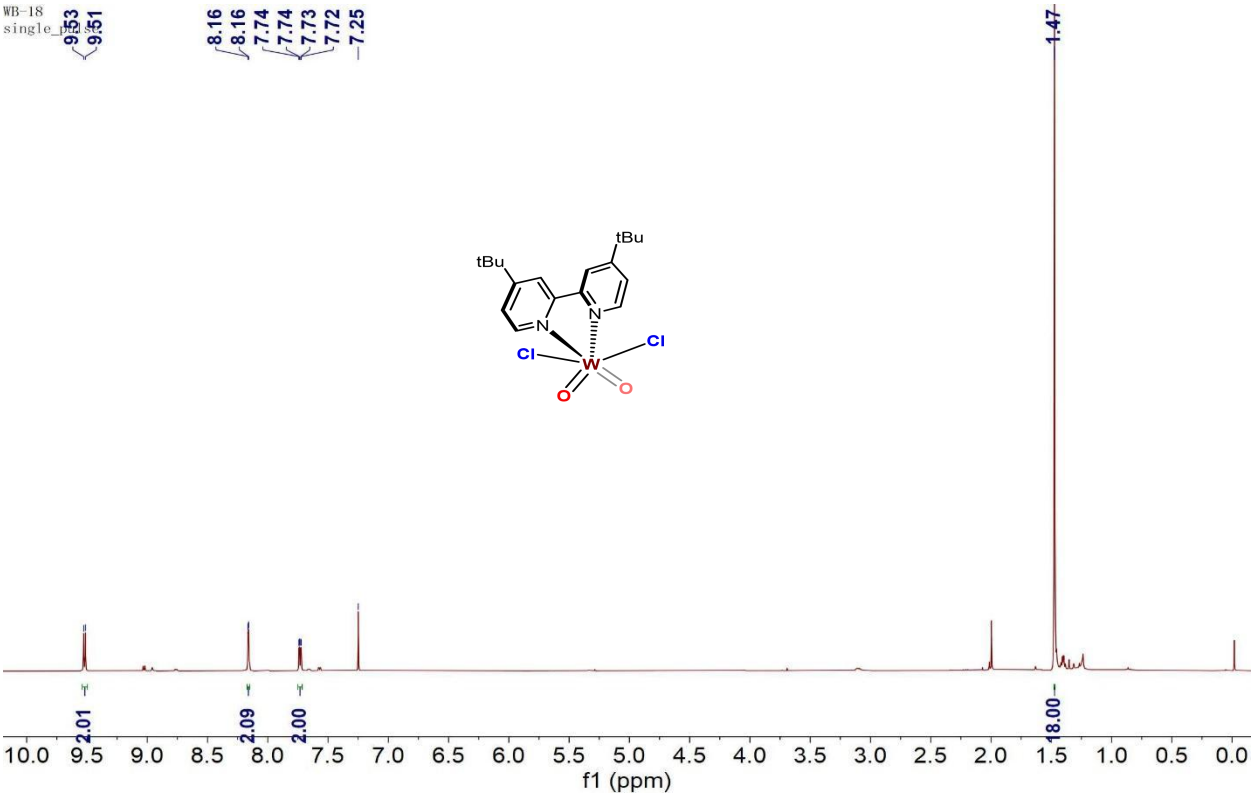

Figure S25. ^{1}H NMR spectrum of **W-1** (400 MHz, Chloroform-d).

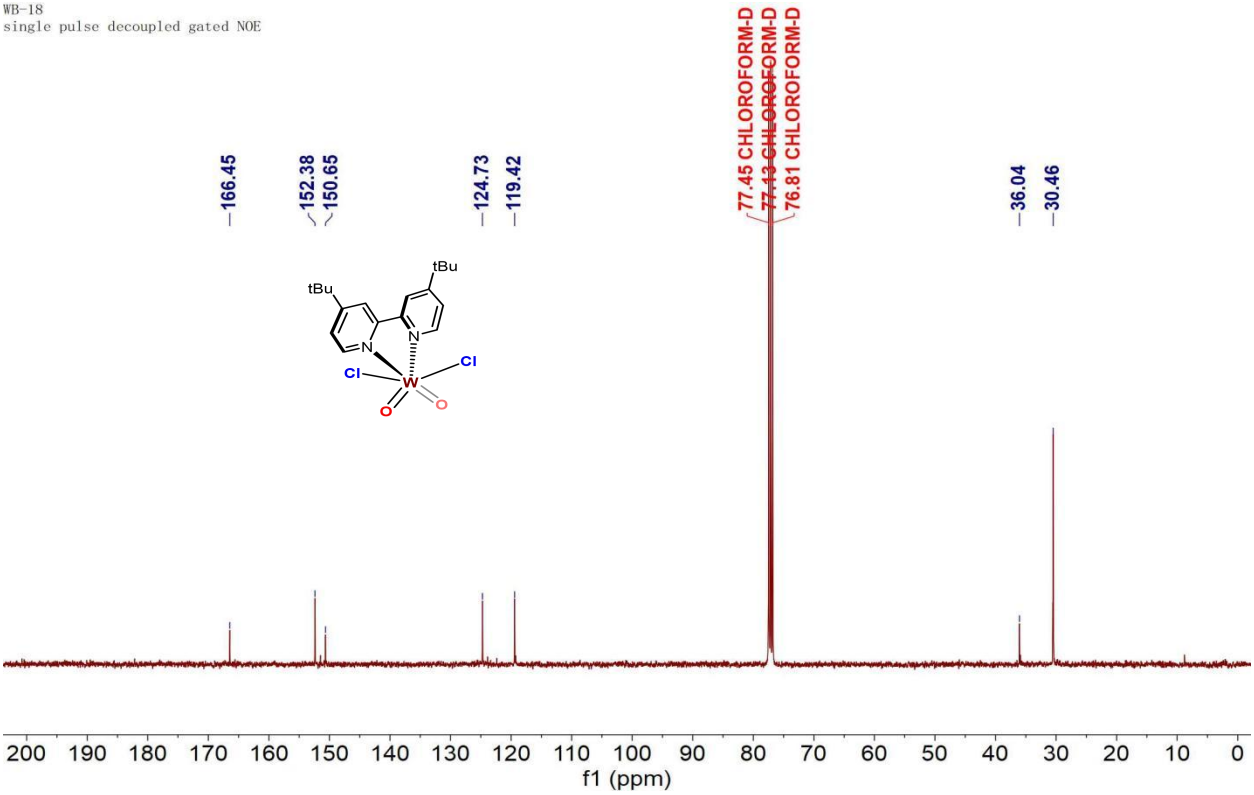

Figure S26. ^{13}C NMR spectrum of **W-1** (101 MHz, Chloroform-d).

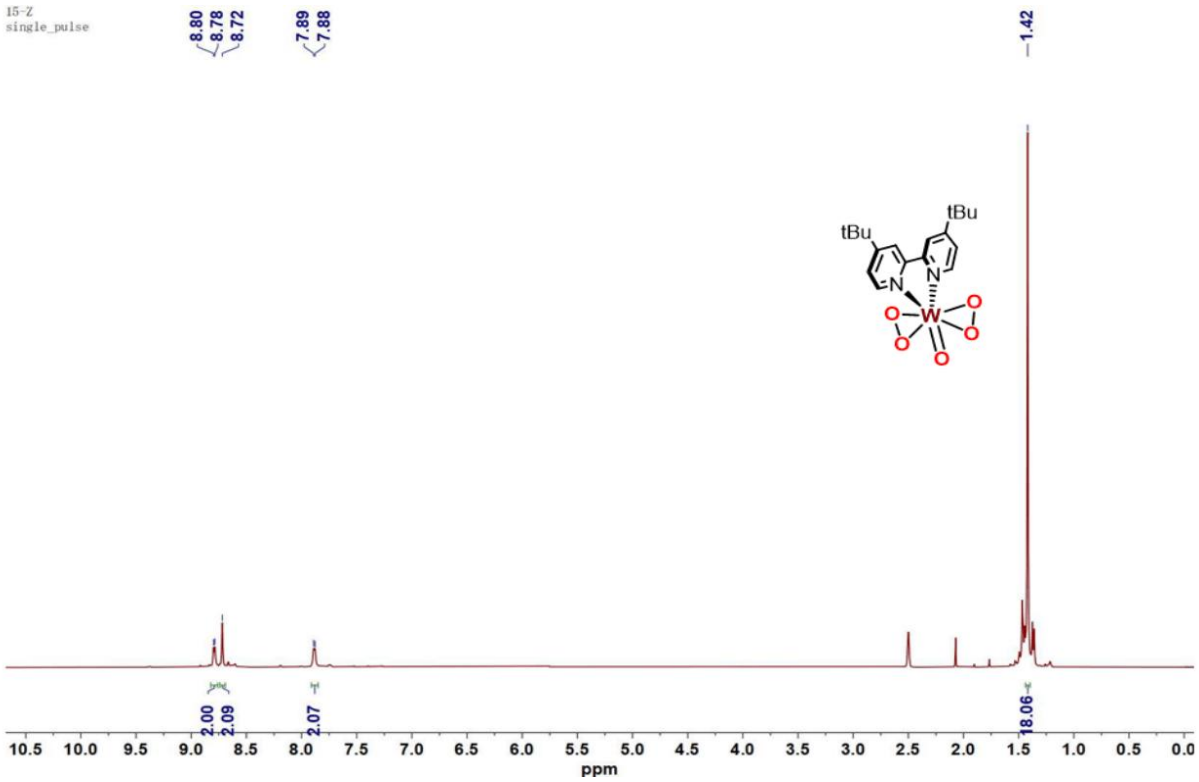

Figure S27. ^{1}H NMR spectrum of **W-2** (400 MHz, DMSO-d_6).

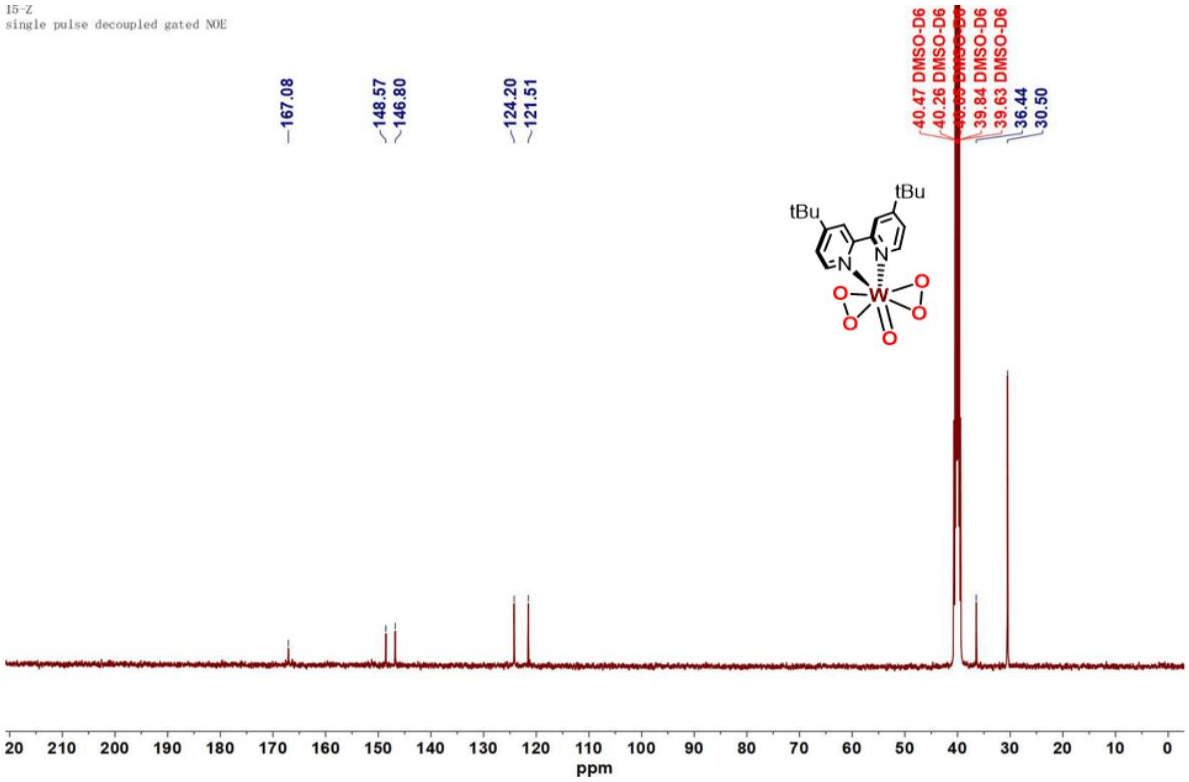

Figure S28. ^{13}C NMR spectrum of **W-2** (101 MHz, DMSO-d_6).

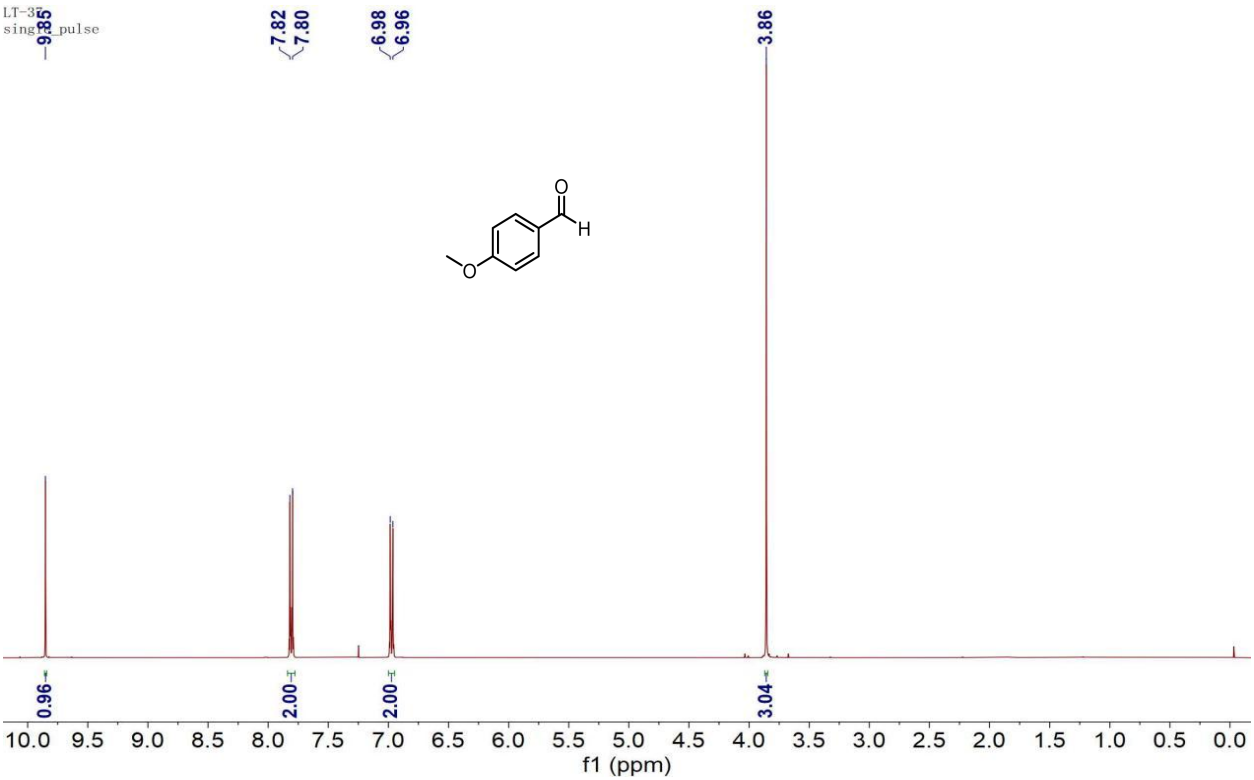

Figure S29. ^{1}H NMR spectrum of **2b** (400 MHz, Chloroform-d).

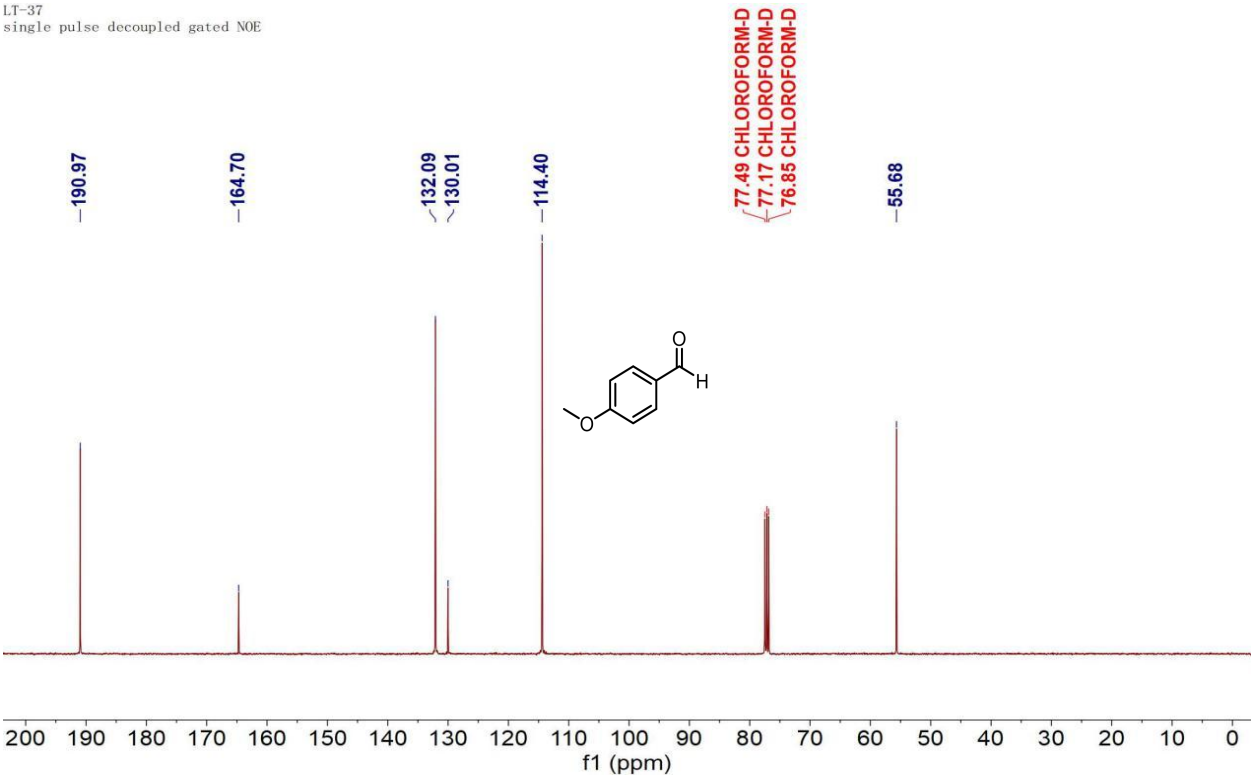

Figure S30. ^{13}C NMR spectrum of **2b** (101 MHz, Chloroform-d).

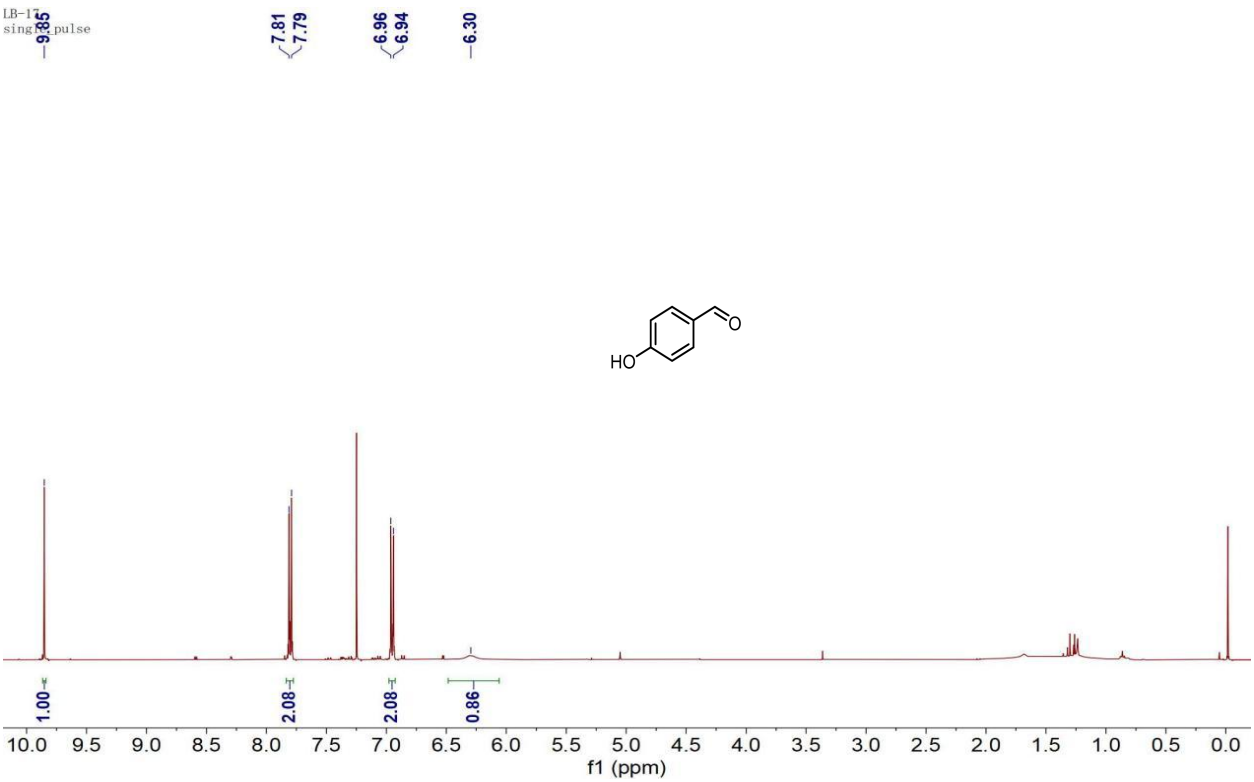

Figure S31. ^{1}H NMR spectrum of **2e** (400 MHz, Chloroform-d).

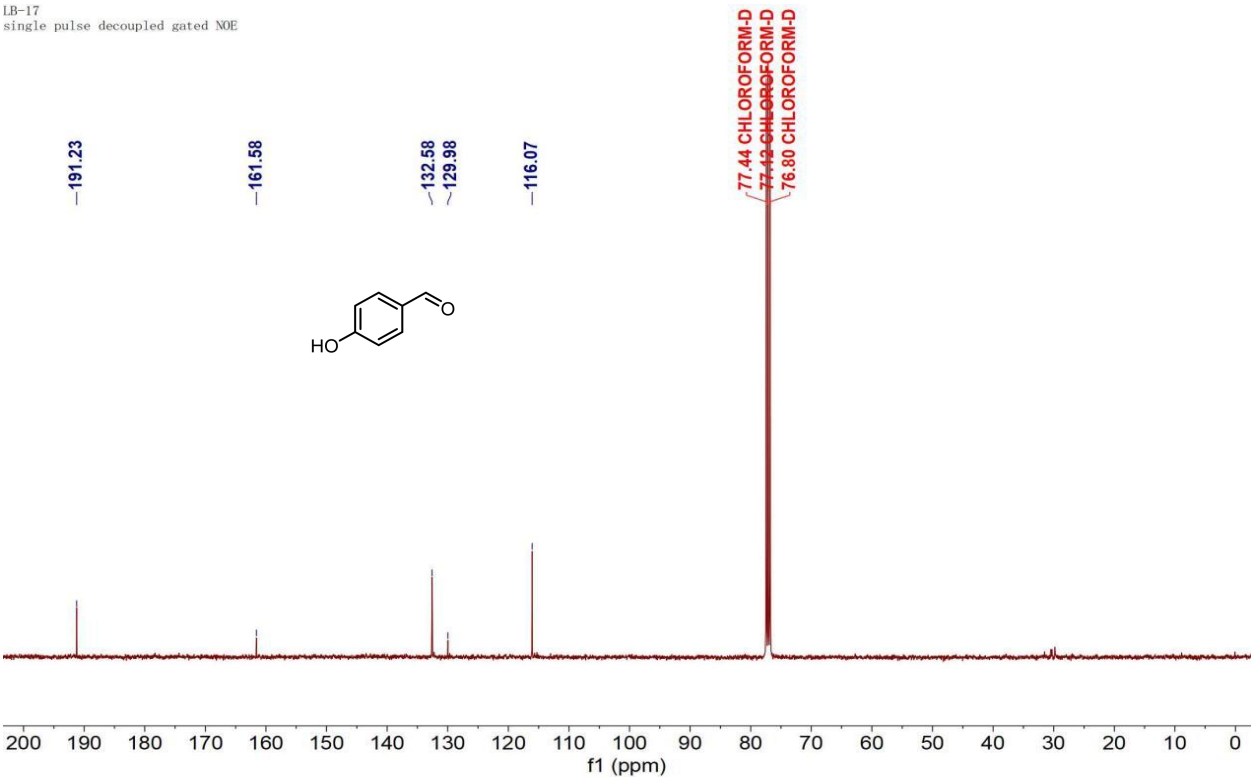

Figure S32. ^{13}C NMR spectrum of **2e** (101 MHz, Chloroform-d).

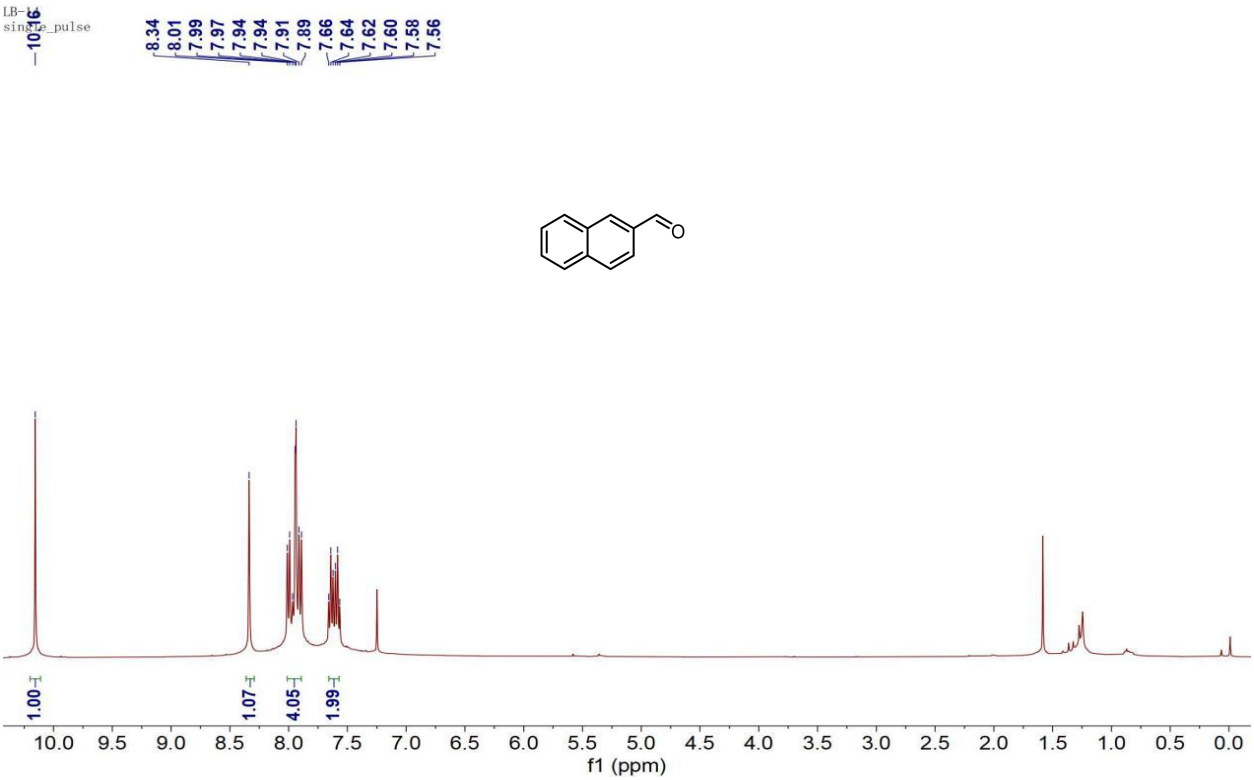

Figure S33. ^{1}H NMR spectrum of **2h** (400 MHz, Chloroform-d).

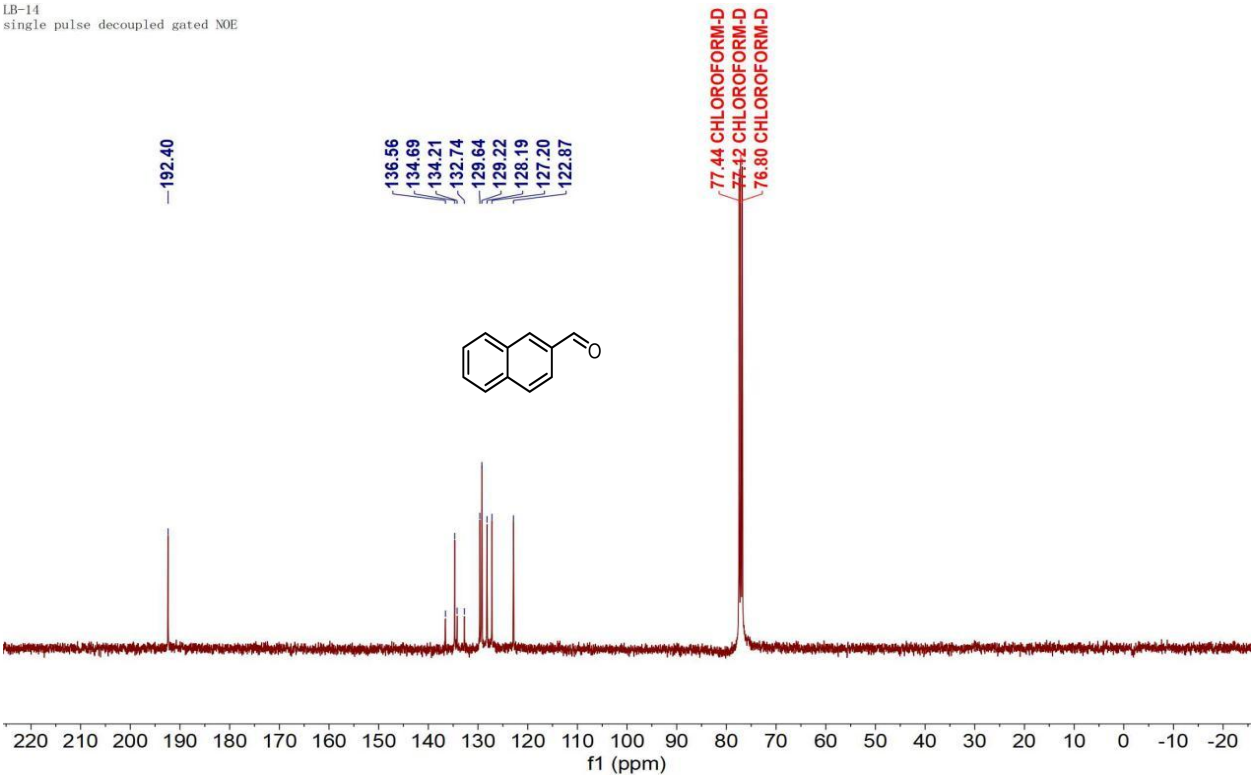

Figure S34. ^{13}C NMR spectrum of **2h** (101 MHz, Chloroform-d).

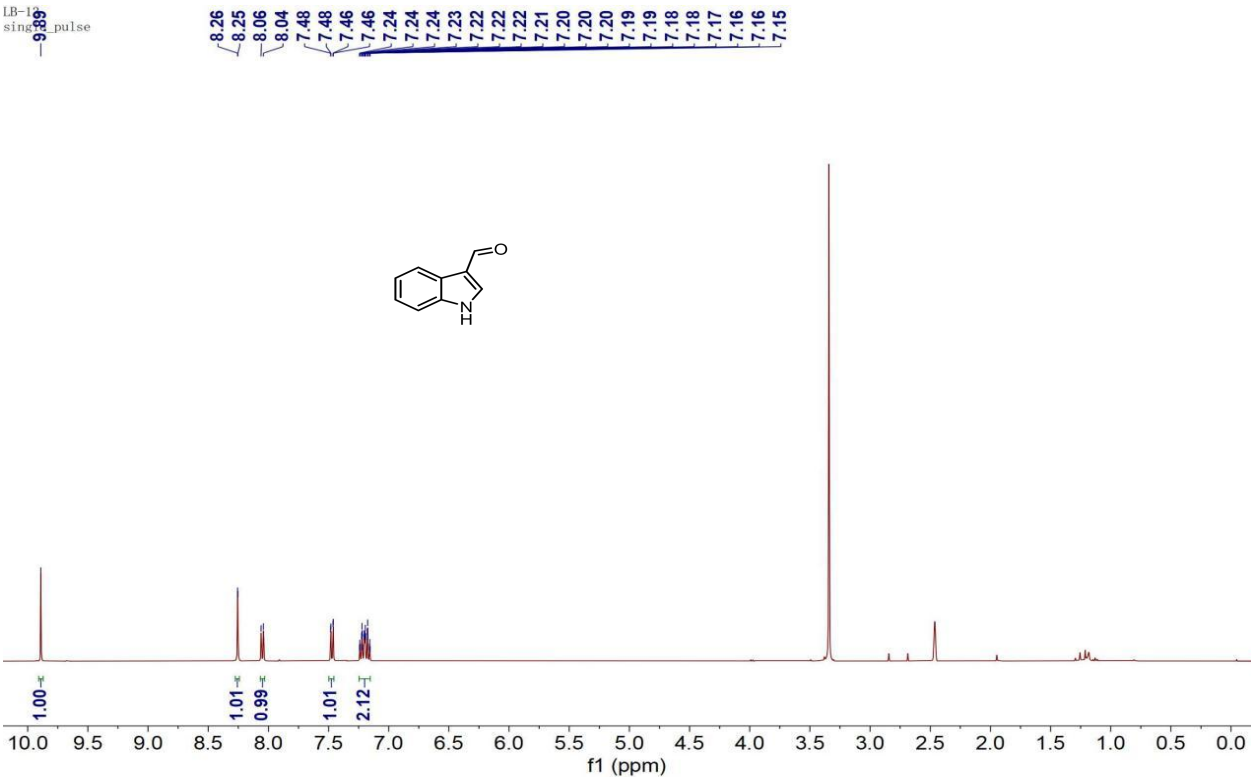

Figure S35. ^{1}H NMR spectrum of **2j** (400 MHz, DMSO-d_6).

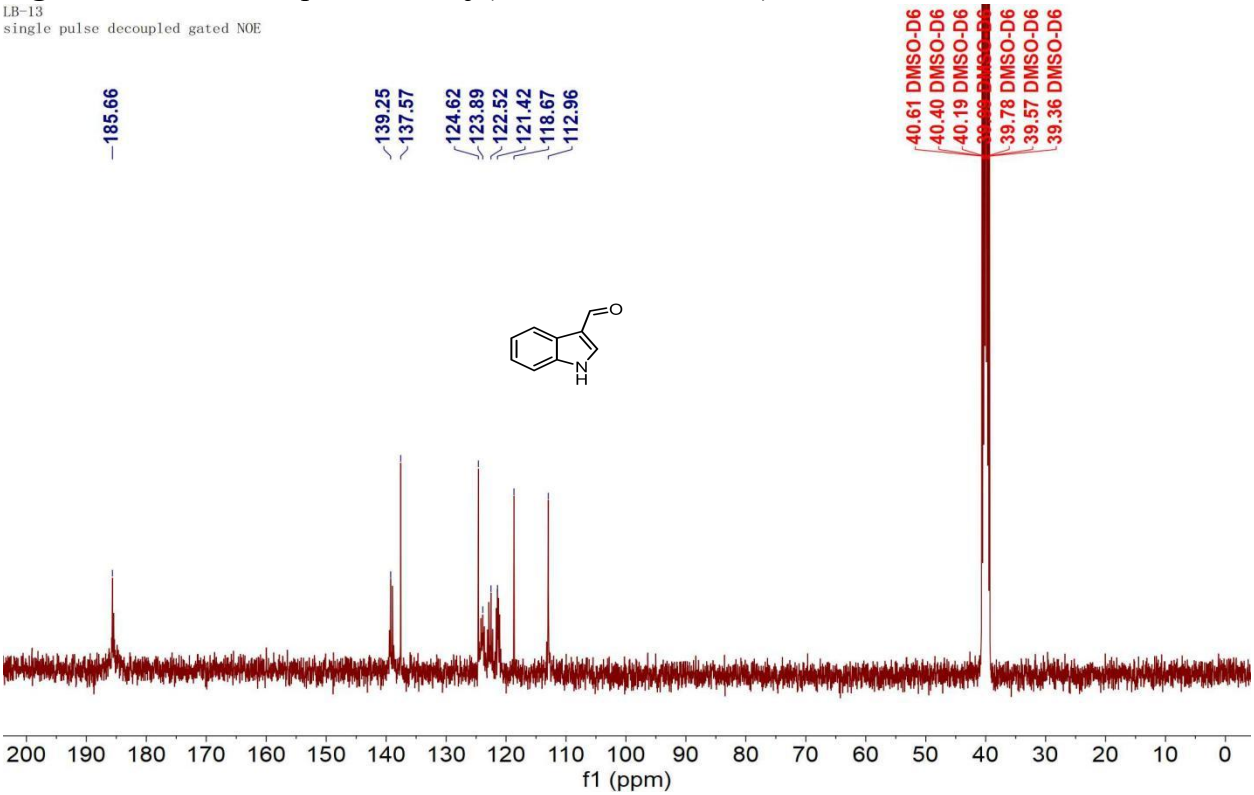

Figure S36. ^{13}C NMR spectrum of **2j** (101 MHz, DMSO-d_6).

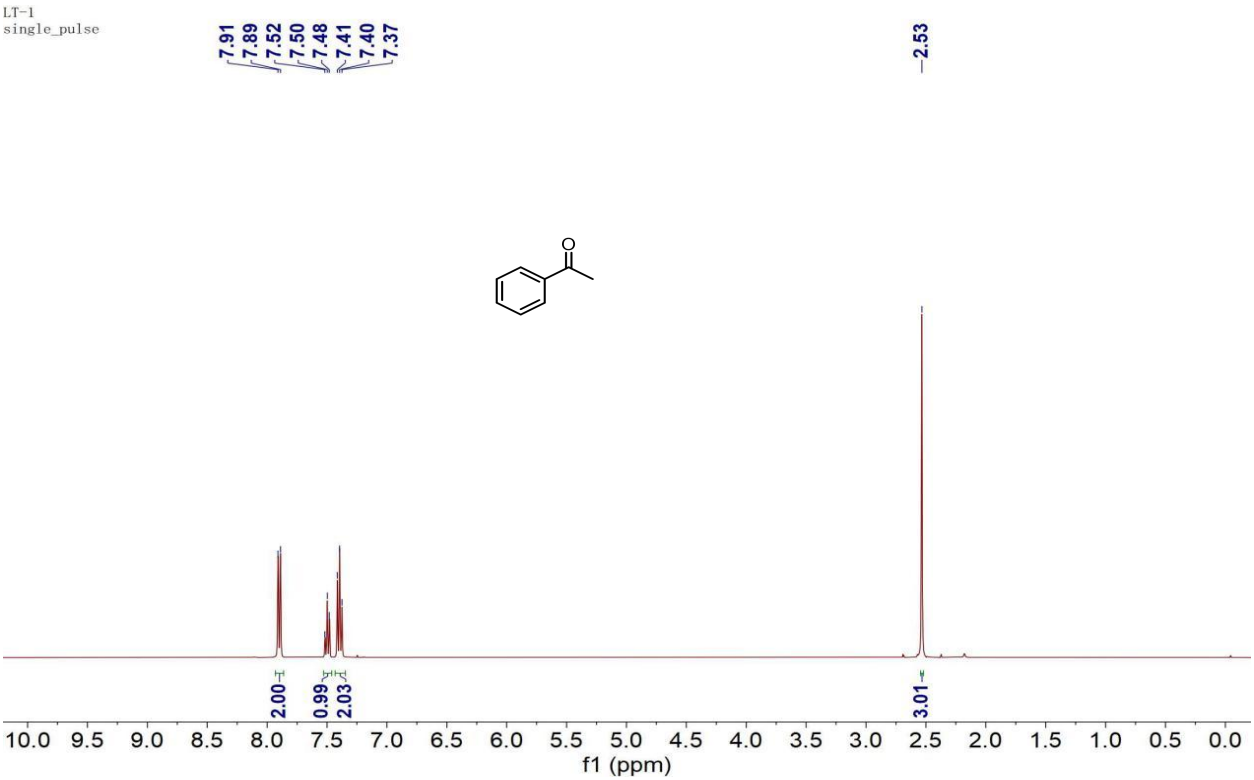

Figure S37. ^{1}H NMR spectrum of **2k** (400 MHz, Chloroform-d).

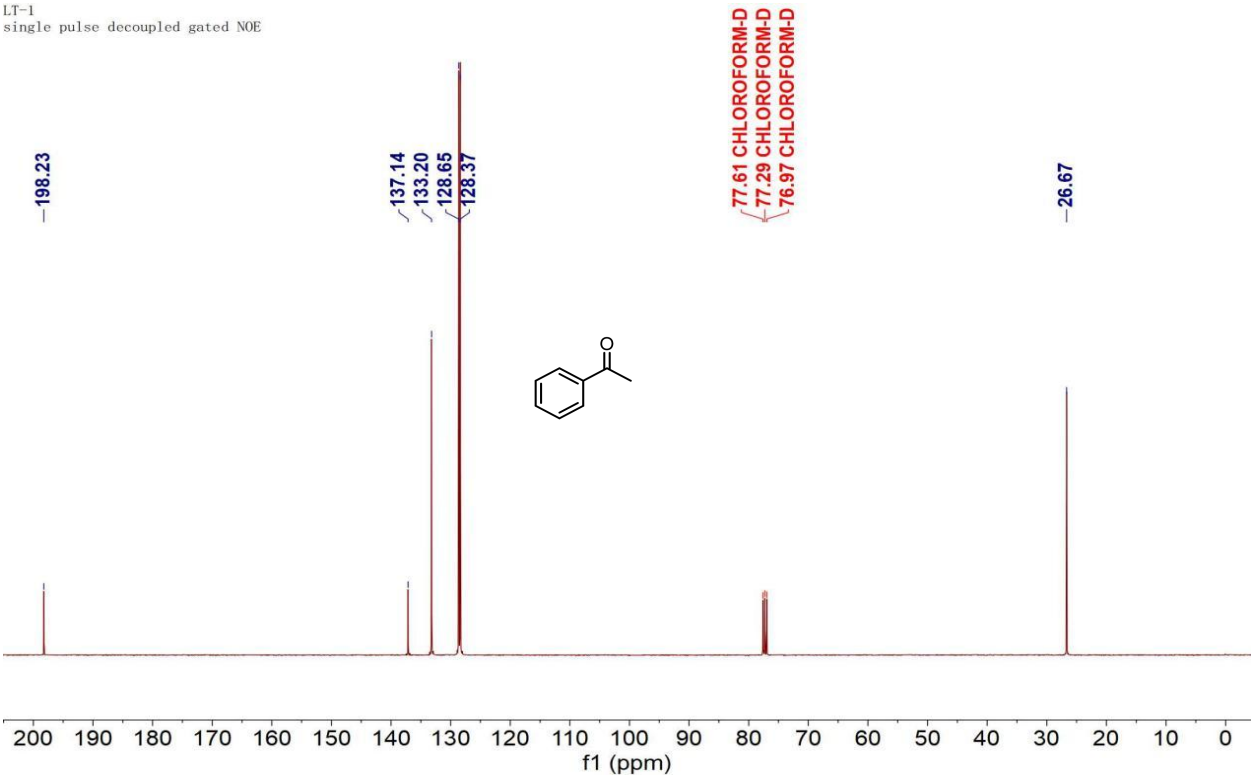

Figure S38. ^{13}C NMR spectrum of **2k** (101 MHz, Chloroform-d).

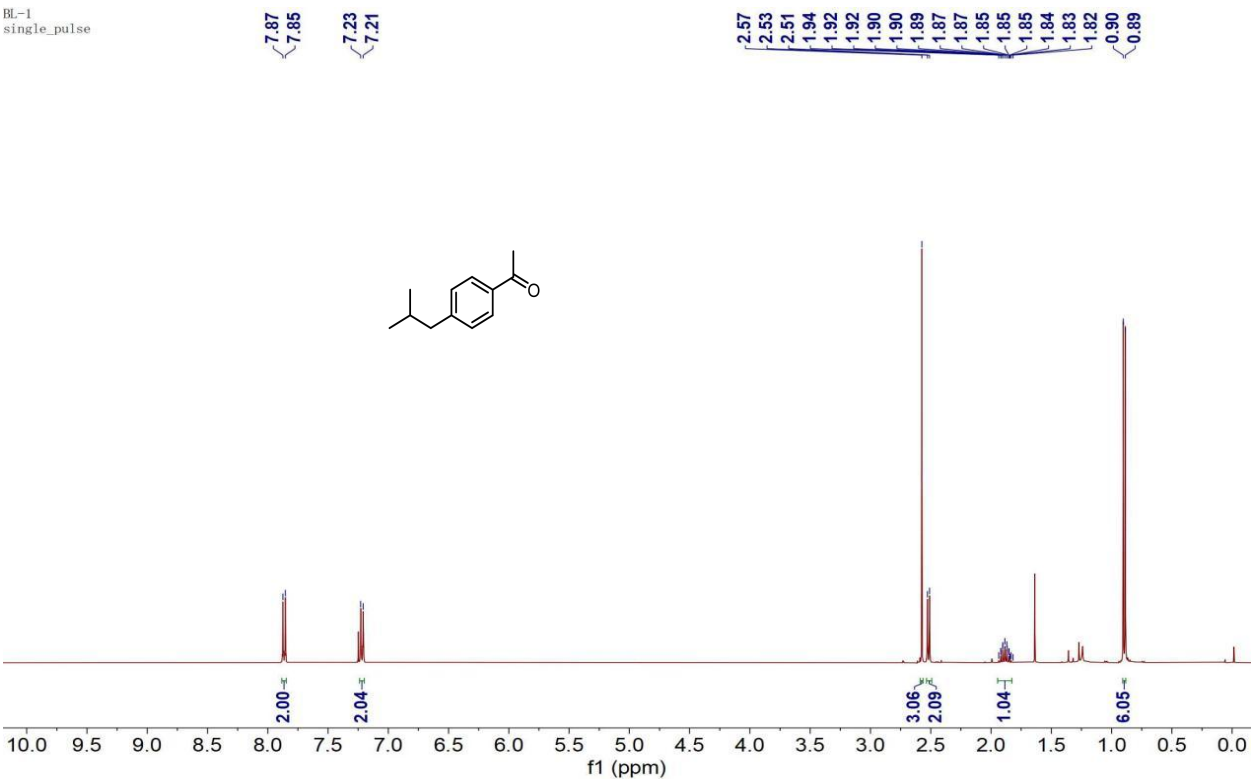

Figure S39. ^{1}H NMR spectrum of **2a** (400 MHz, Chloroform-d).

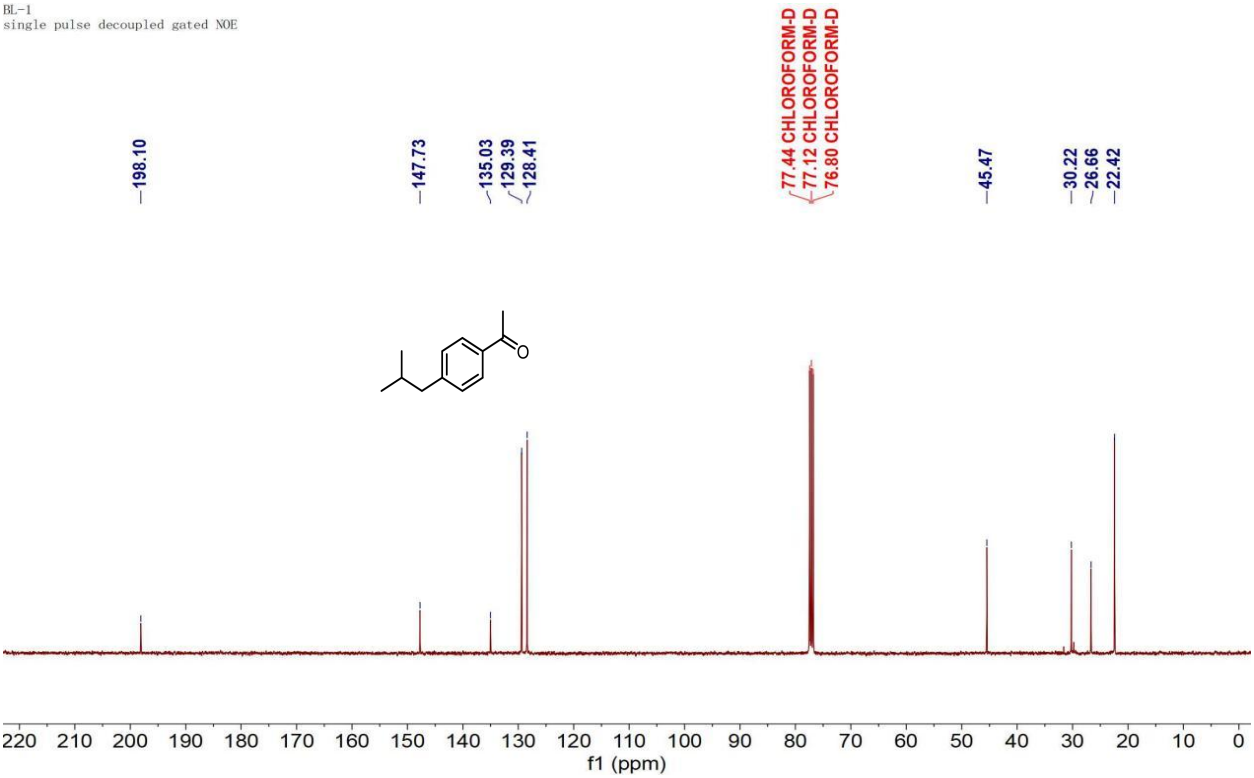

Figure S40. ^{13}C NMR spectrum of **2a** (101 MHz, Chloroform-d).

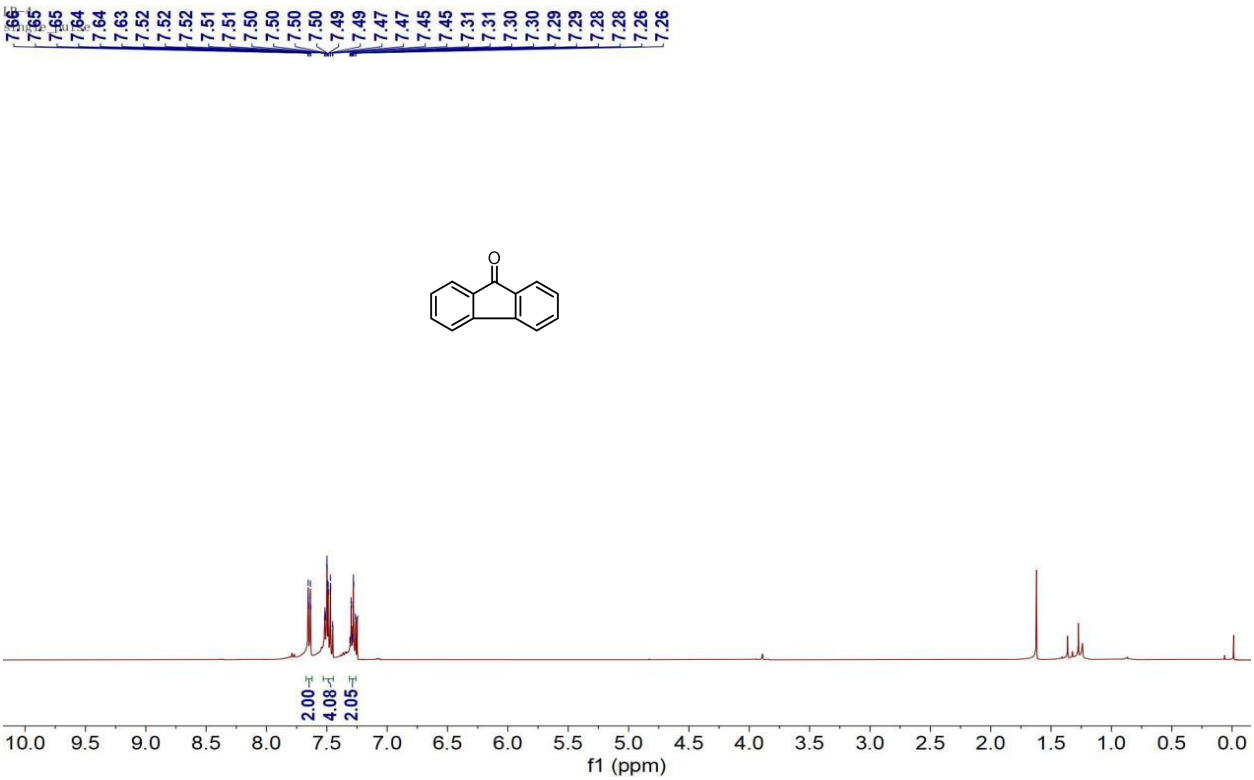

Figure S41. [1]H NMR spectrum of **2p** (400 MHz, Chloroform-d).

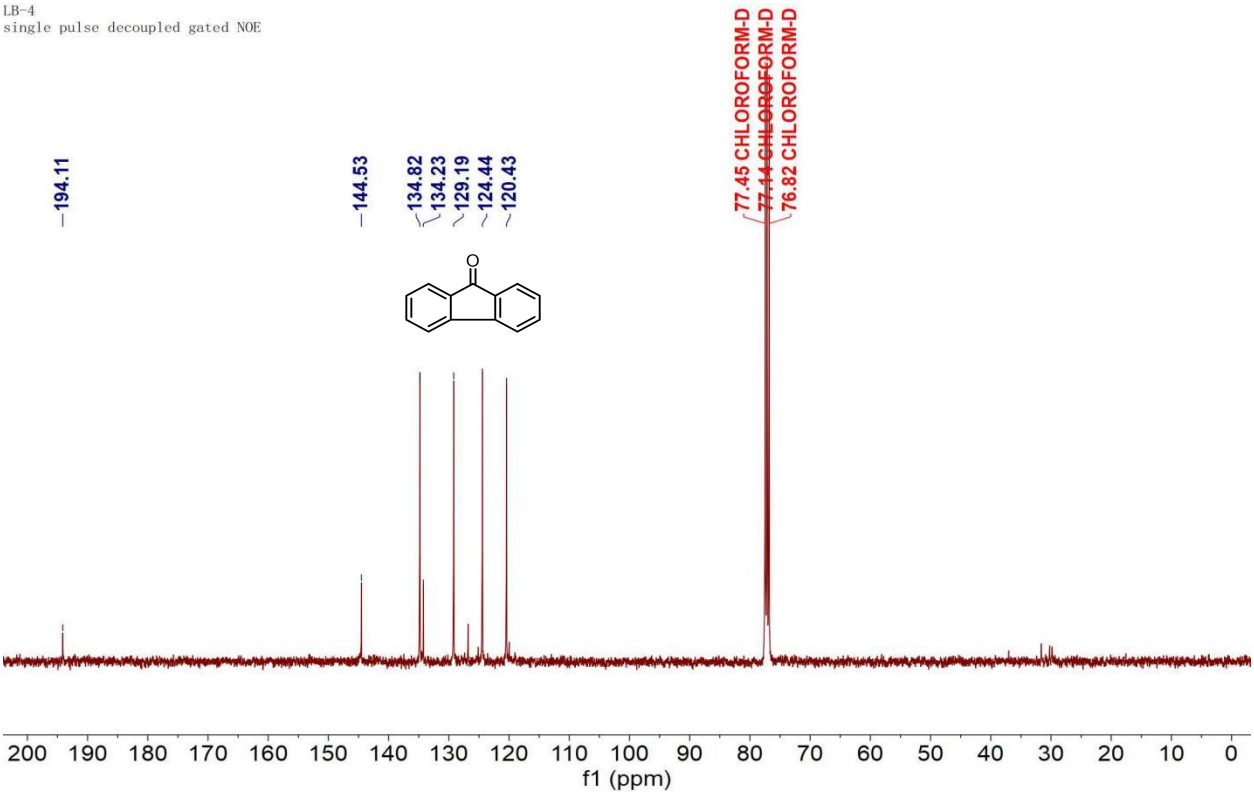

Figure S42. [13]C NMR spectrum of **2p** (101 MHz, Chloroform-d).

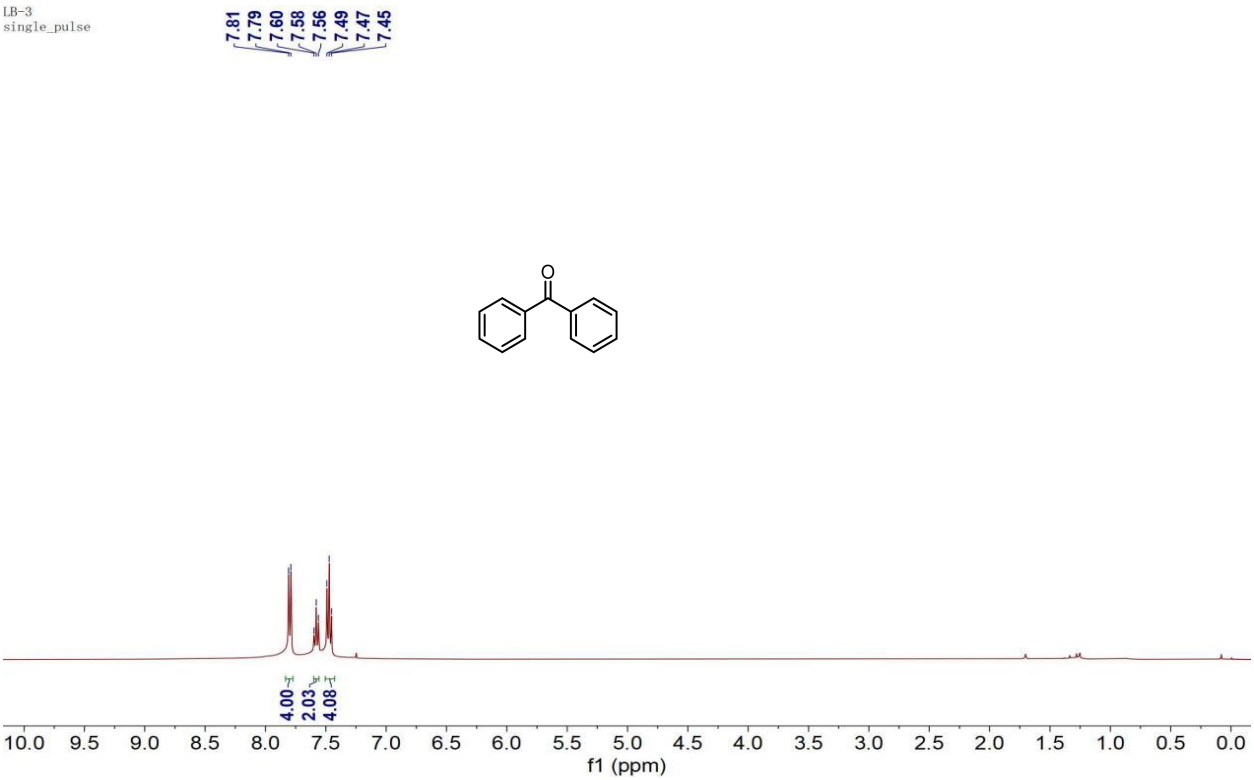

Figure S43. ^{1}H NMR spectrum of **2u** (400 MHz, Chloroform-d).

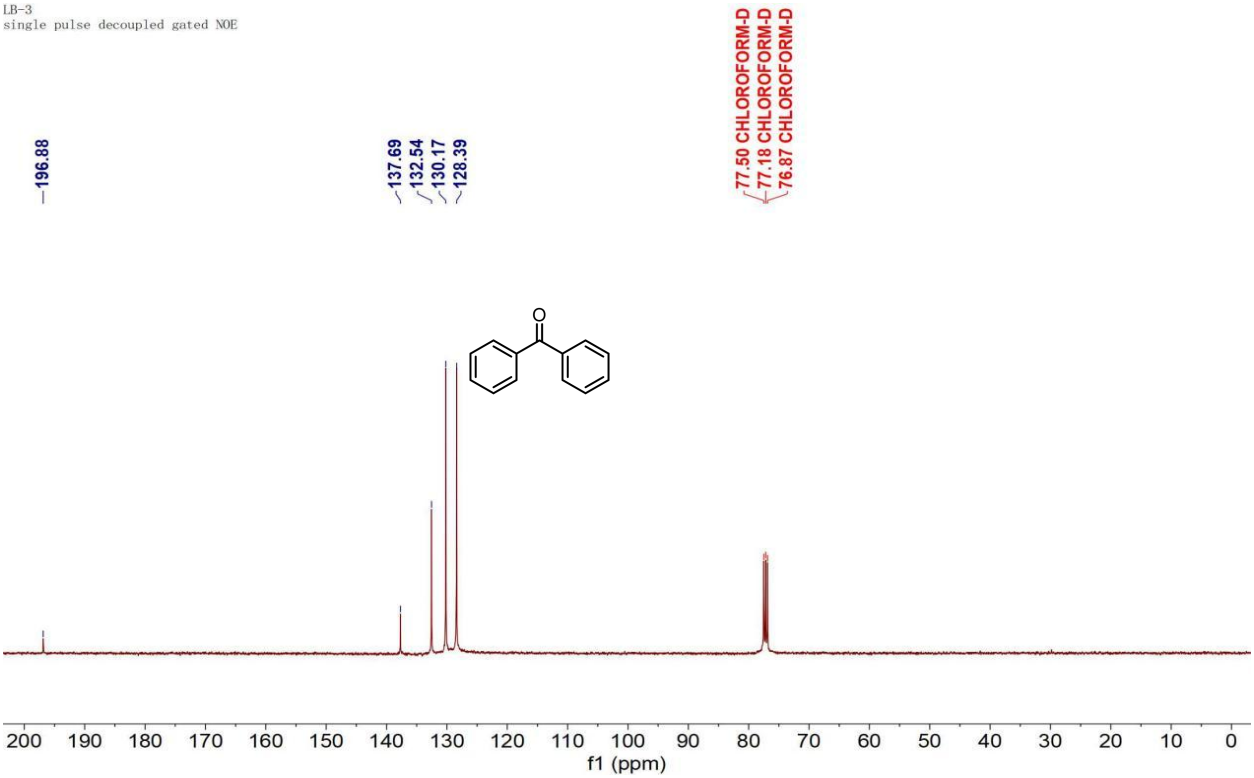

Figure S44. ^{13}C NMR spectrum of **2u** (101 MHz, Chloroform-d).

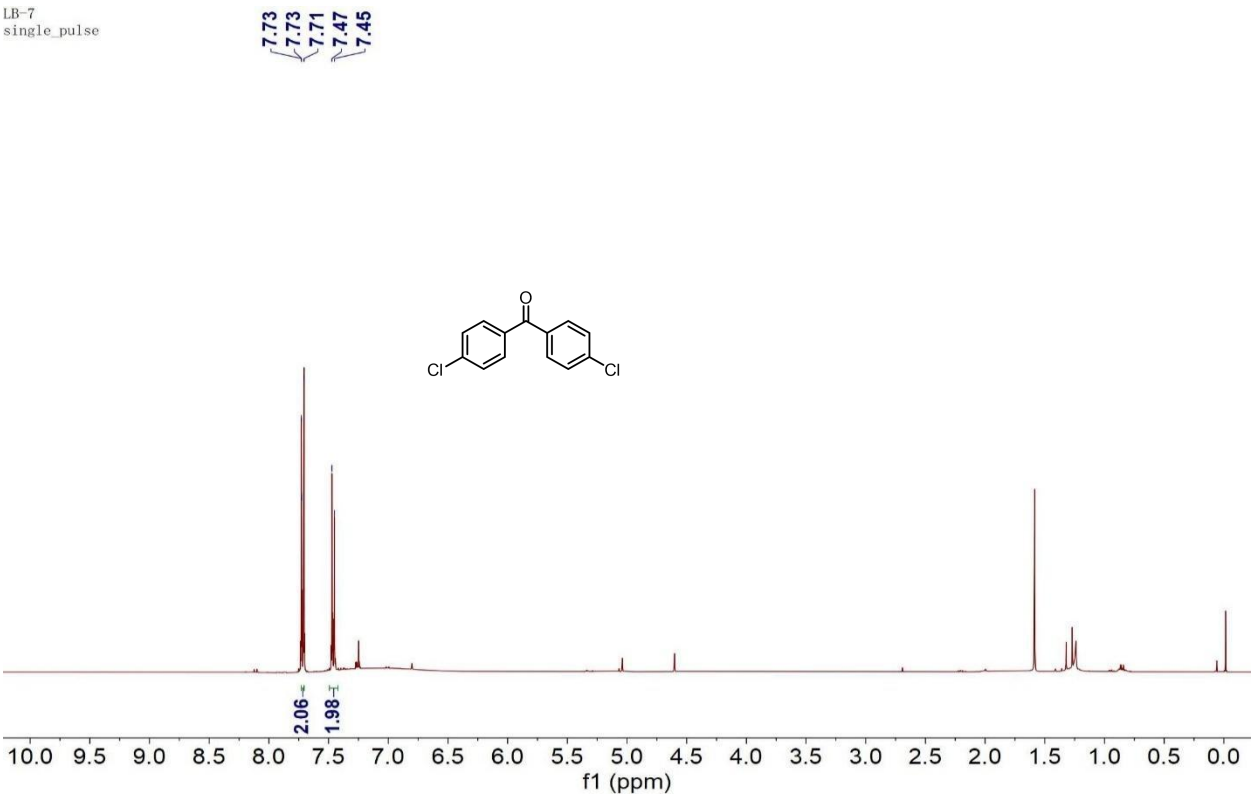

Figure S45. ^{1}H NMR spectrum of **2t** (400 MHz, Chloroform-d).

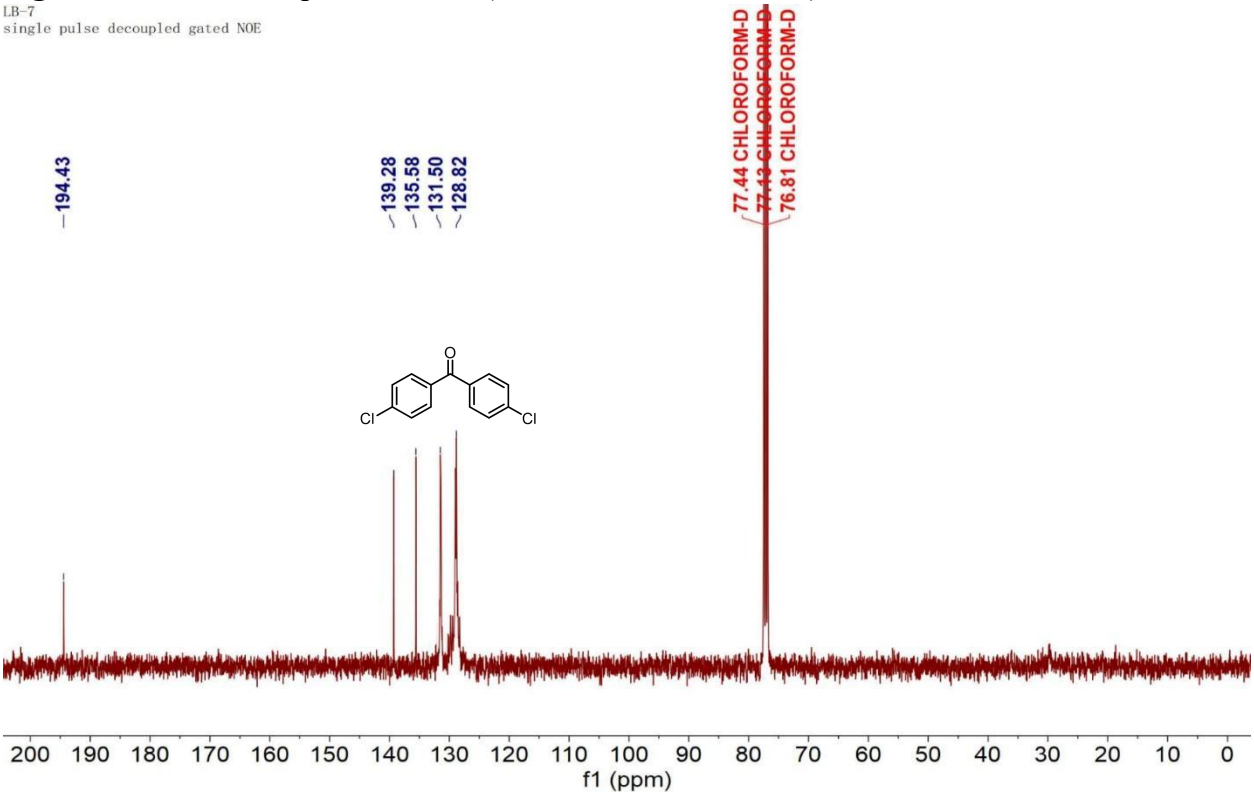

Figure S46. ^{13}C NMR spectrum of **2t** (101 MHz, Chloroform-d).

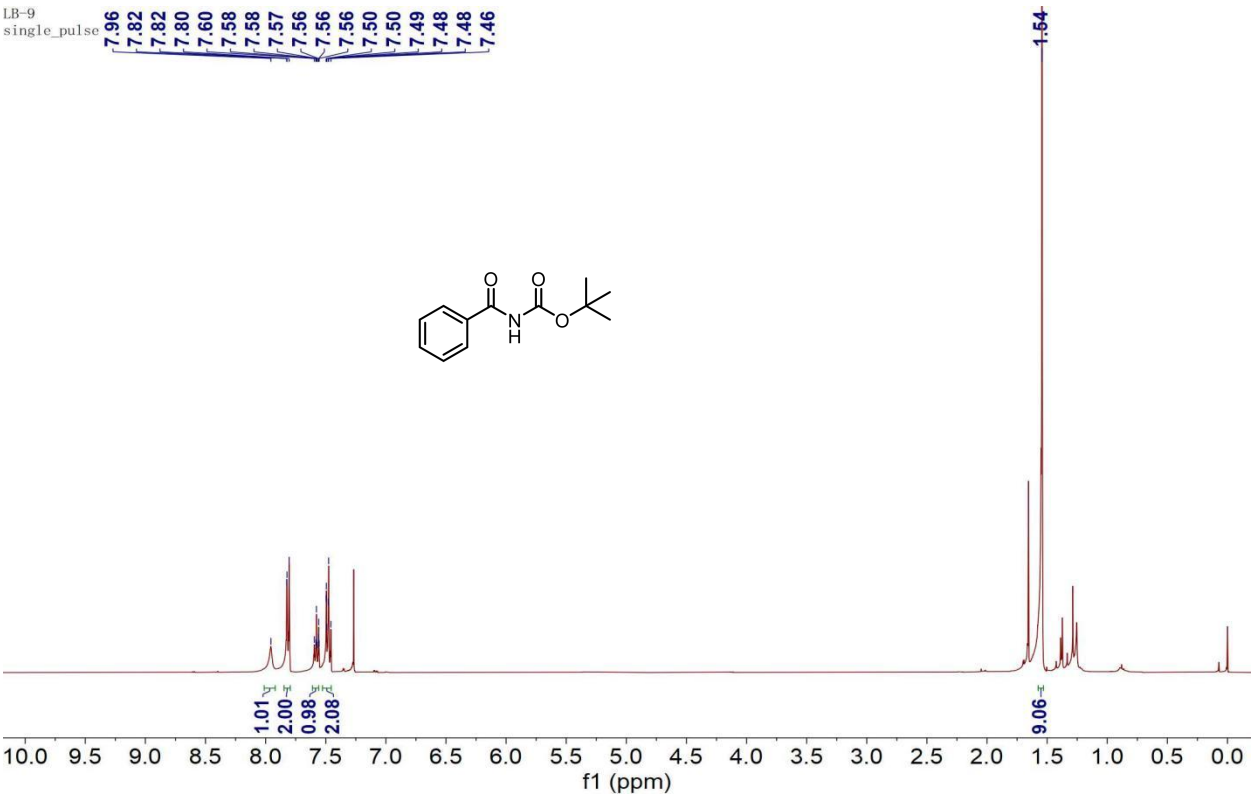

Figure S47. ^{1}H NMR spectrum of **2s** (400 MHz, Chloroform-d).

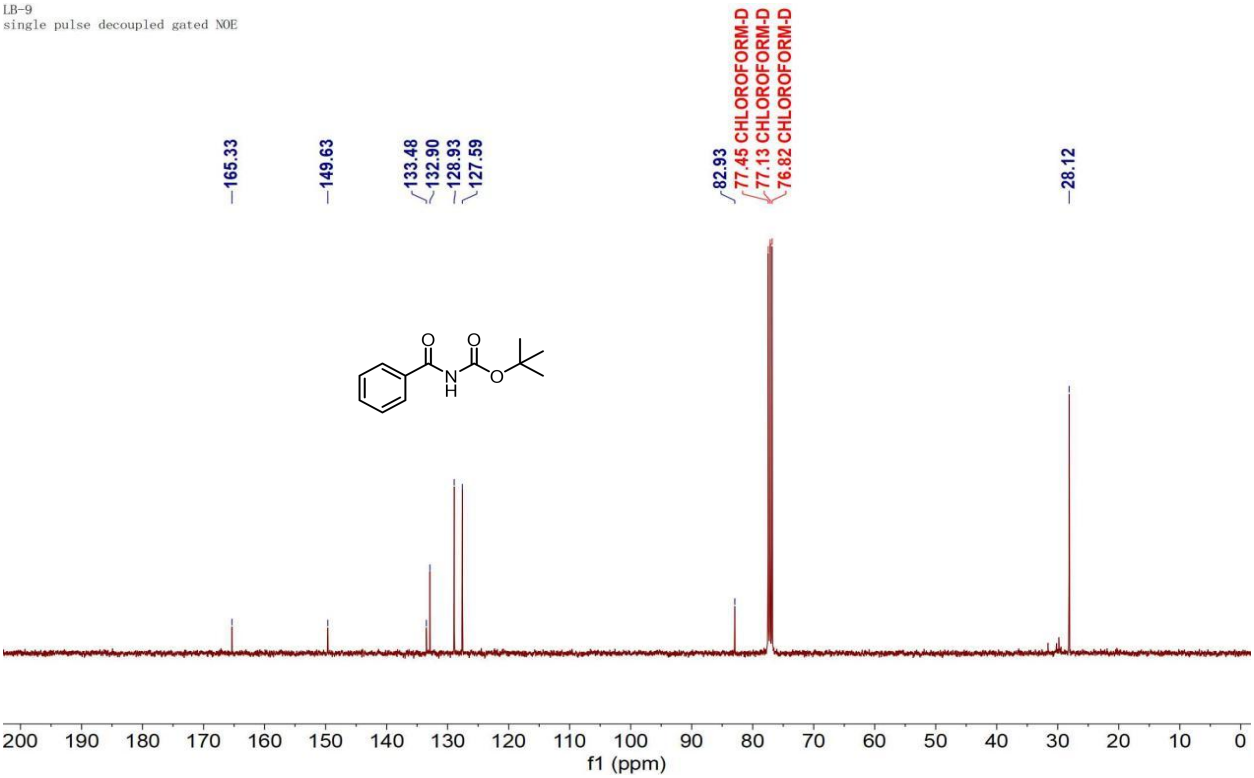

Figure S48. ^{13}C NMR spectrum of **2s** (101 MHz, Chloroform-d).

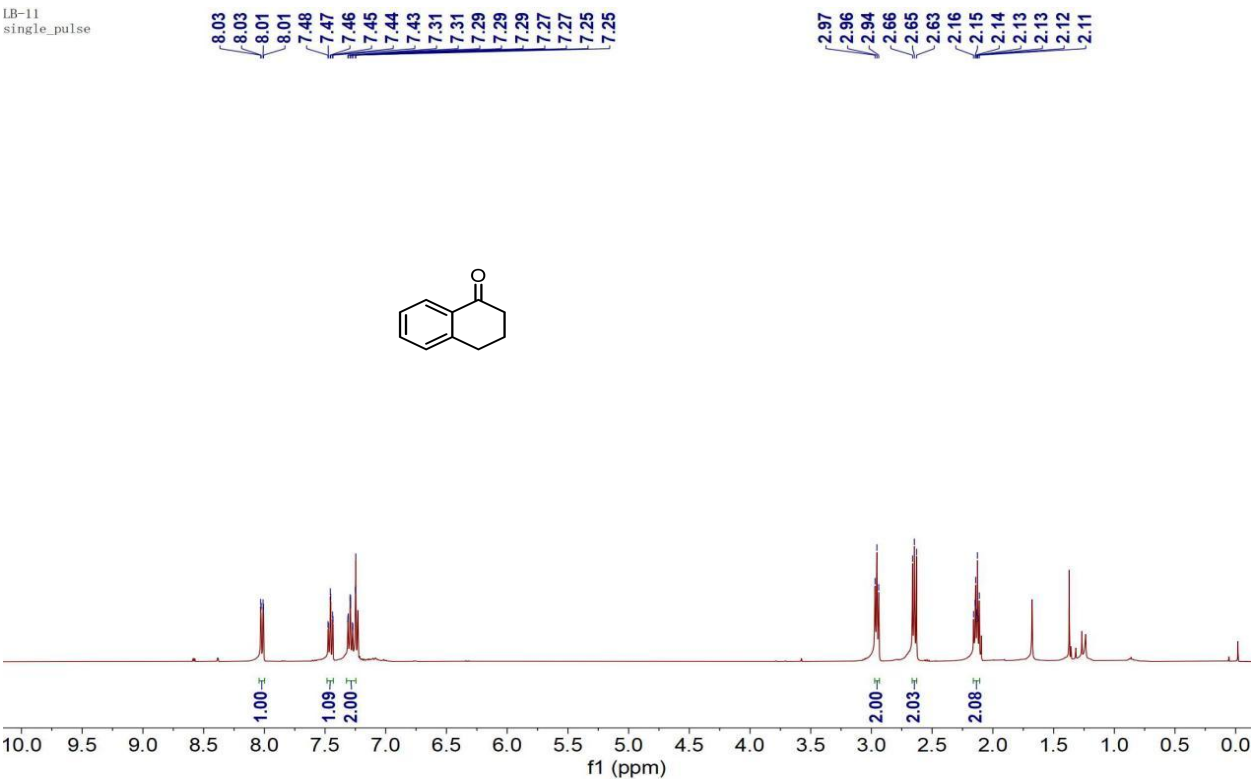

Figure S49. ^{1}H NMR spectrum of **2o** (400 MHz, Chloroform-d).

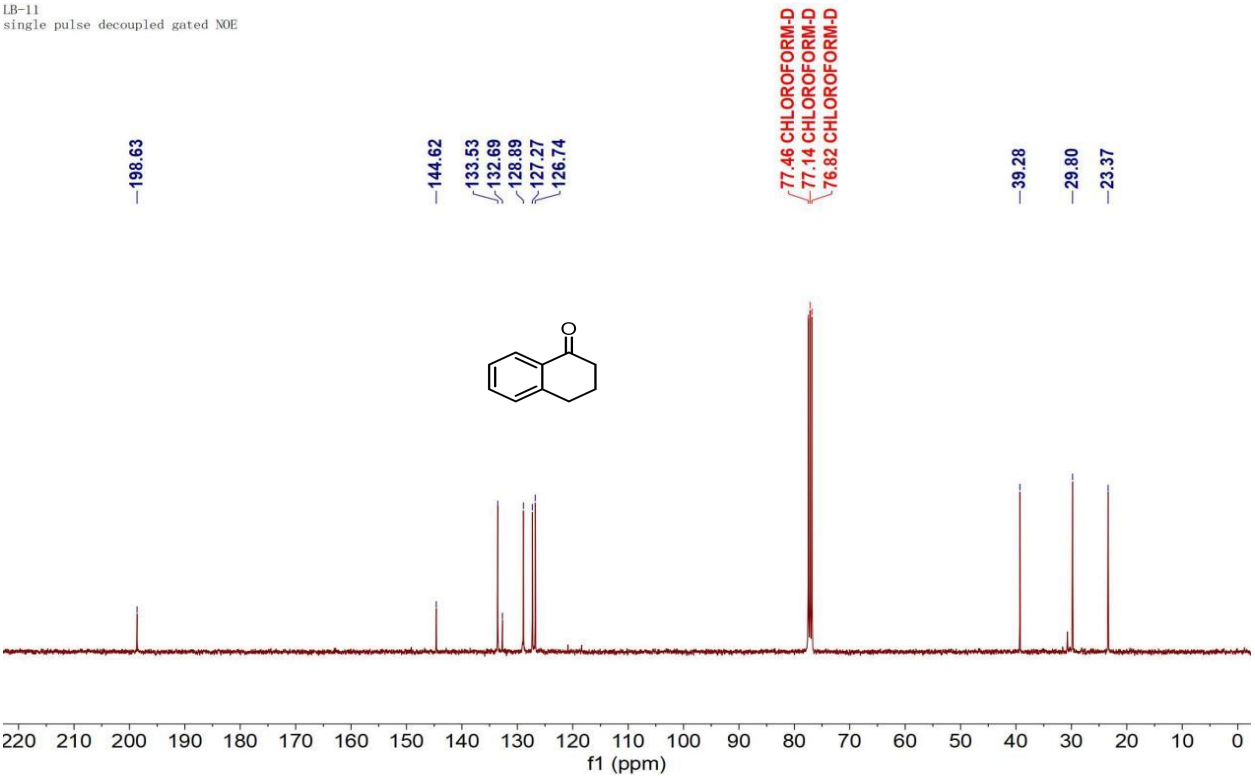

Figure S50. ^{13}C NMR spectrum of **2o** (101 MHz, Chloroform-d).

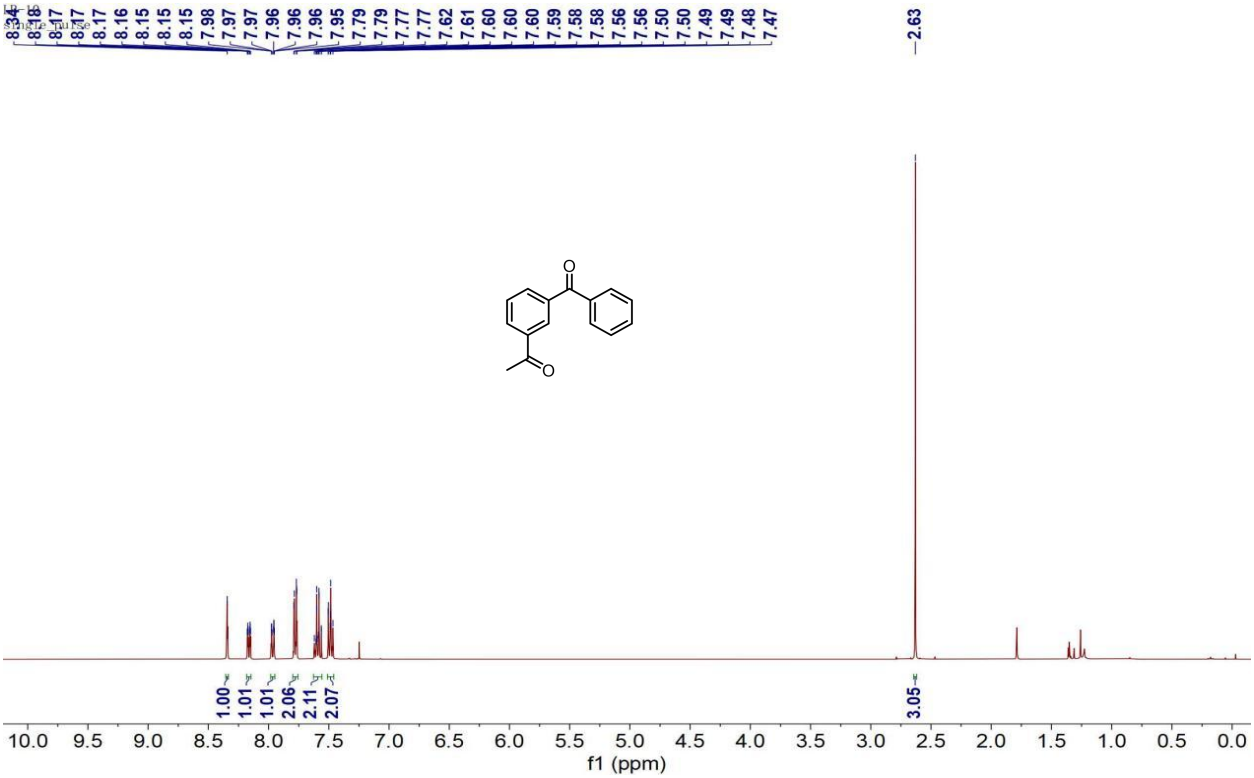

Figure S51. ^{1}H NMR spectrum of **2z** (400 MHz, Chloroform-d).

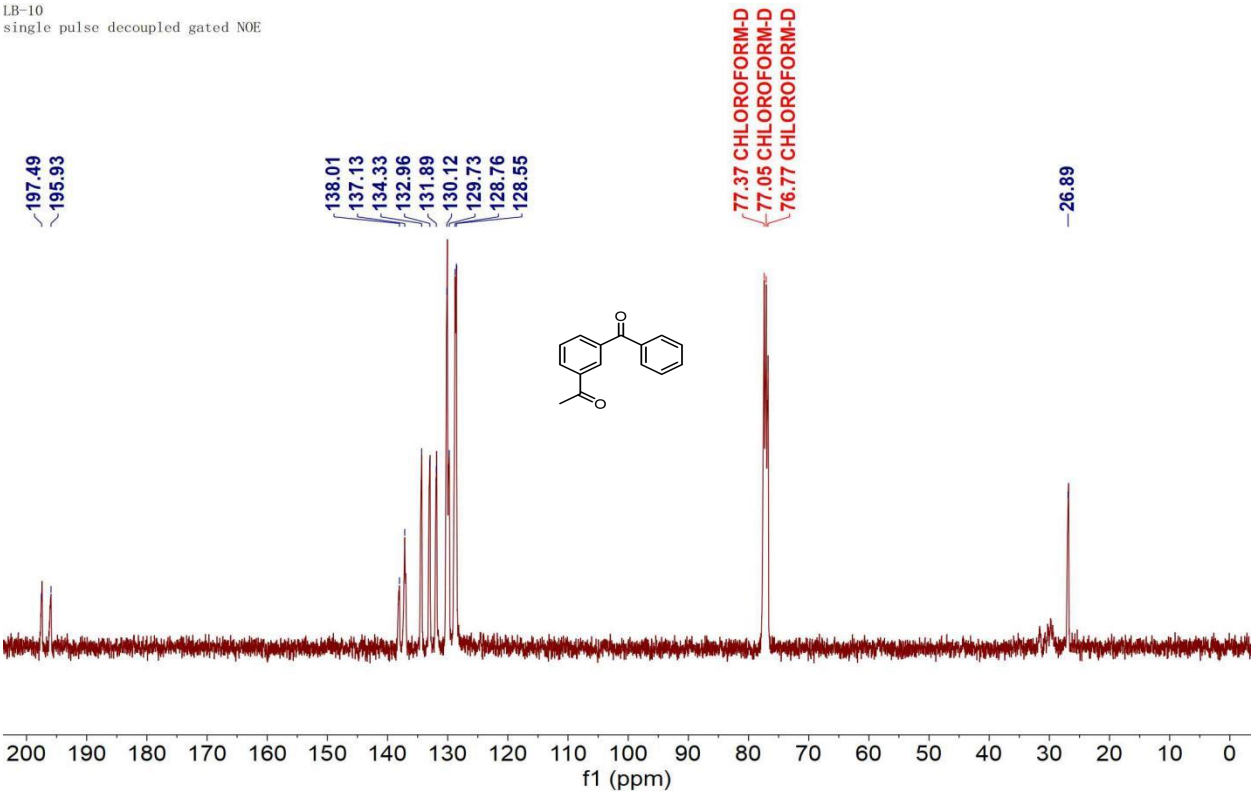

Figure S52. ^{13}C NMR spectrum of **2z** (101 MHz, Chloroform-d).

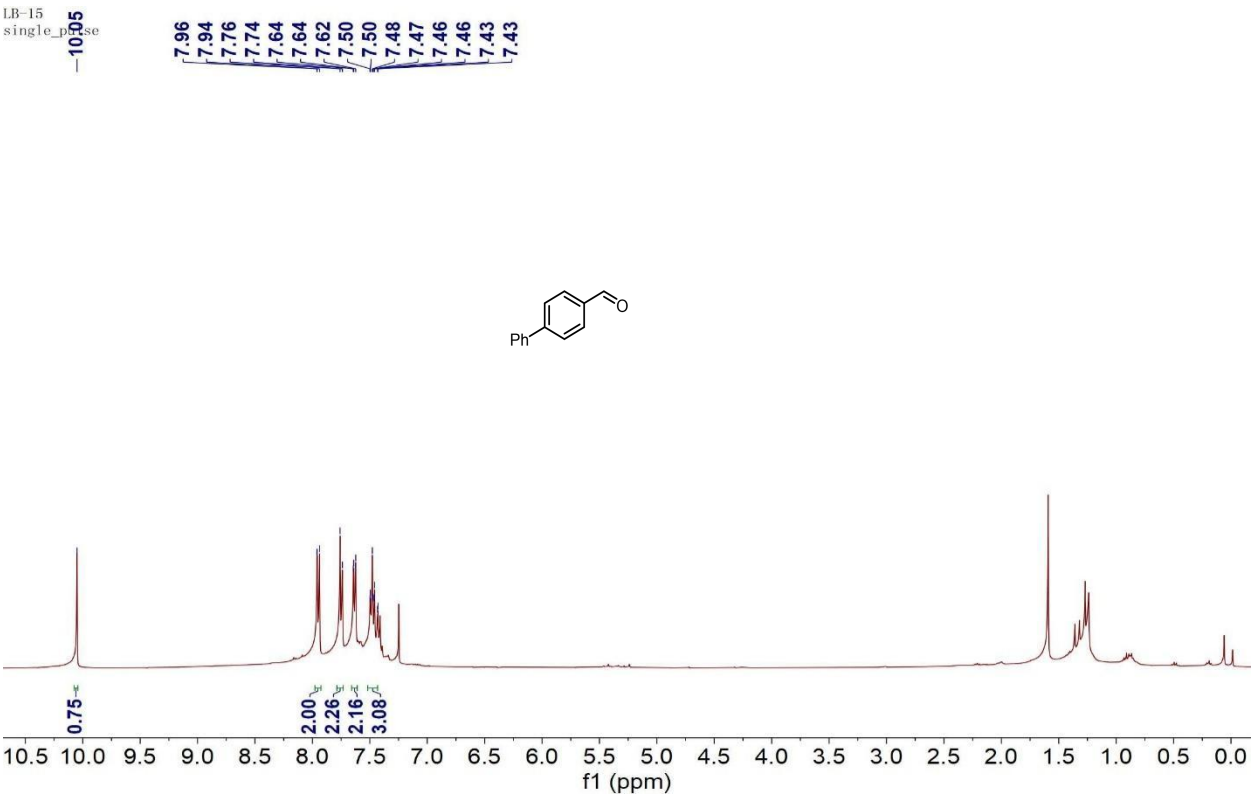

Figure S53. ^{1}H NMR spectrum of **2af** (400 MHz, Chloroform-d).

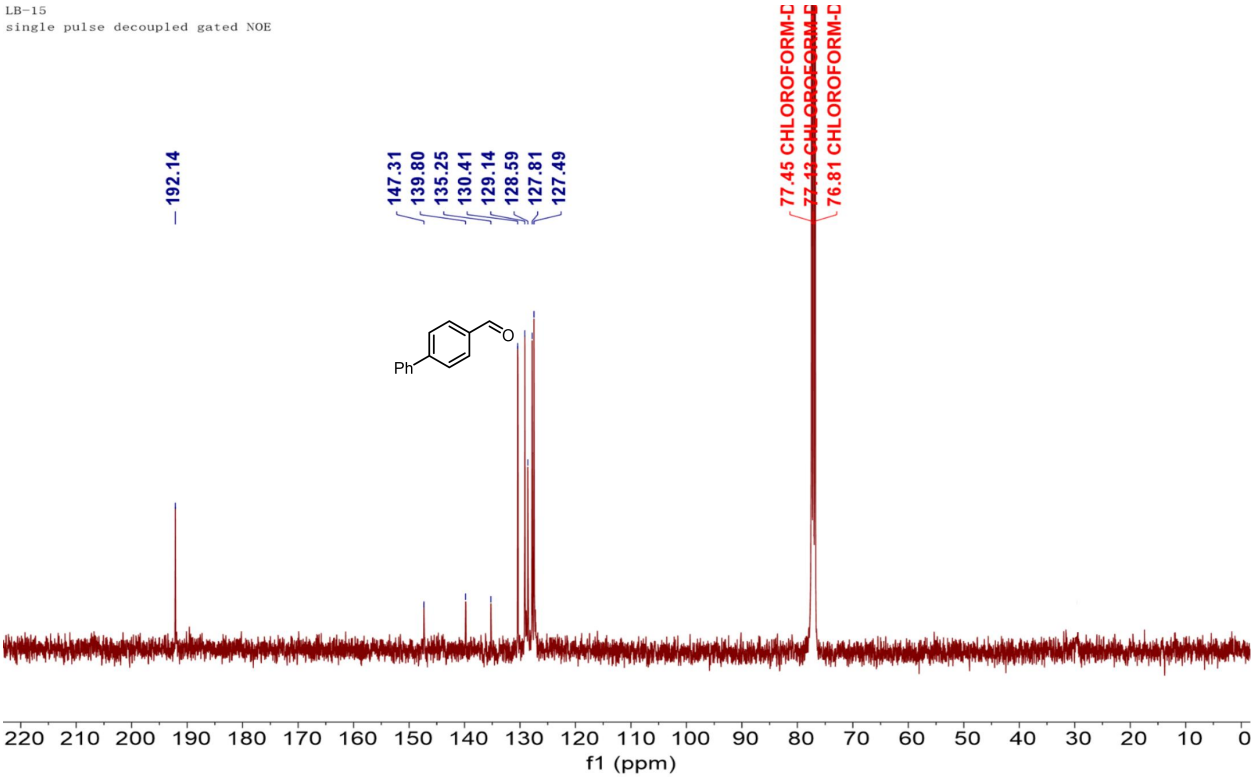

Figure S54. ^{13}C NMR spectrum of **2af** (101 MHz, Chloroform-d).

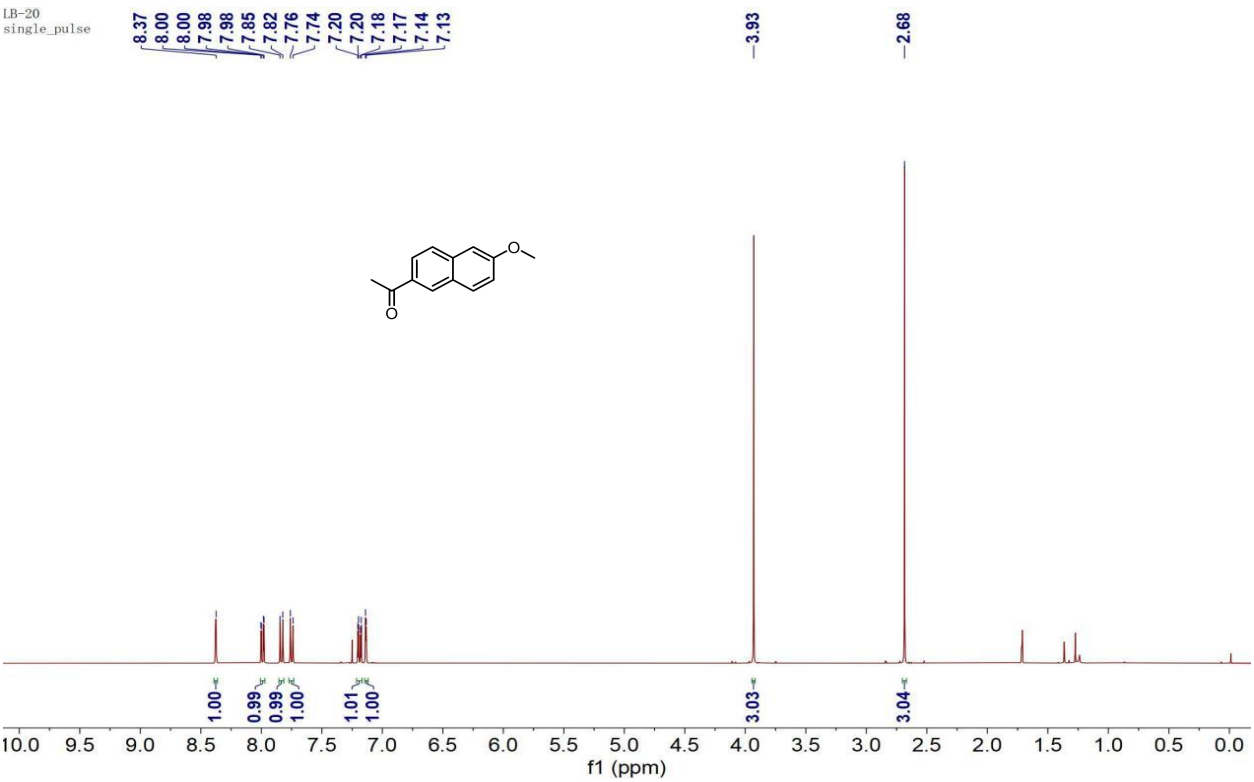

Figure S55. ^{1}H NMR spectrum of **2ab** (400 MHz, Chloroform-d).

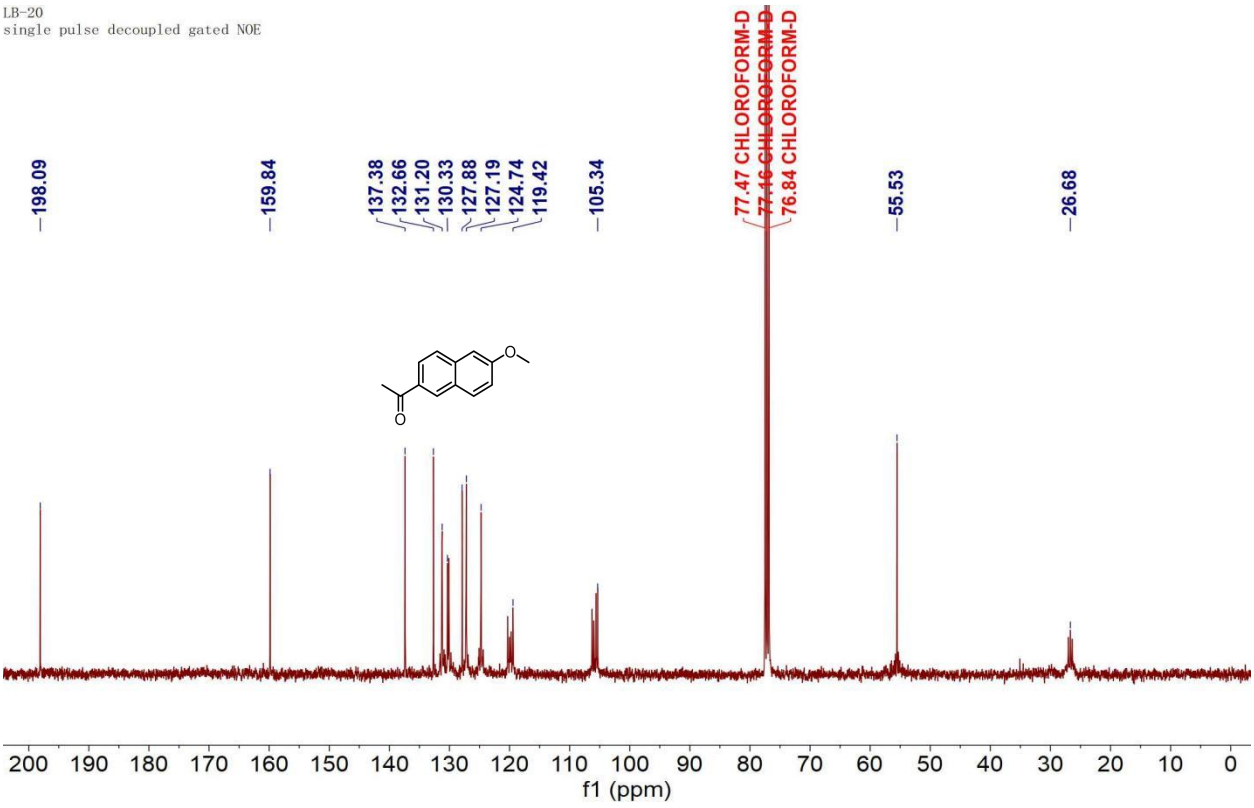

Figure S56. ^{13}C NMR spectrum of **2ab** (101 MHz, Chloroform-d).

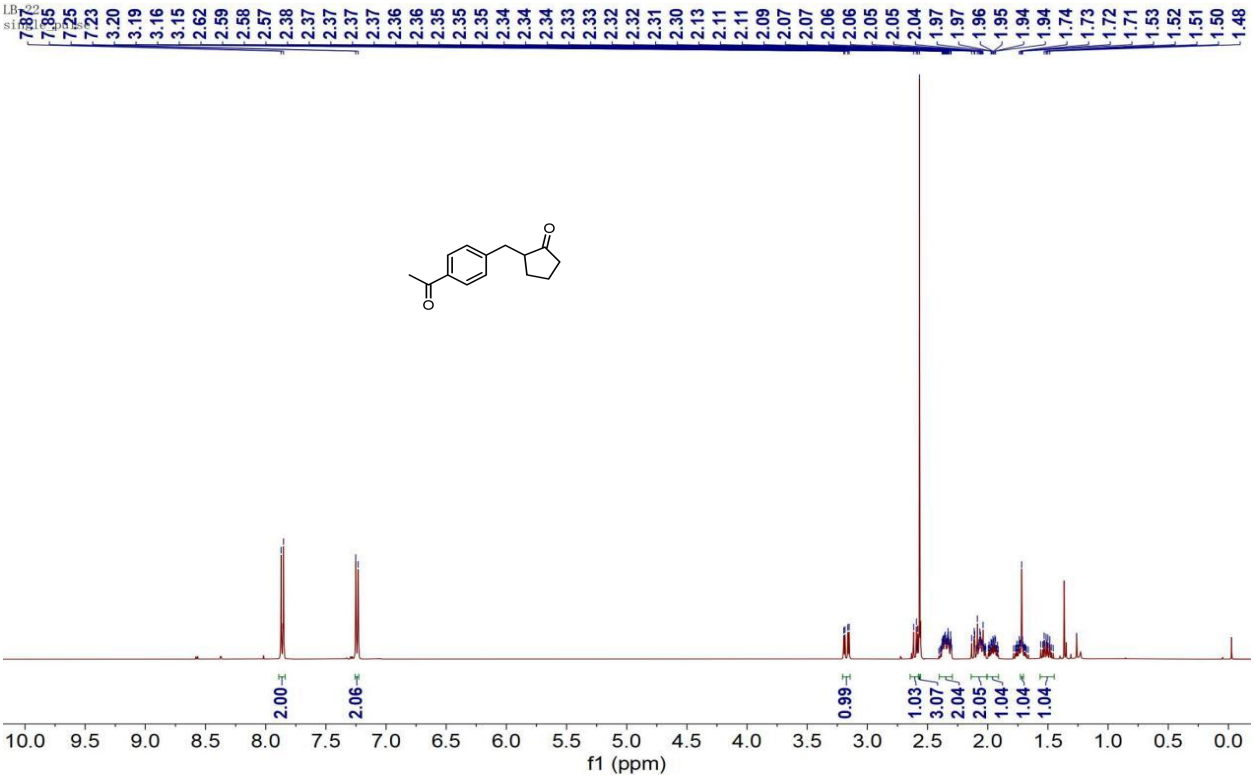

Figure S57. ^{1}H NMR spectrum of **2ac** (400 MHz, Chloroform-d).

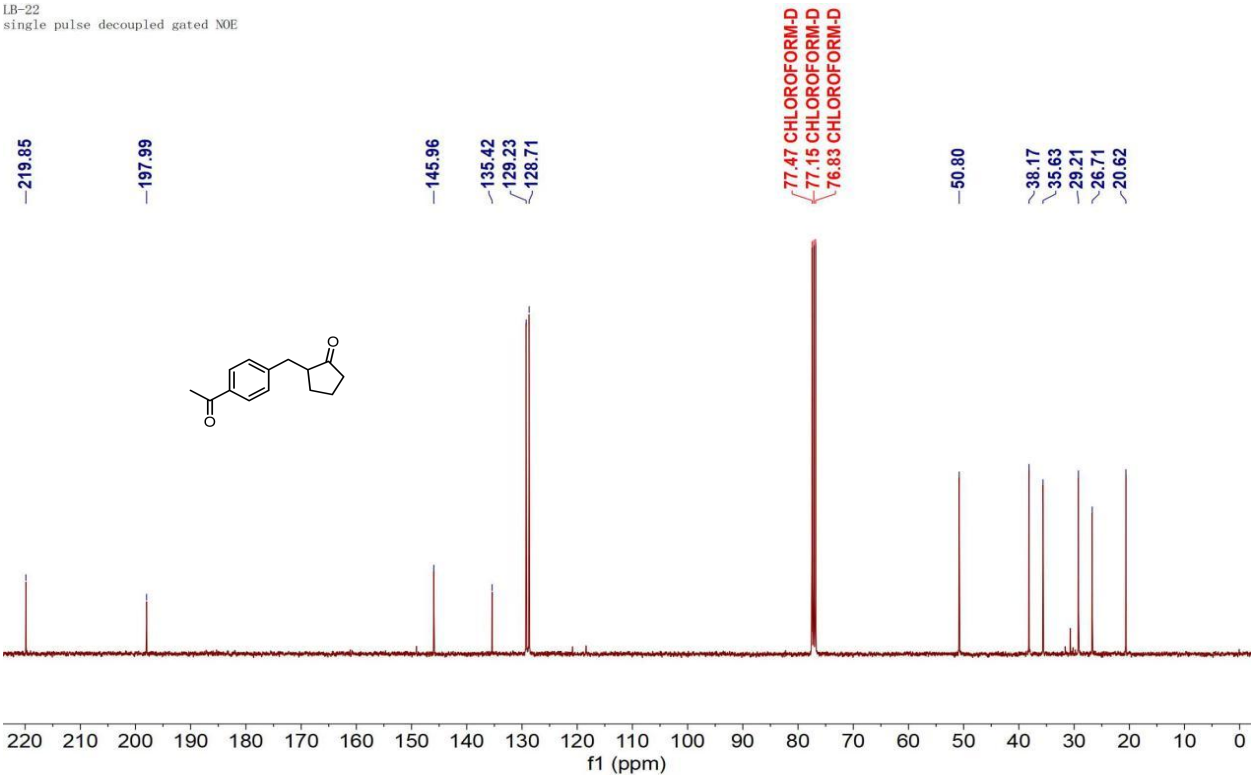

Figure S58. ^{13}C NMR spectrum of **2ac** (101 MHz, Chloroform-d).

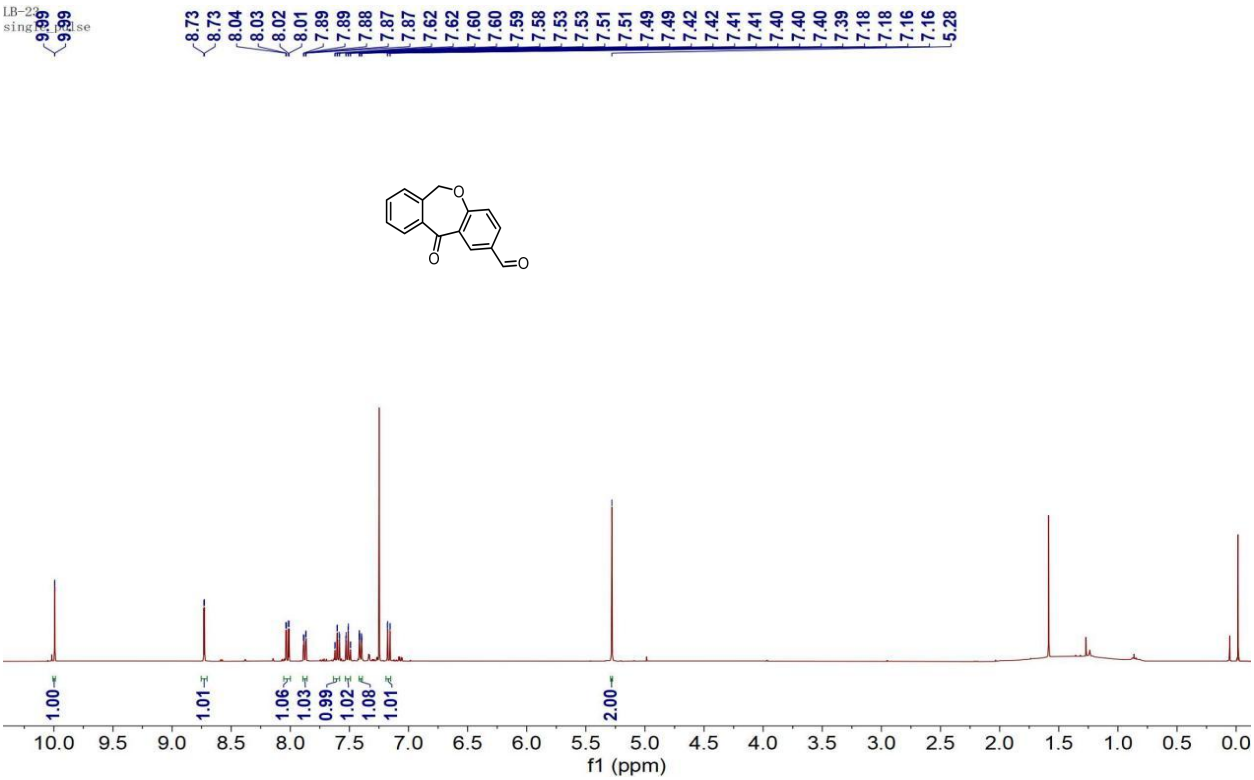

Figure S59. ^{1}H NMR spectrum of **2ah** (400 MHz, Chloroform-d).

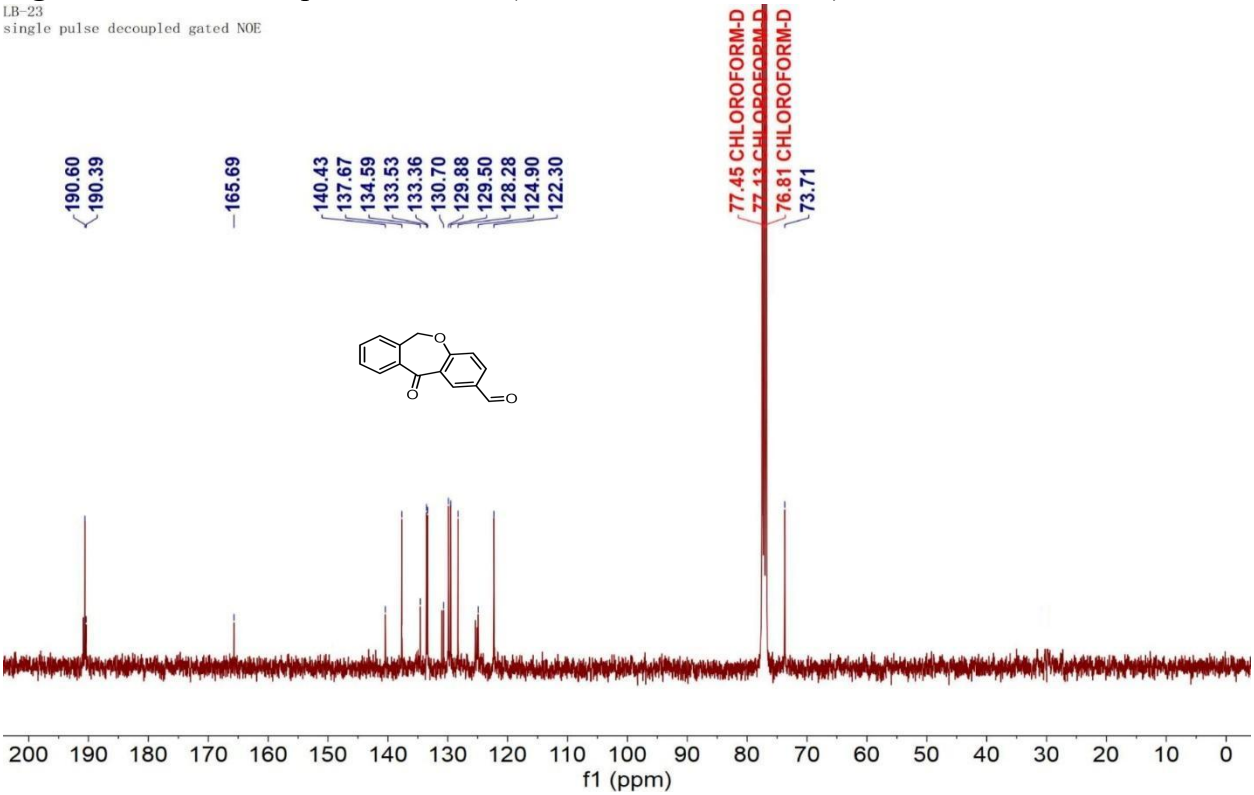

Figure S60. ^{13}C NMR spectrum of **2ah** (101 MHz, Chloroform-d).

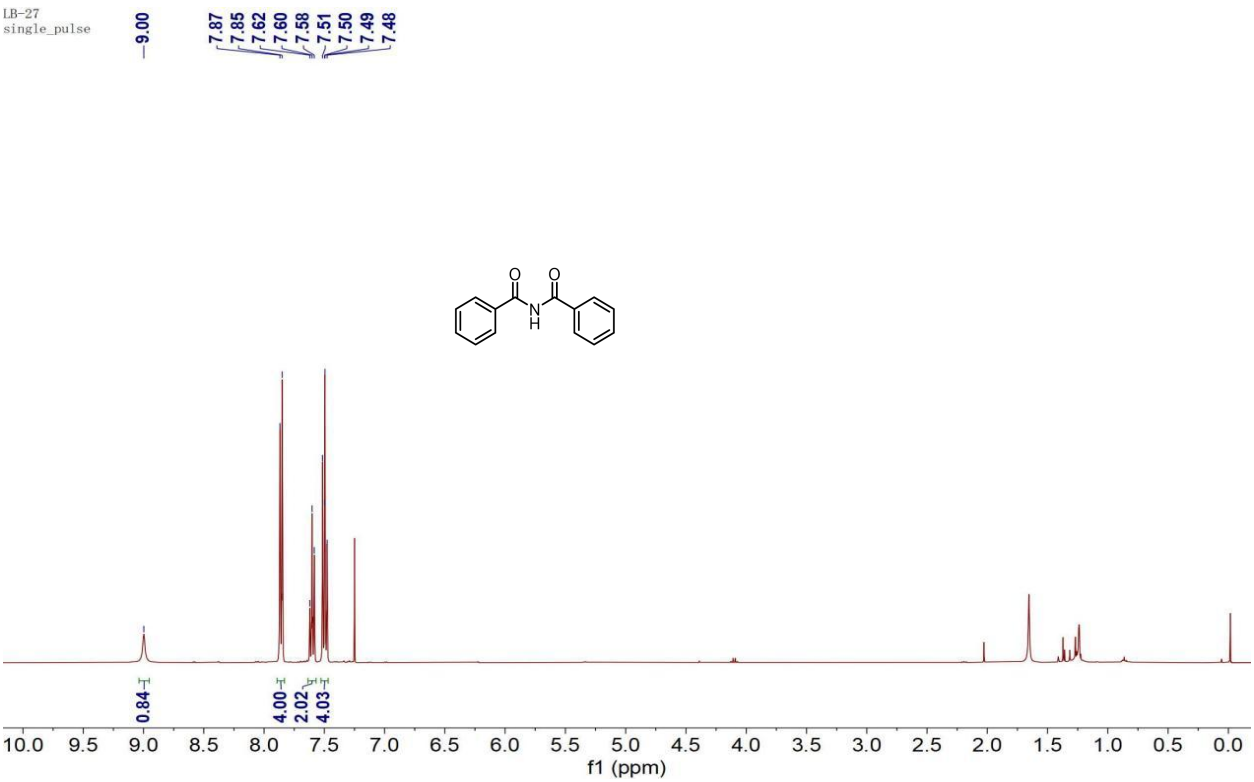

Figure S61. ^{1}H NMR spectrum of **2r** (400 MHz, Chloroform-d).

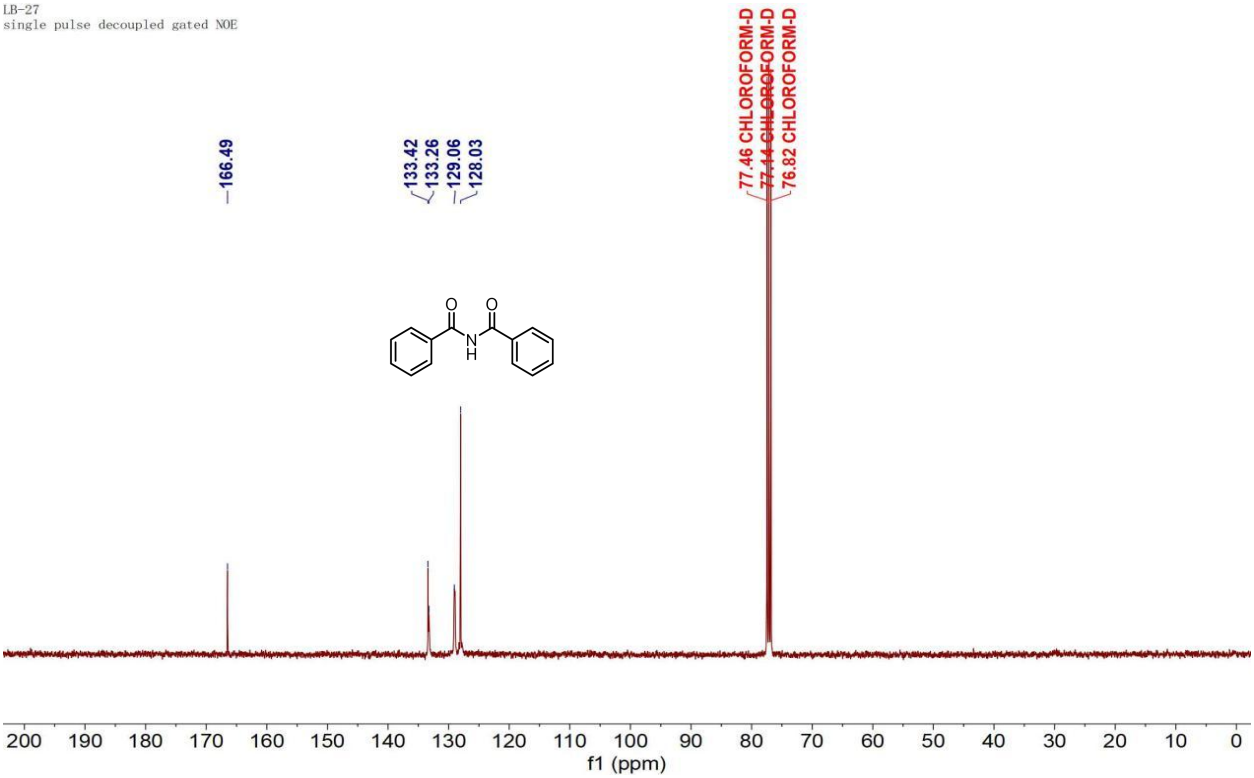

Figure S62. ^{13}C NMR spectrum of **2r** (101 MHz, Chloroform-d).

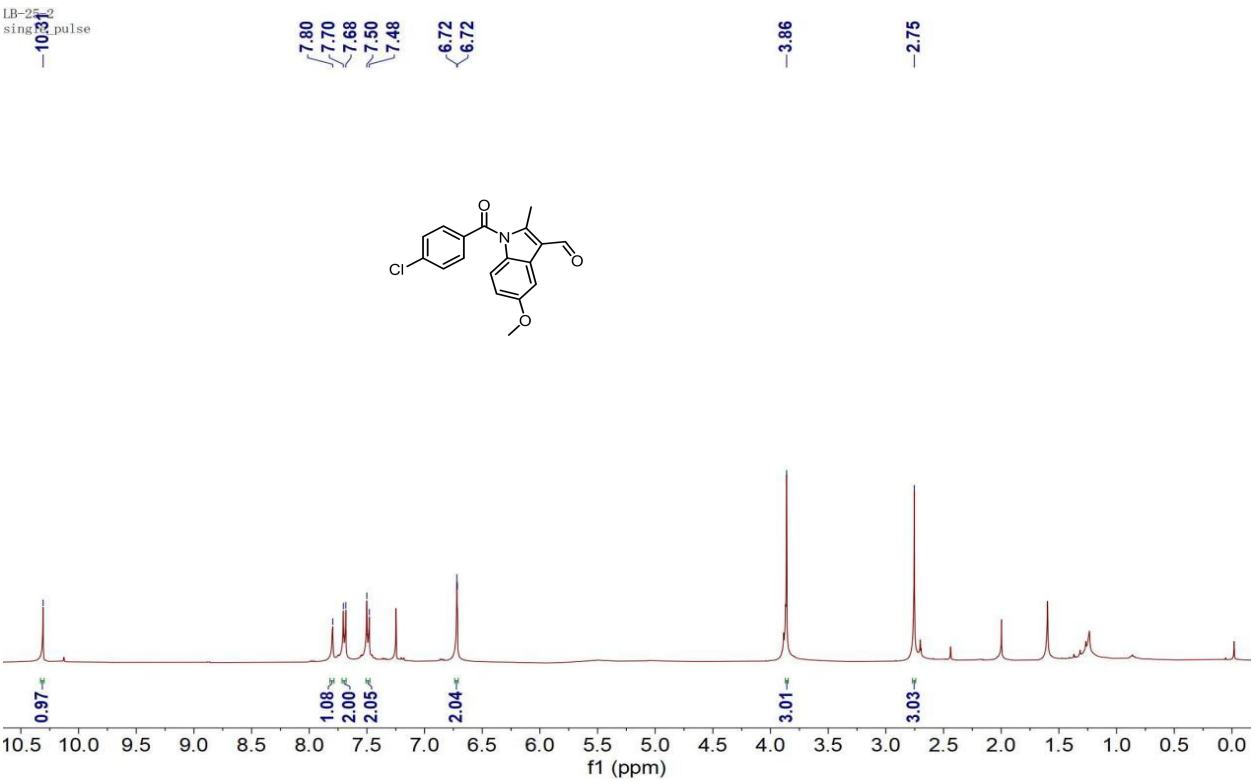

Figure S63. ^{1}H NMR spectrum of **2ai** (400 MHz, Chloroform-d).

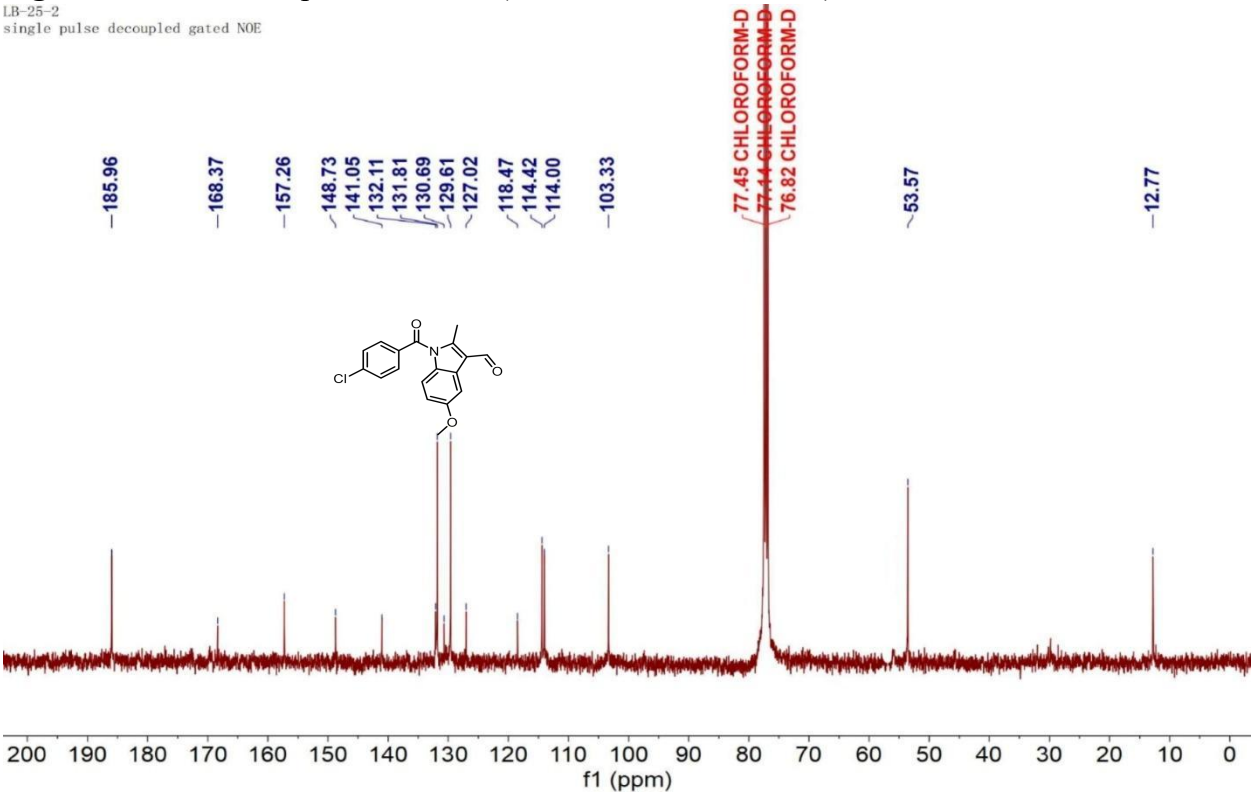

Figure S64. ^{13}C NMR spectrum of **2ai** (101 MHz, Chloroform-d).

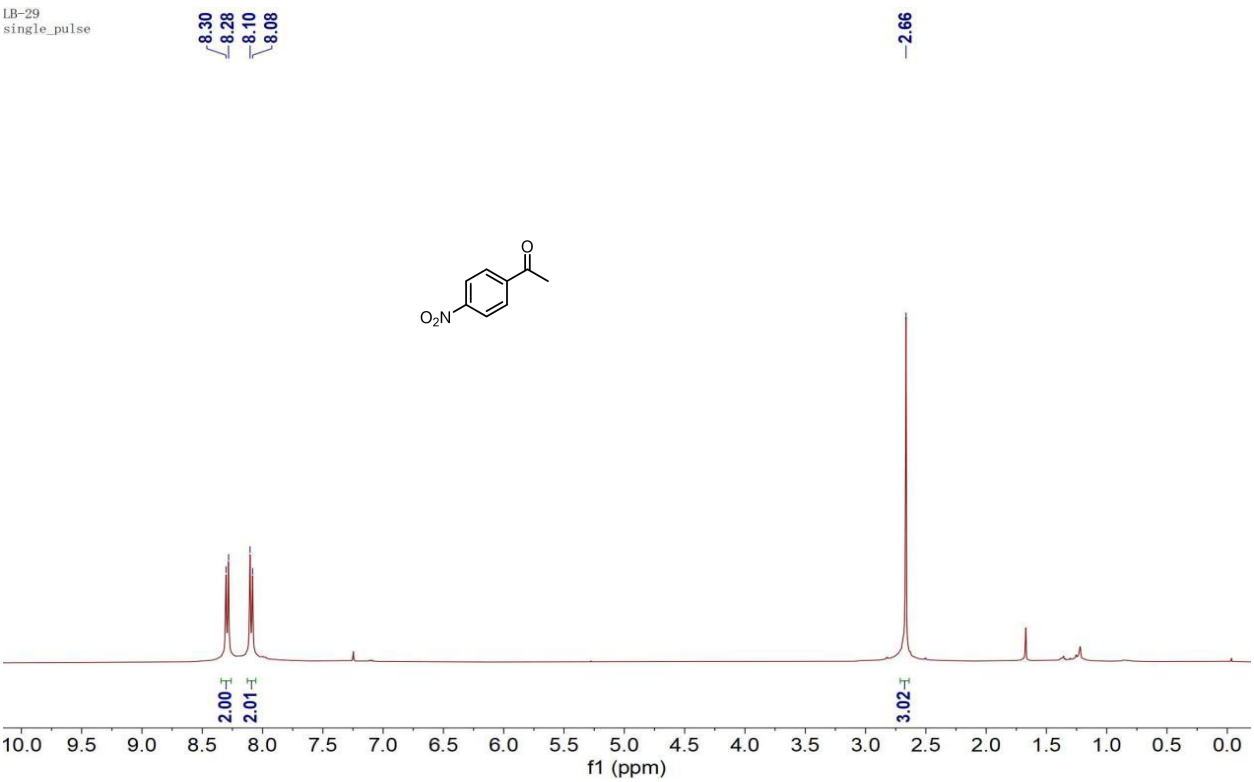

Figure S65. ^{1}H NMR spectrum of **2m** (400 MHz, Chloroform-d).

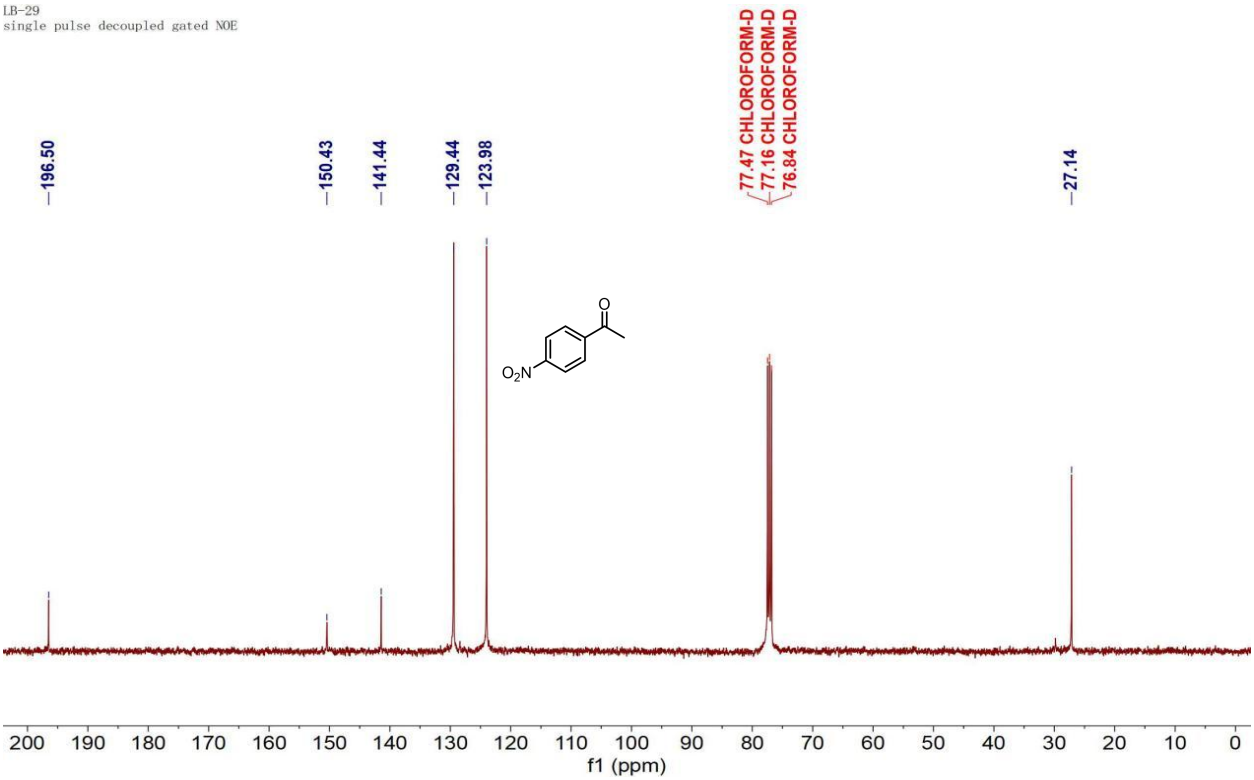

Figure S66. ^{13}C NMR spectrum of **2m** (101 MHz, Chloroform-d).

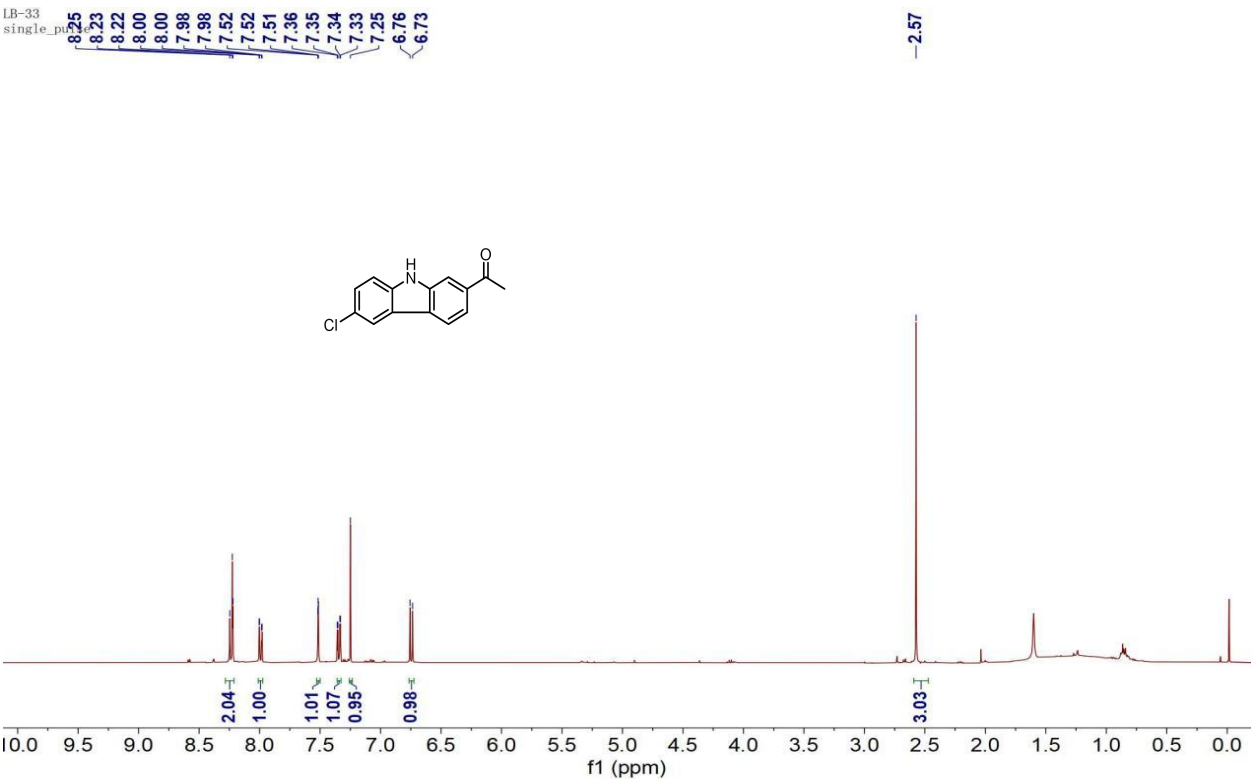

Figure S67. ^{1}H NMR spectrum of **2ae** (400 MHz, Chloroform-d).

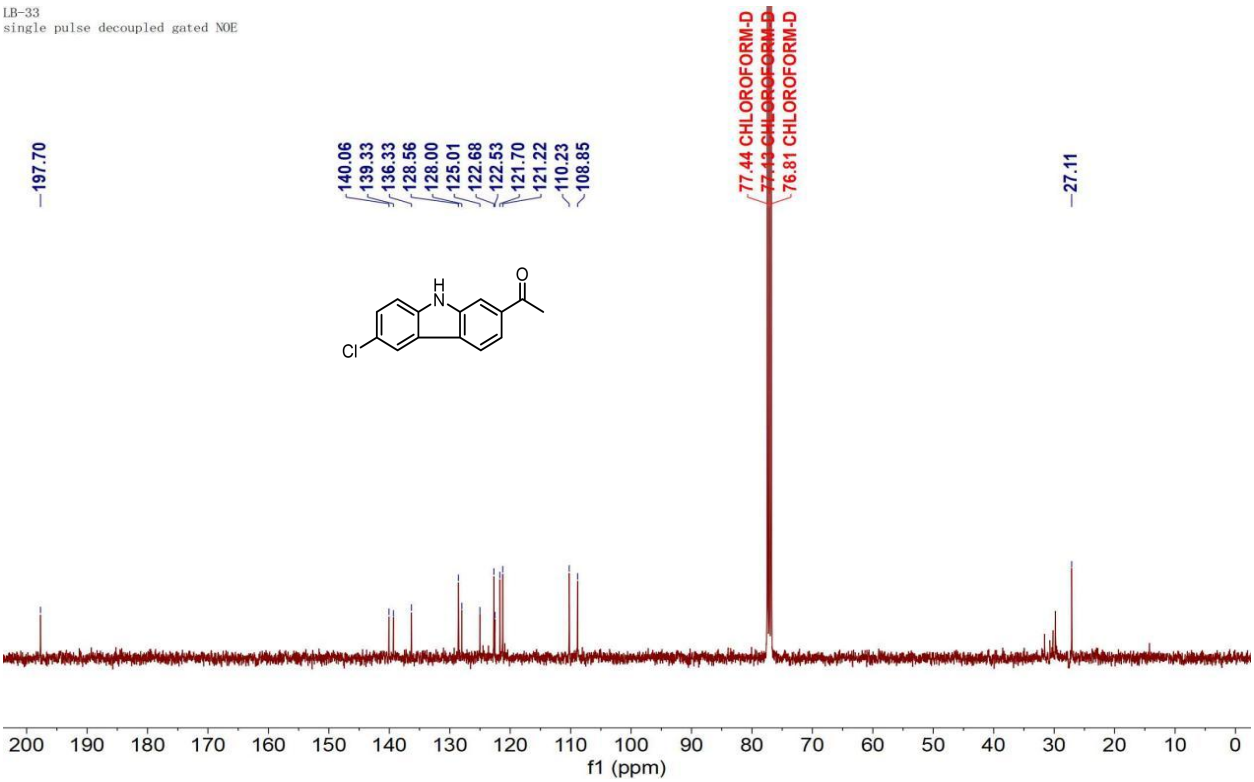

Figure S68. ^{13}C NMR spectrum of **2ae** (101 MHz, Chloroform-d).

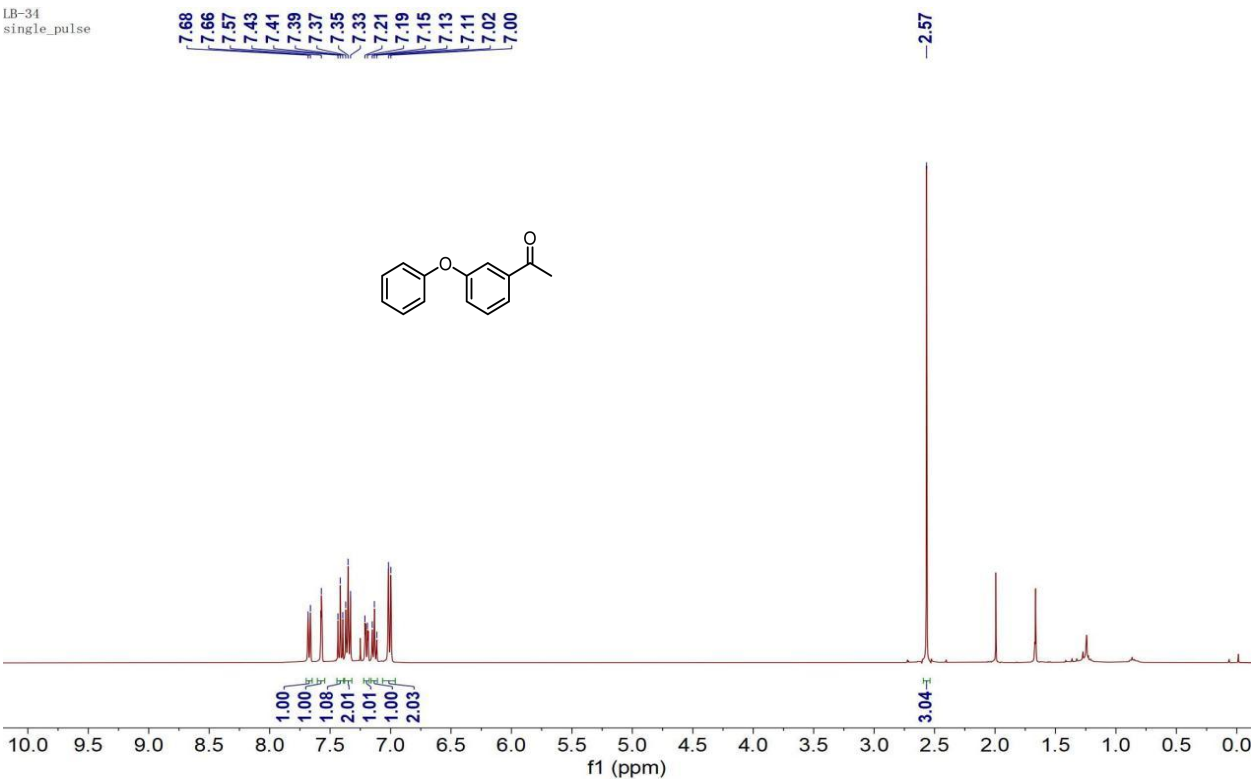

Figure S69. ^{1}H NMR spectrum of **2ad** (400 MHz, Chloroform-d).

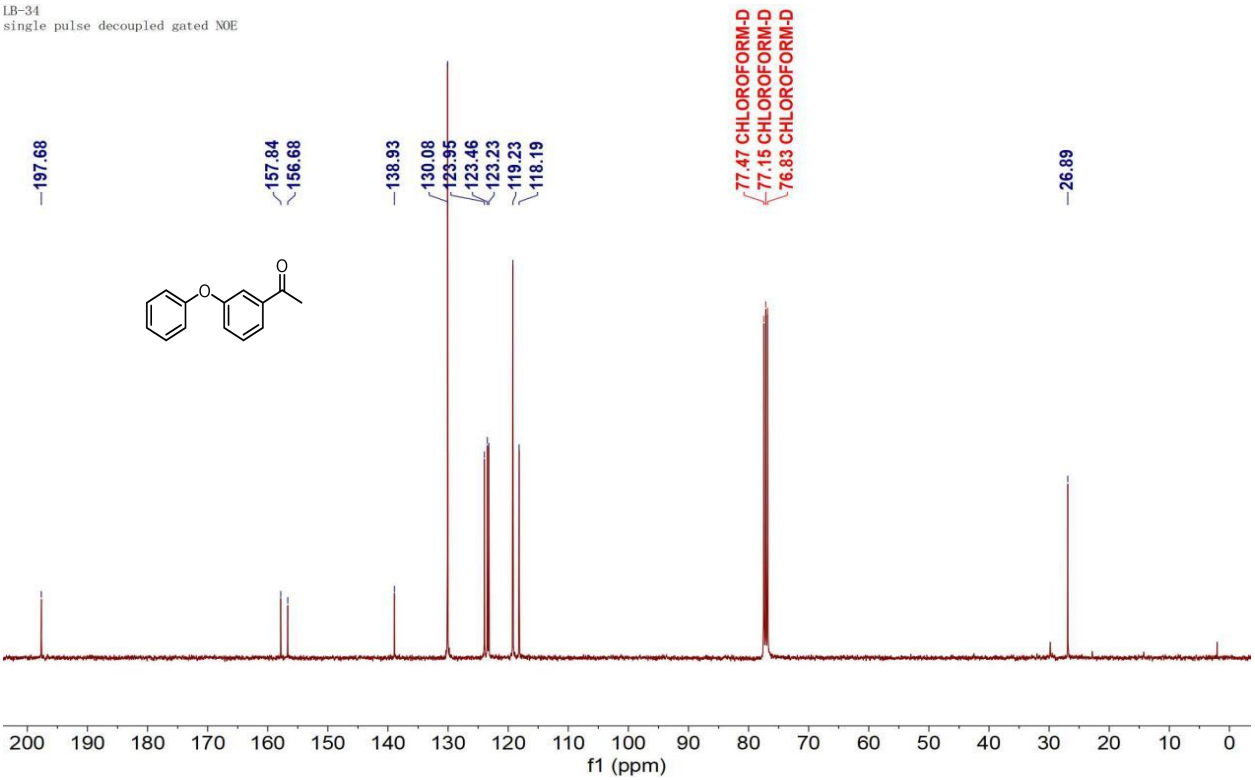

Figure S70. ^{13}C NMR spectrum of **2ad** (101 MHz, Chloroform-d).

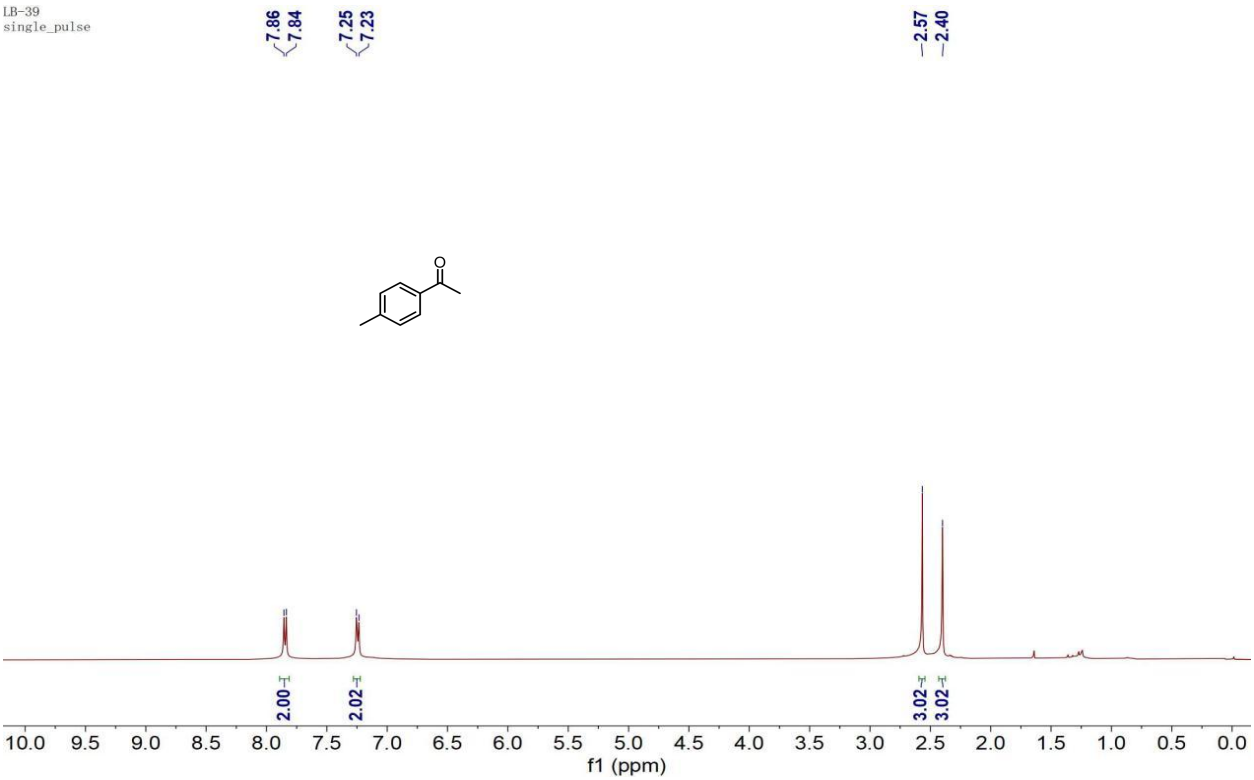

Figure S71. ^{1}H NMR spectrum of **2l** (400 MHz, Chloroform-d).

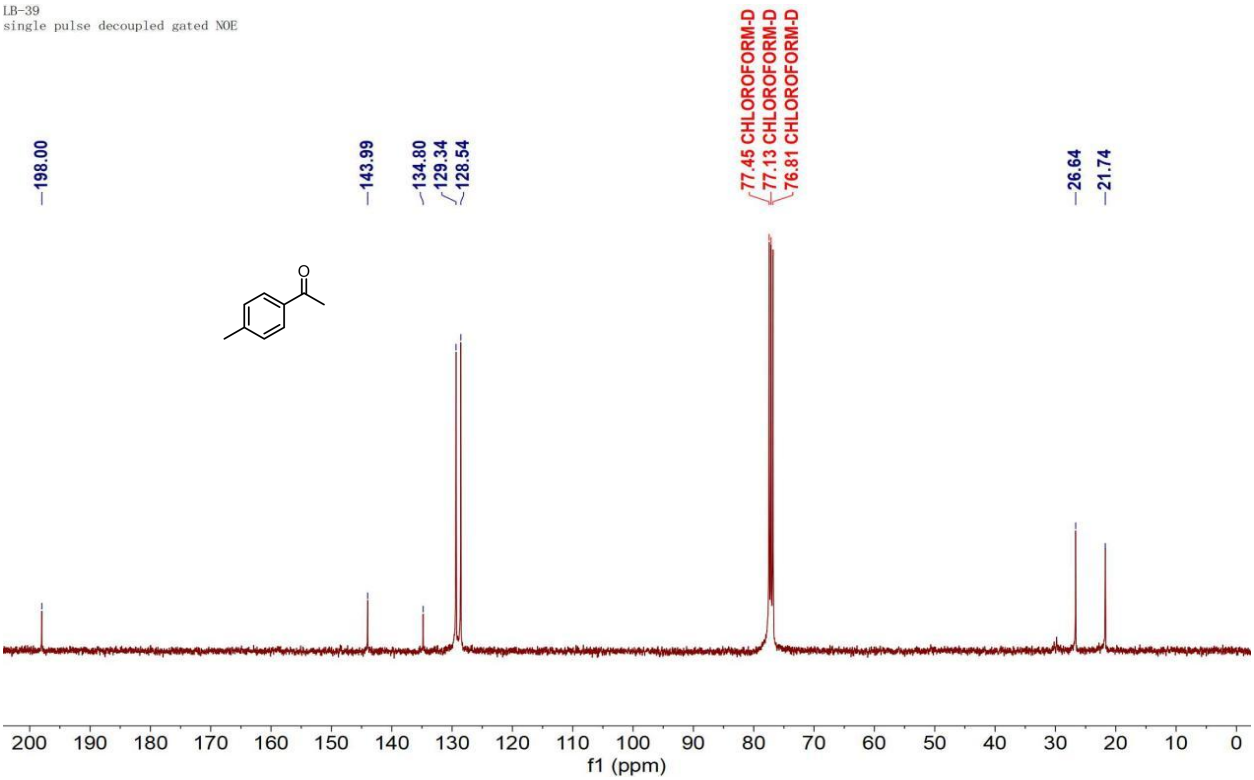

Figure S72. ^{13}C NMR spectrum of **2l** (101 MHz, Chloroform-d).

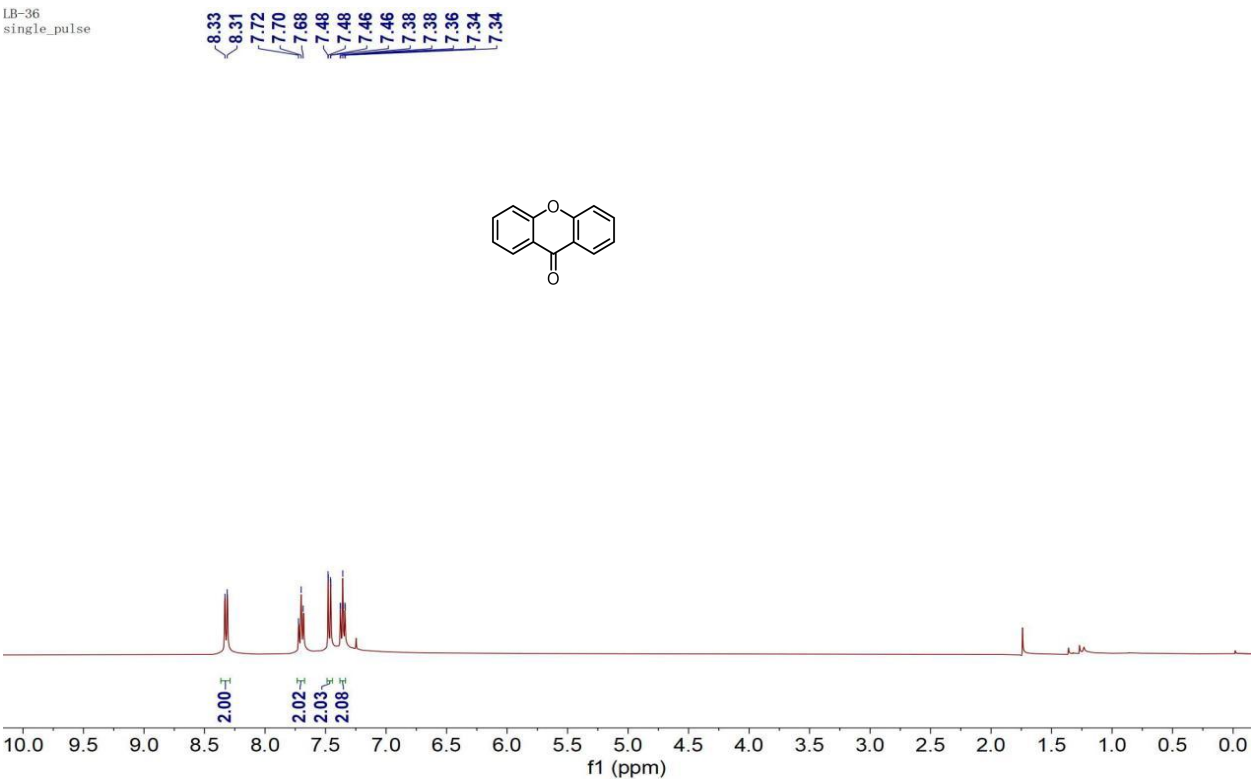

Figure S73. ^{1}H NMR spectrum of **2q** (400 MHz, Chloroform-d).

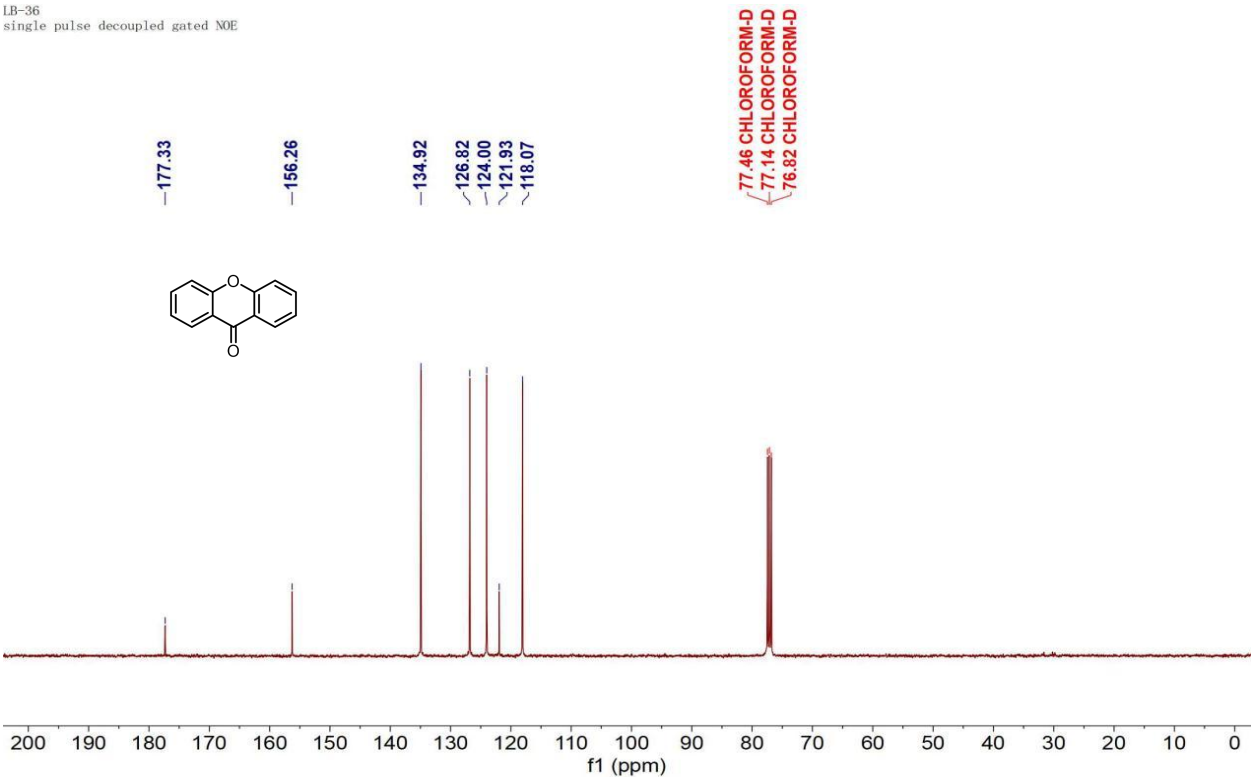

Figure S74. ^{13}C NMR spectrum of **2q** (101 MHz, Chloroform-d).

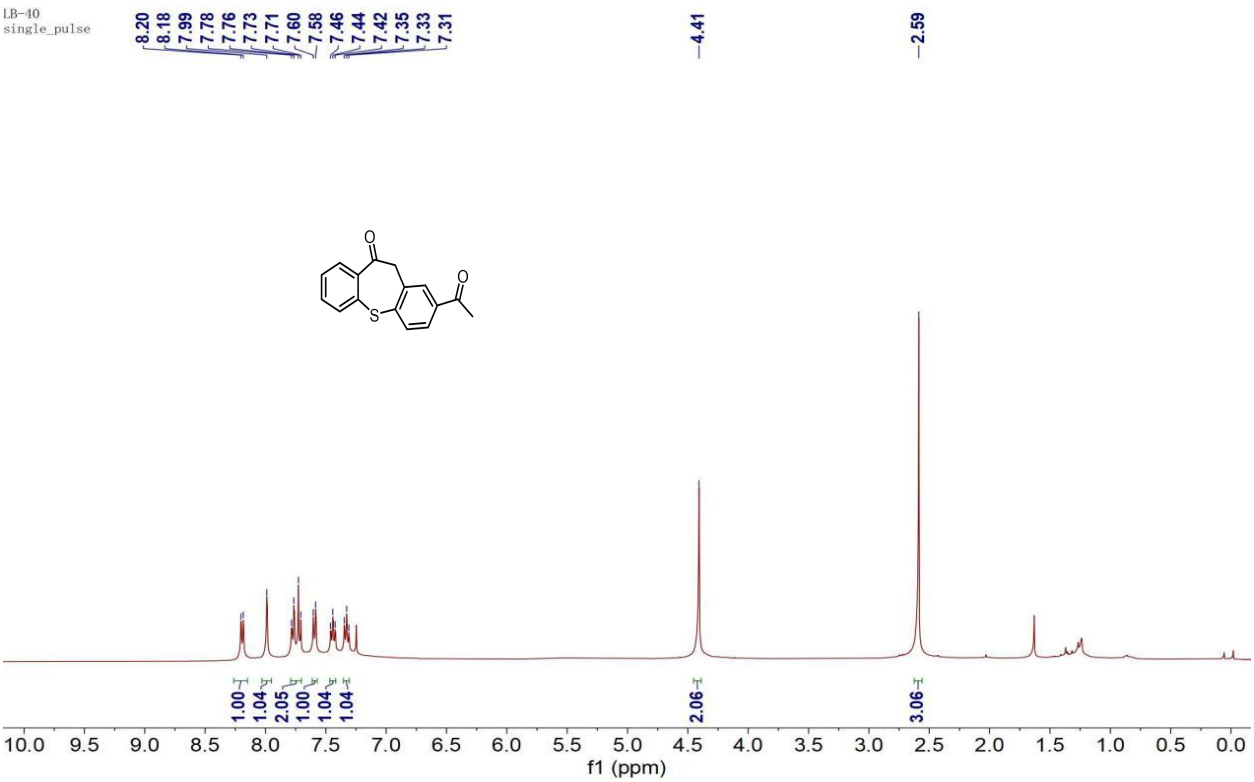

Figure S75. ^{1}H NMR spectrum of **2aa** (400 MHz, Chloroform-d).

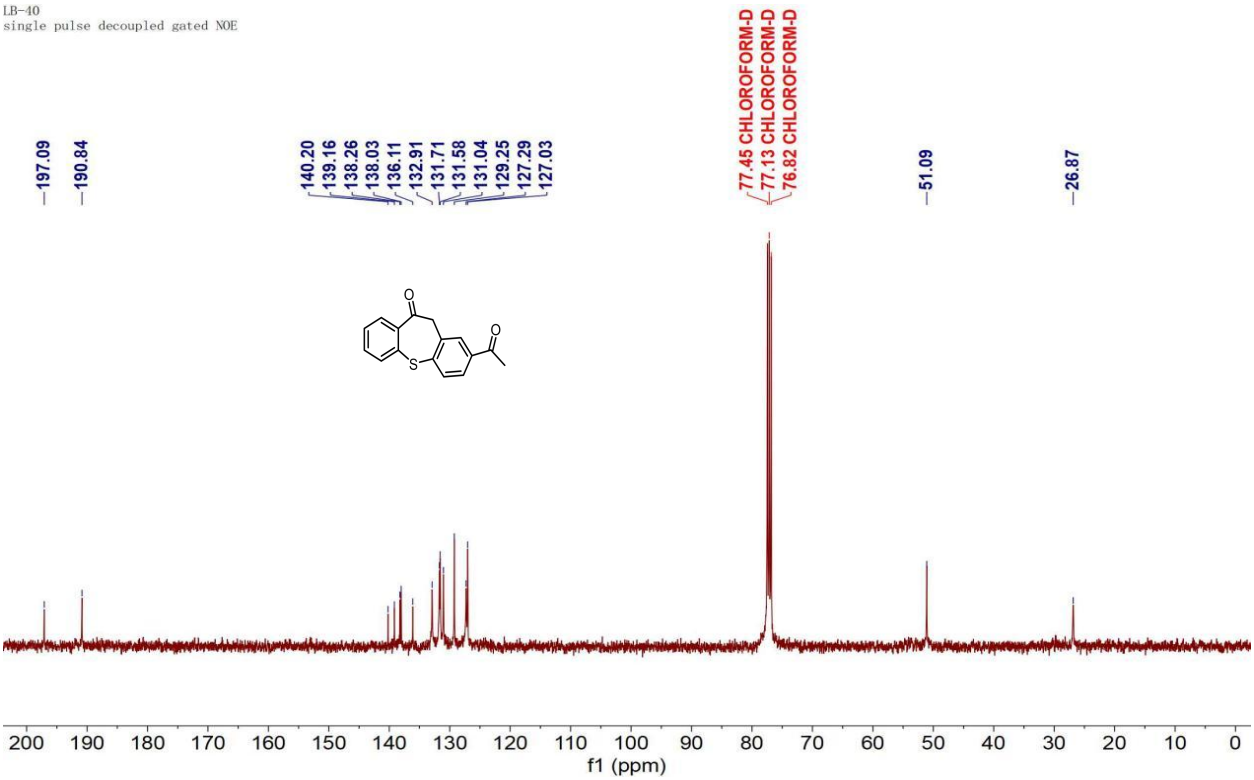

Figure S76. ^{13}C NMR spectrum of **2aa** (101 MHz, Chloroform-d).

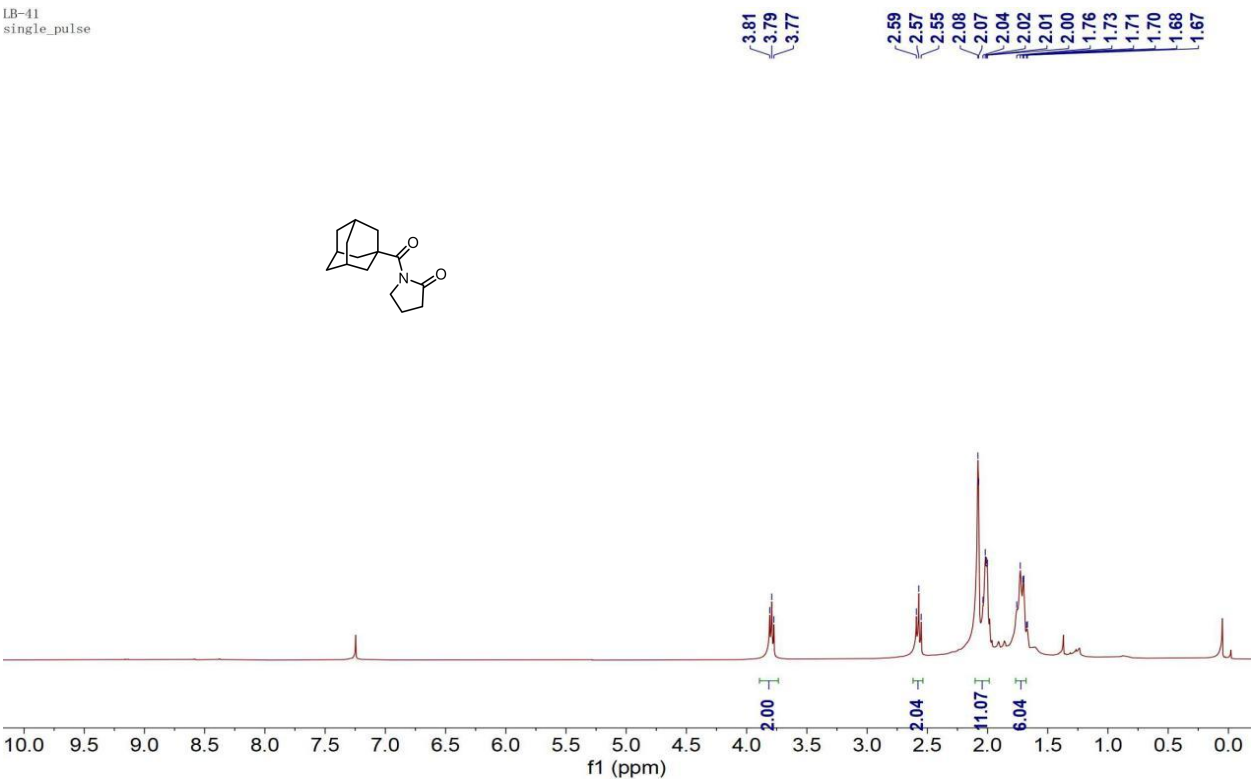

Figure S77. ^{1}H NMR spectrum of **2v** (400 MHz, Chloroform-d).

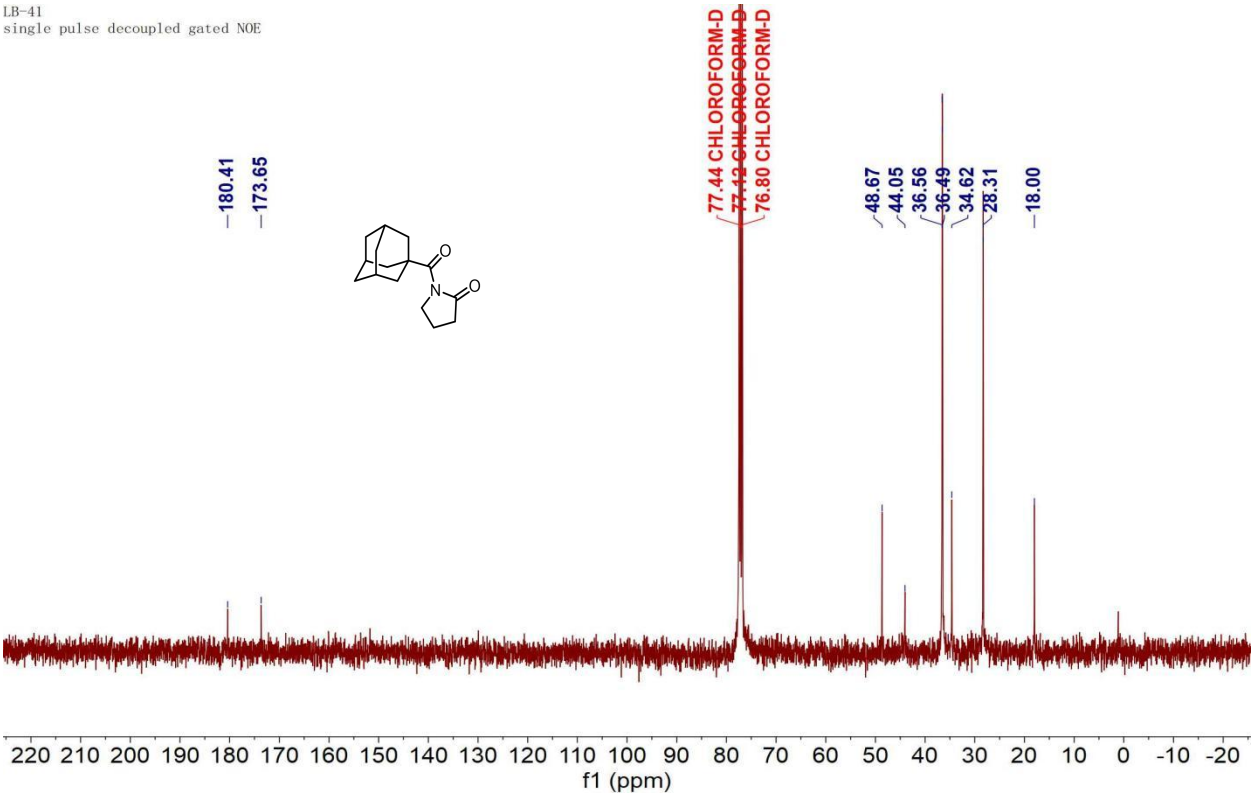

Figure S78. ^{13}C NMR spectrum of **2v** (101 MHz, Chloroform-d).

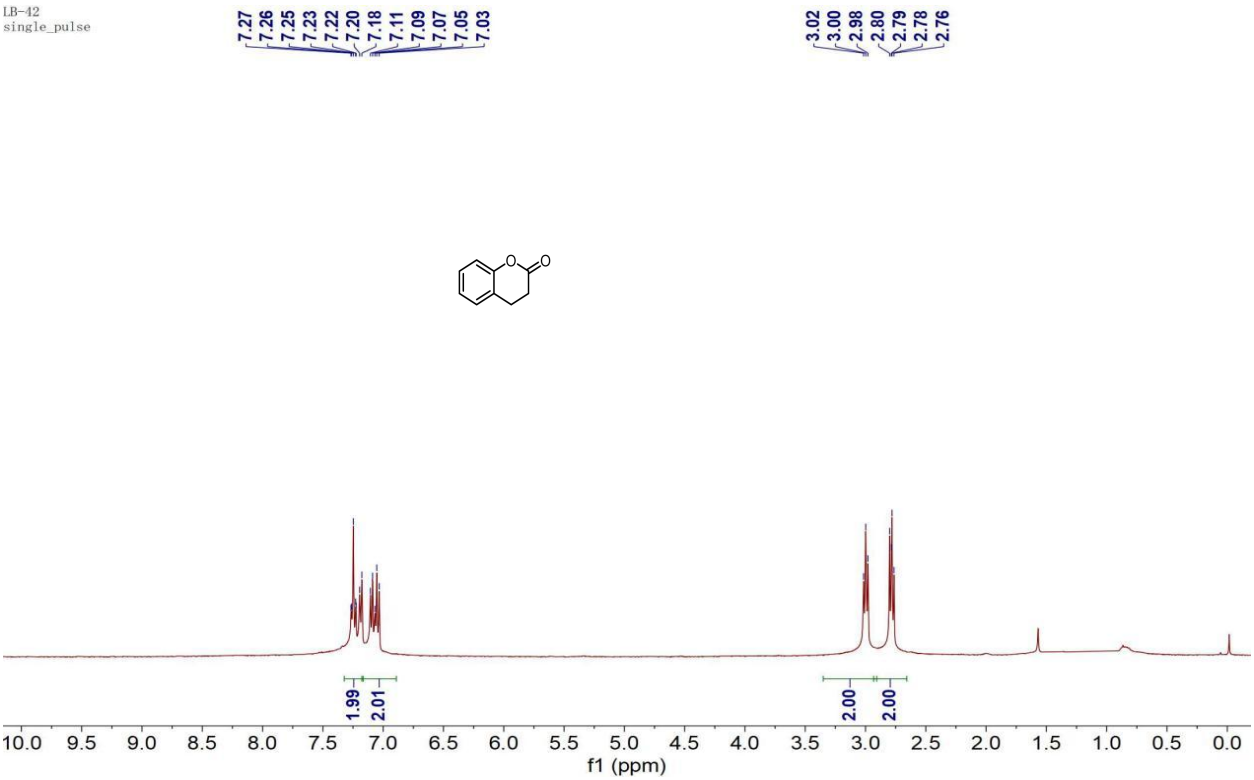

Figure S79. ^{1}H NMR spectrum of **2w** (400 MHz, Chloroform-d).

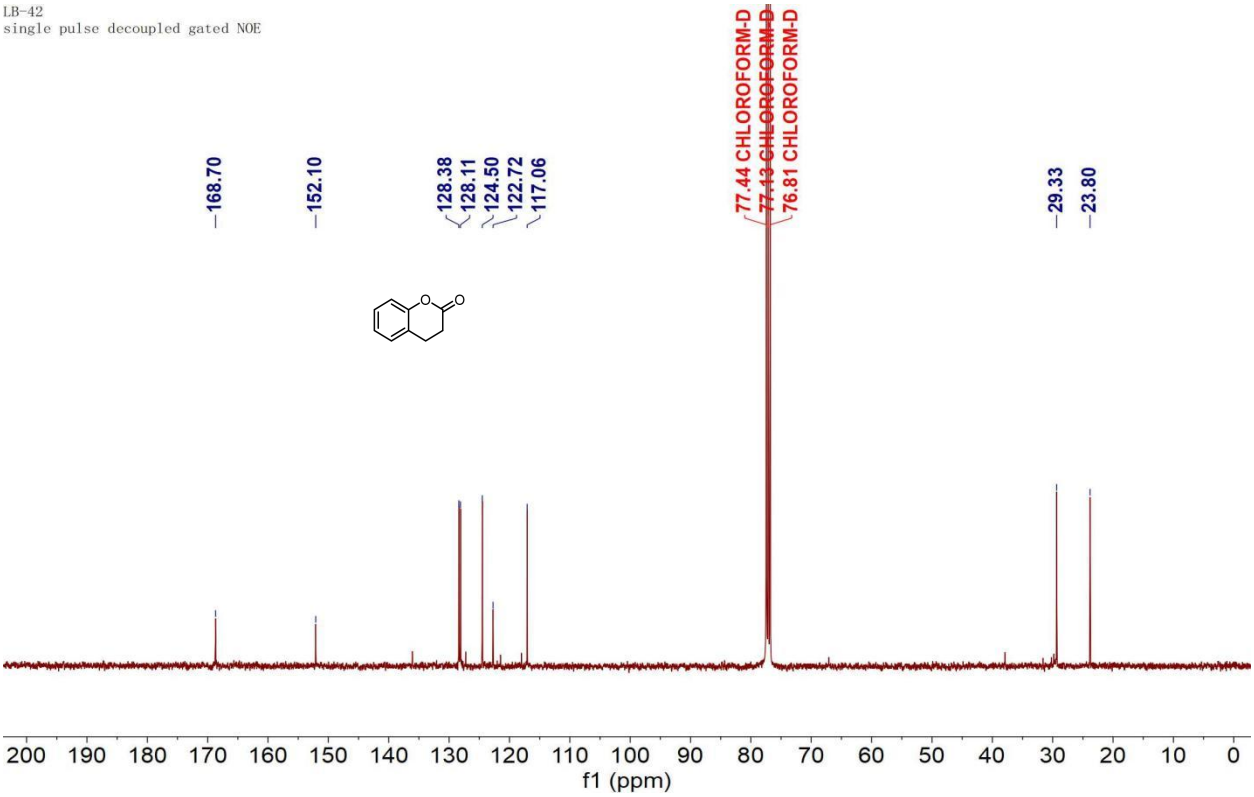

Figure S80. ^{13}C NMR spectrum of **2w** (101 MHz, Chloroform-d).

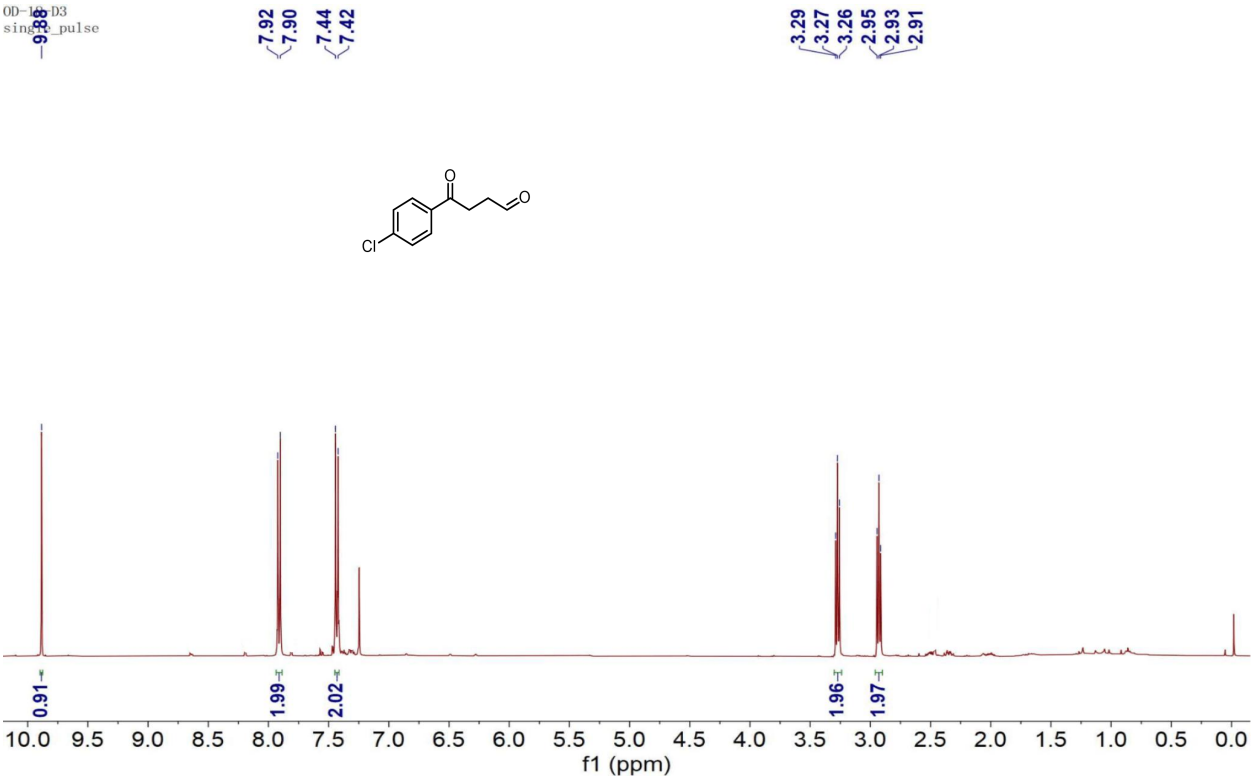

Figure S81. [1]H NMR spectrum of **4b** (400 MHz, Chloroform-d).

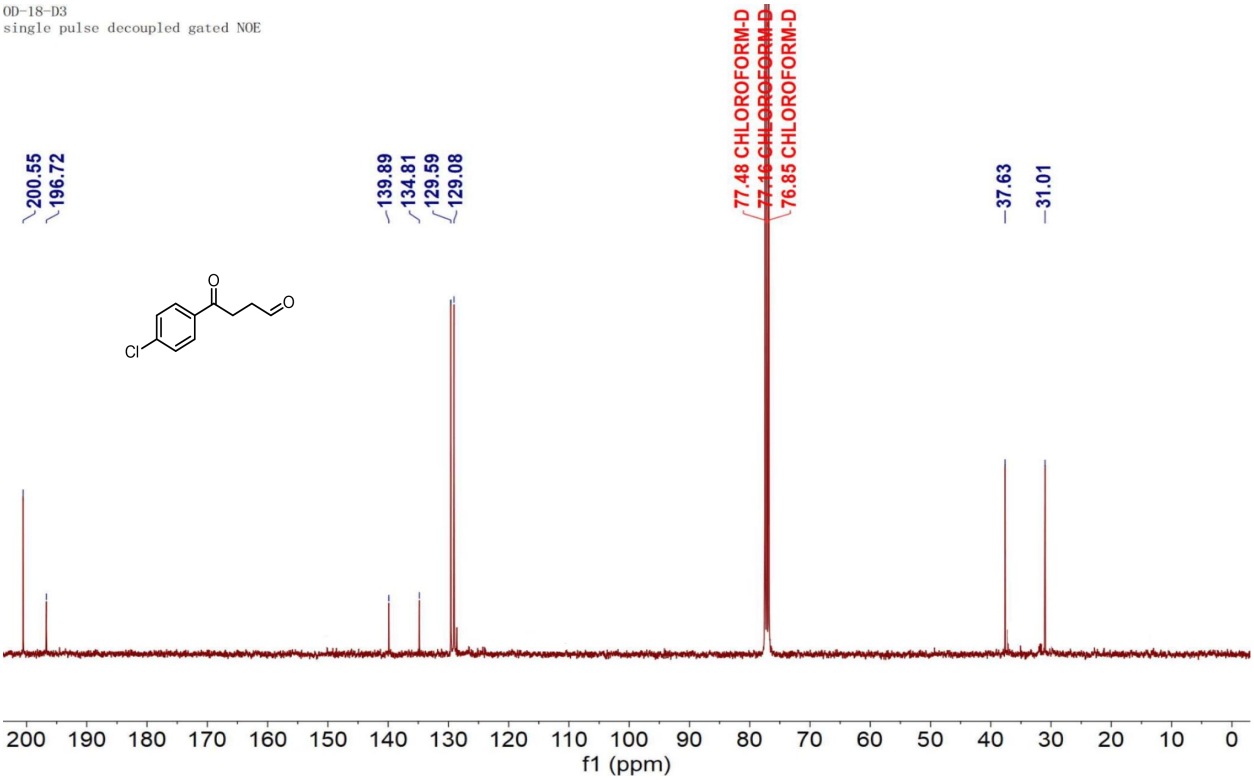

Figure S82. [13]C NMR spectrum of **4b** (101 MHz, Chloroform-d).

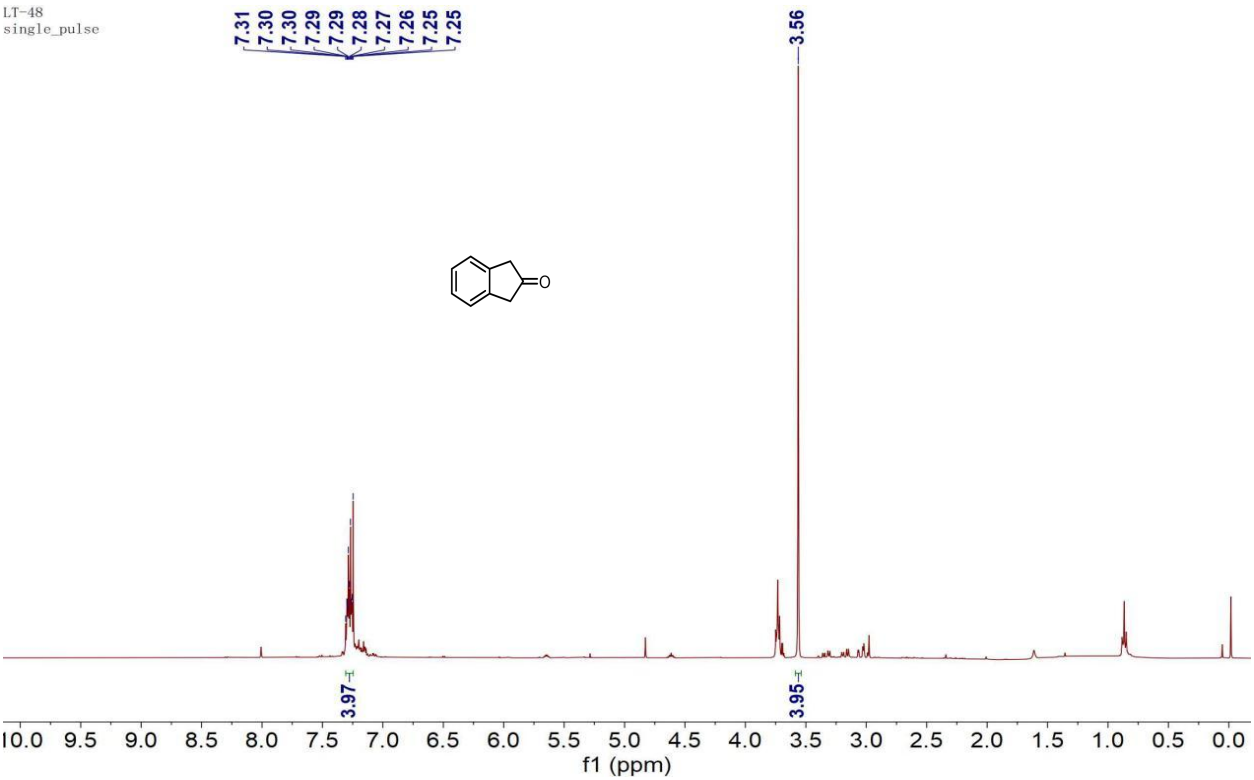

Figure S83. ^{1}H NMR spectrum of **2x** (400 MHz, Chloroform-d).

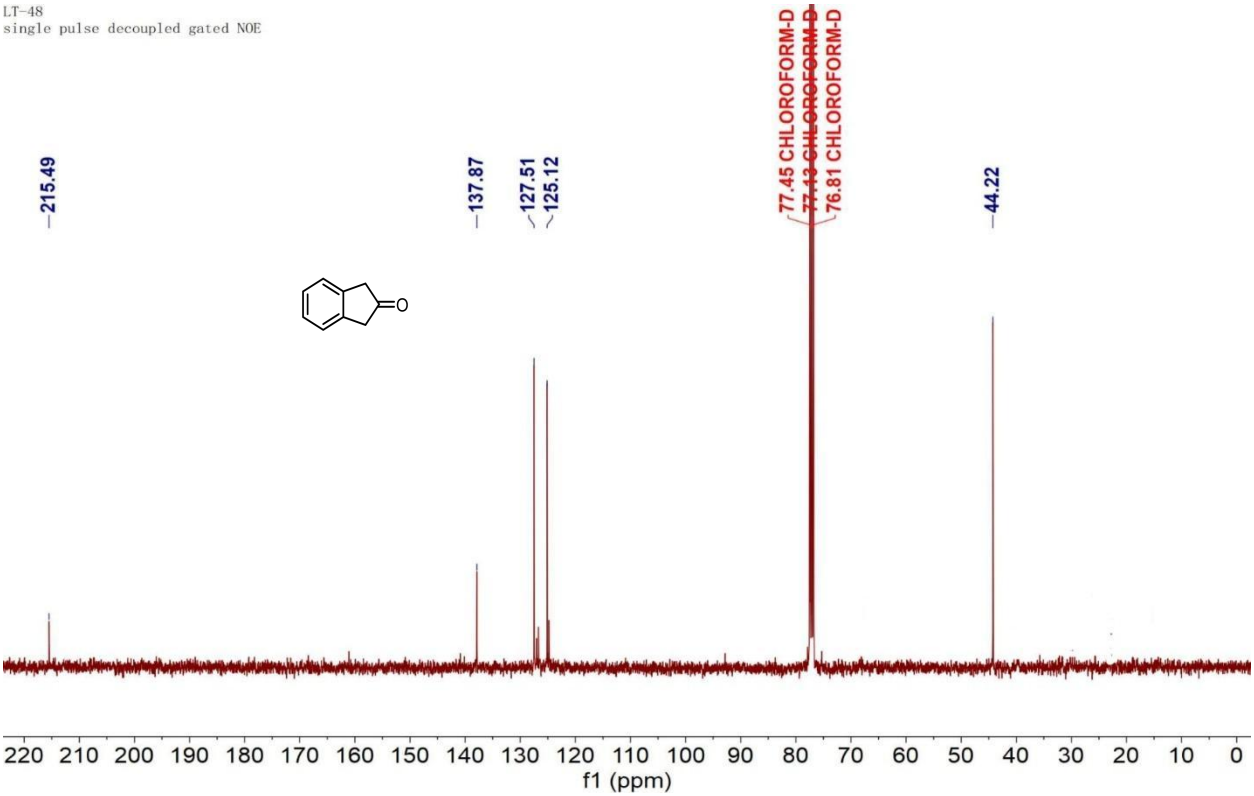

Figure S84. ^{13}C NMR spectrum of **2x** (101 MHz, Chloroform-d).

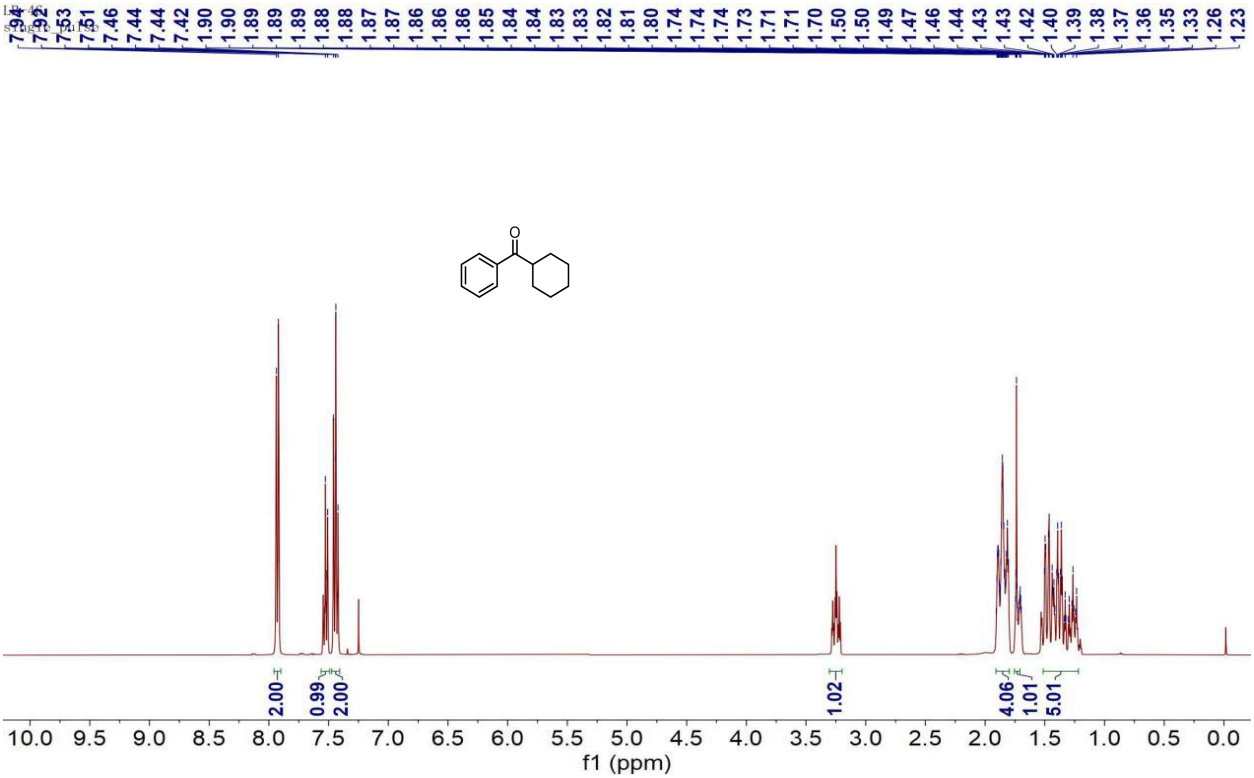

Figure S85. ^{1}H NMR spectrum of **2n** (400 MHz, Chloroform-d).

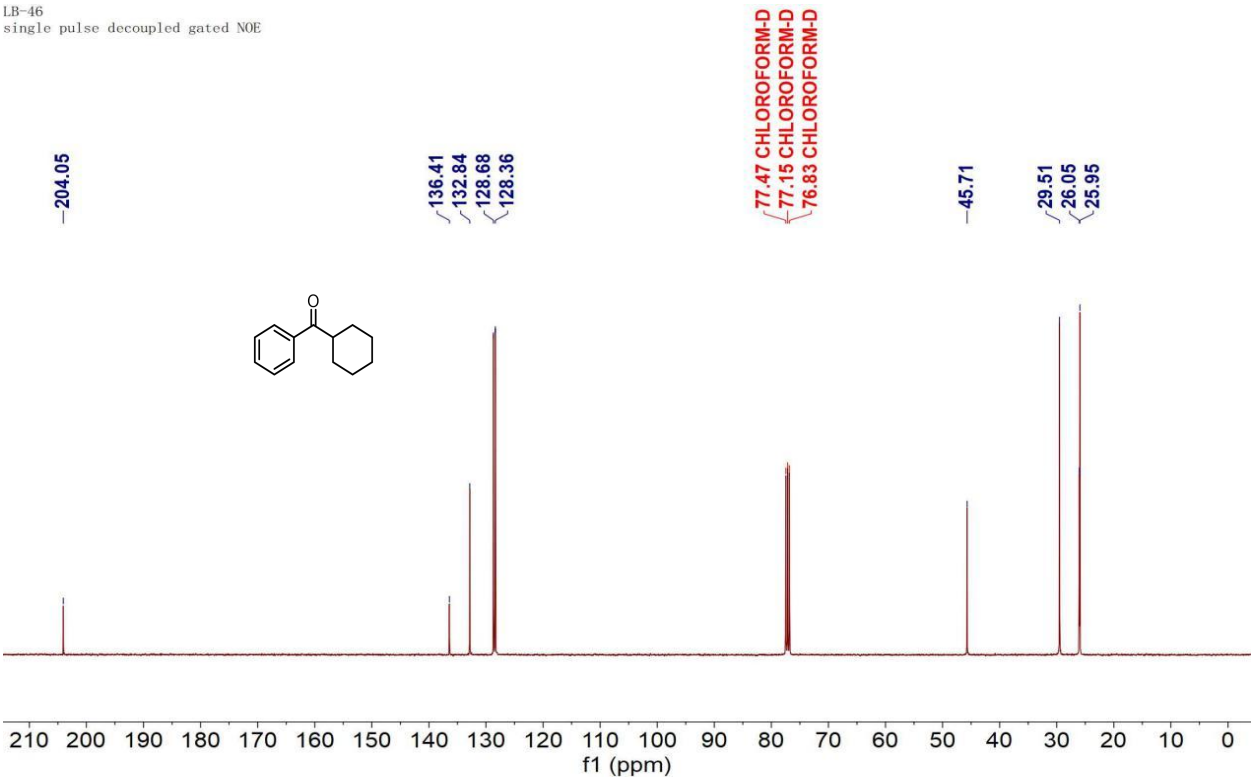

Figure S86. ^{13}C NMR spectrum of **2n** (101 MHz, Chloroform-d).

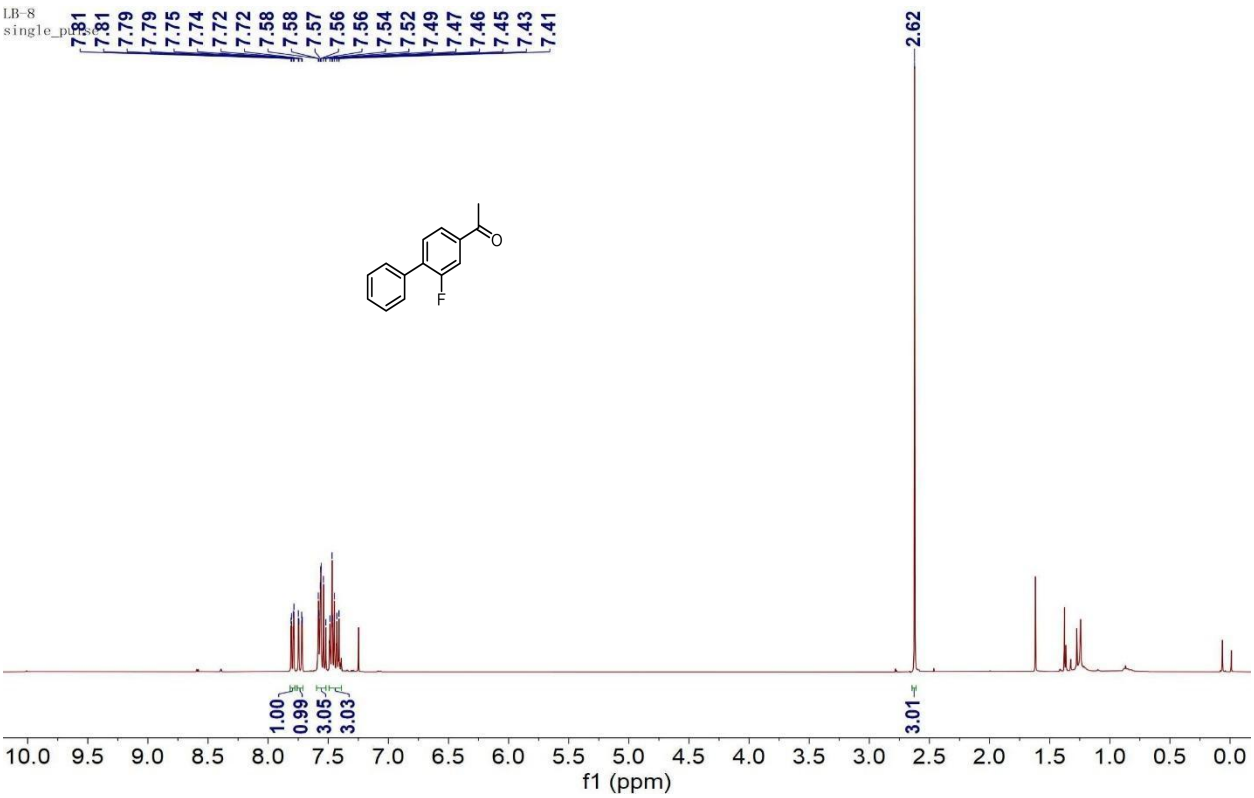

Figure S87. ^{1}H NMR spectrum of **2y** (400 MHz, Chloroform-d).

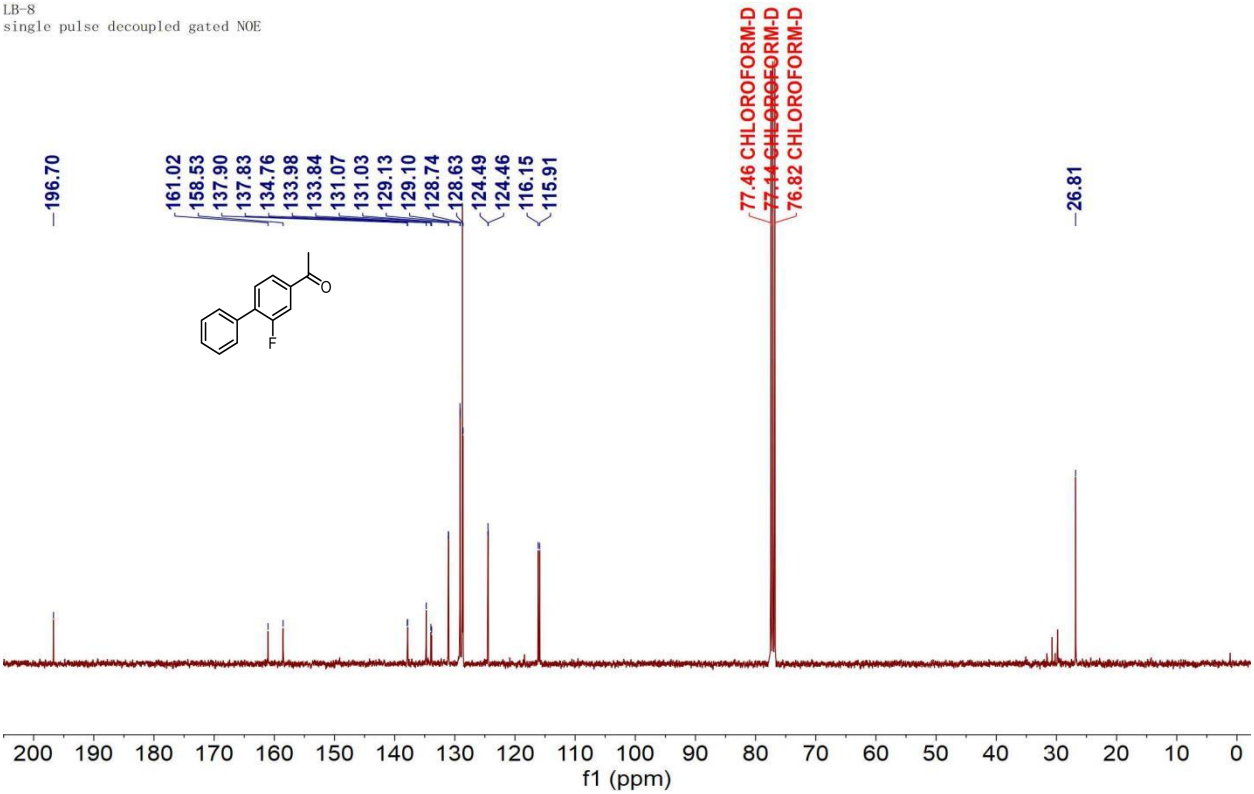

Figure S88. ^{13}C NMR spectrum of **2y** (101 MHz, Chloroform-d).

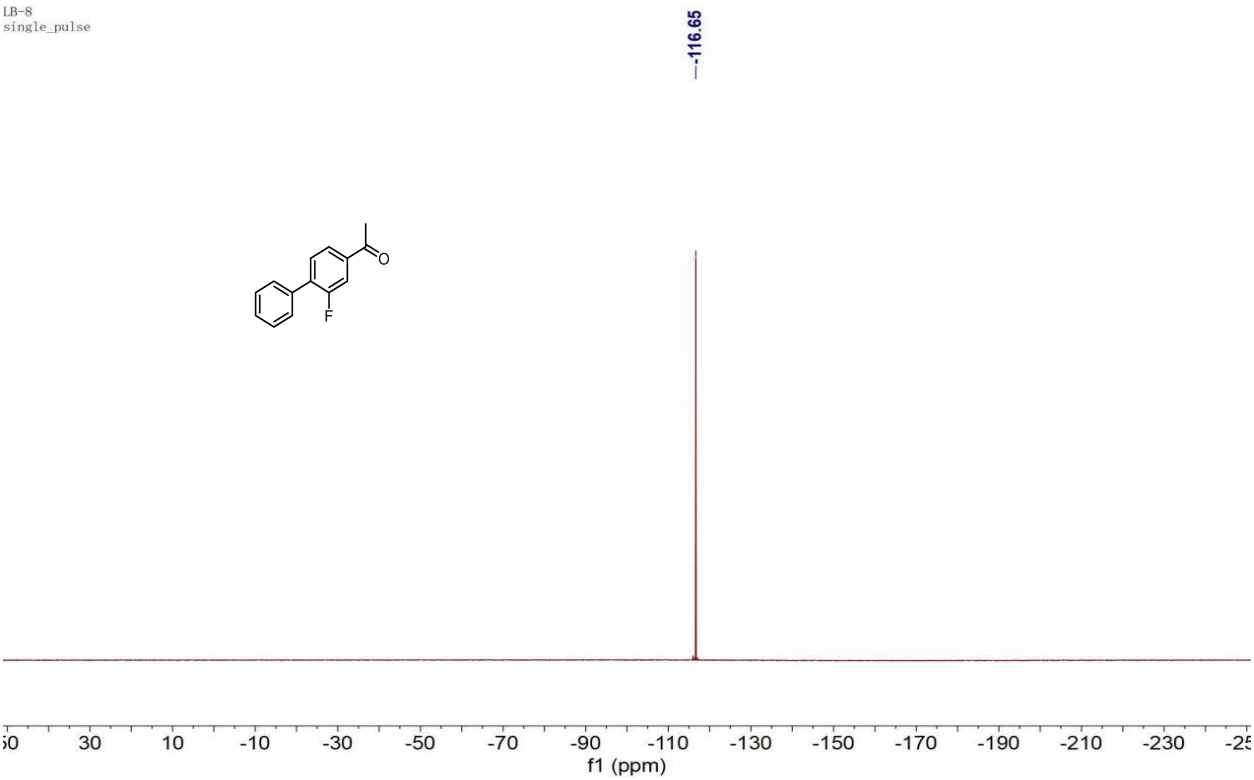

Figure S89. ^{19}F NMR spectrum of **2y** (376 MHz, Chloroform-d).

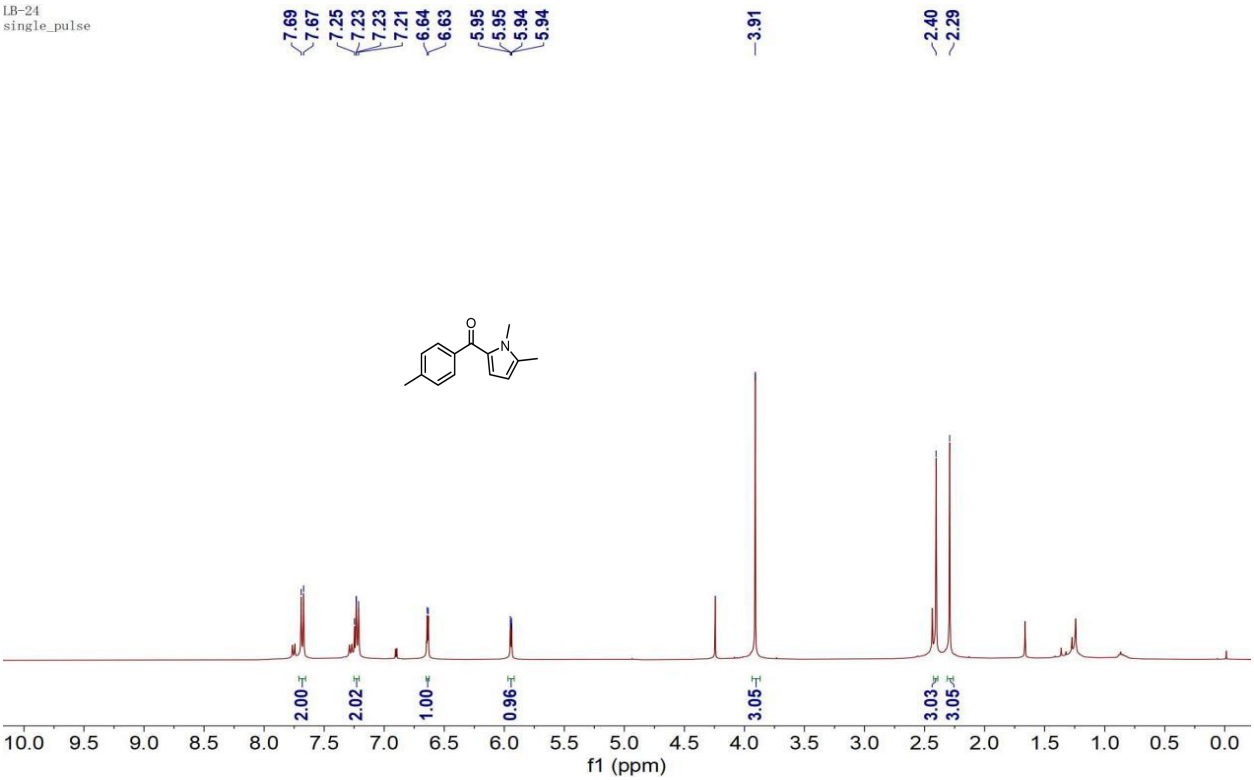

Figure S90. ^{1}H NMR spectrum of **2aj'** (400 MHz, Chloroform-d).

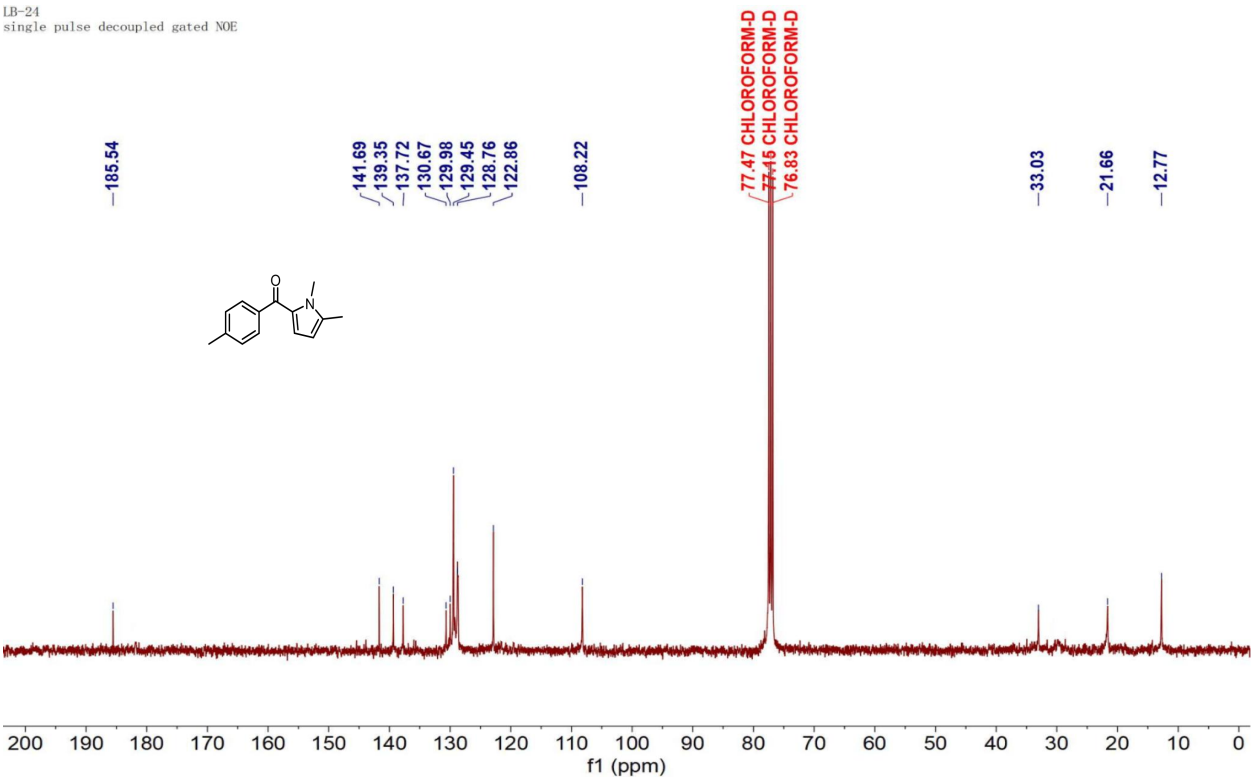

Figure S91. ^{13}C NMR spectrum of **2aj'** (101 MHz, Chloroform-d).

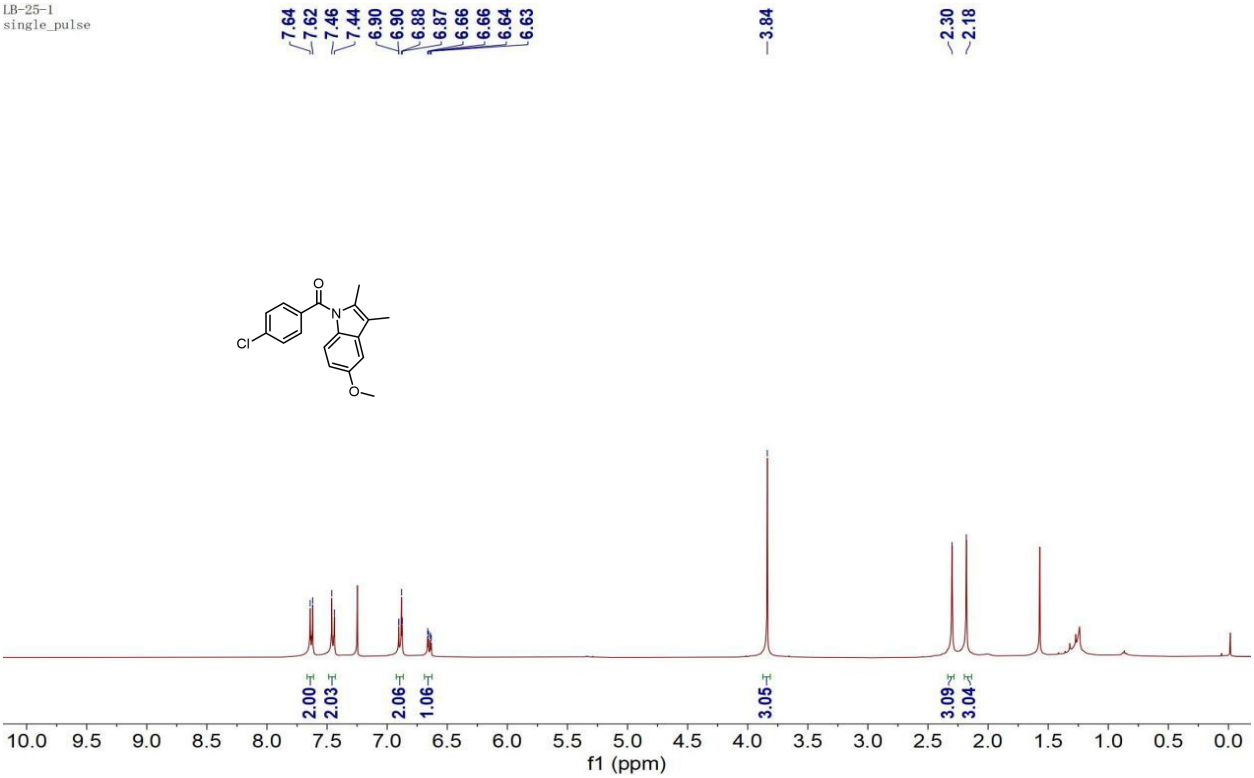

Figure S92. ^{1}H NMR spectrum of **2ai'** (400 MHz, Chloroform-d).

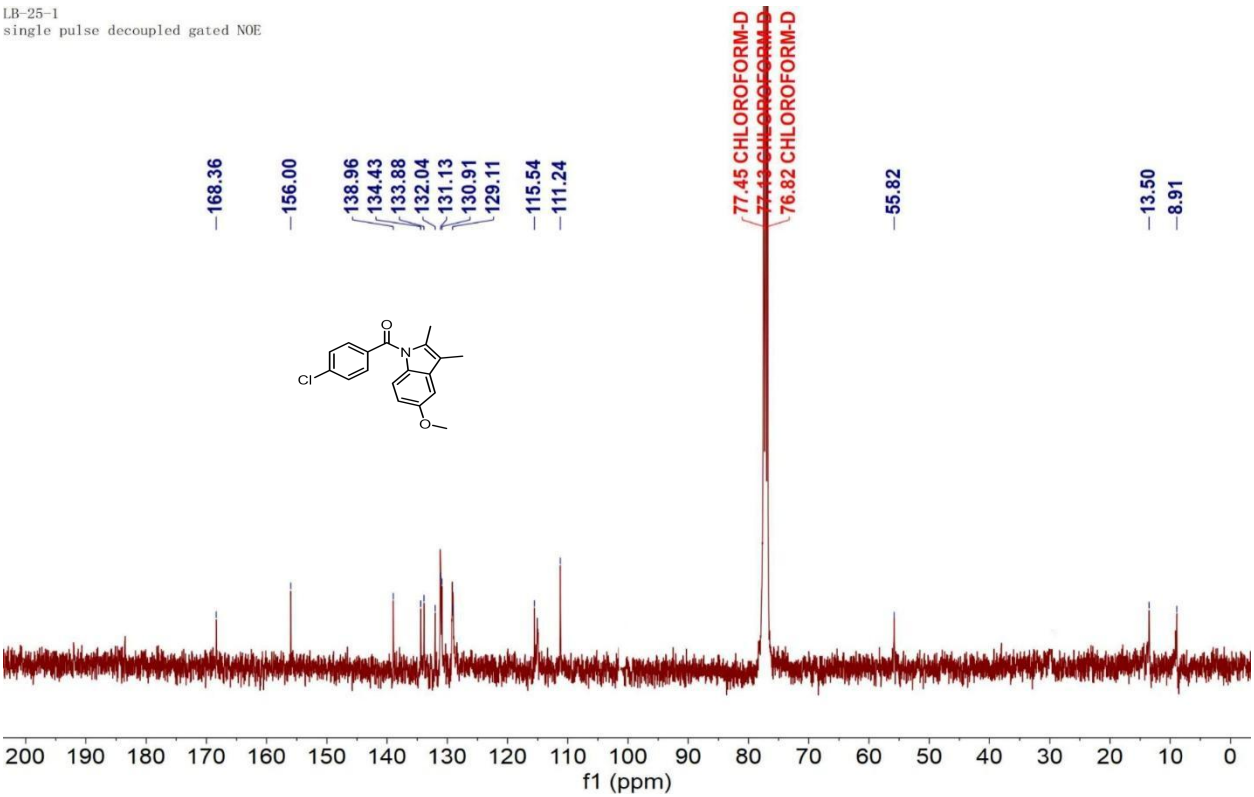

Figure S93. ^{13}C NMR spectrum of **2ai'** (101 MHz, Chloroform-d).

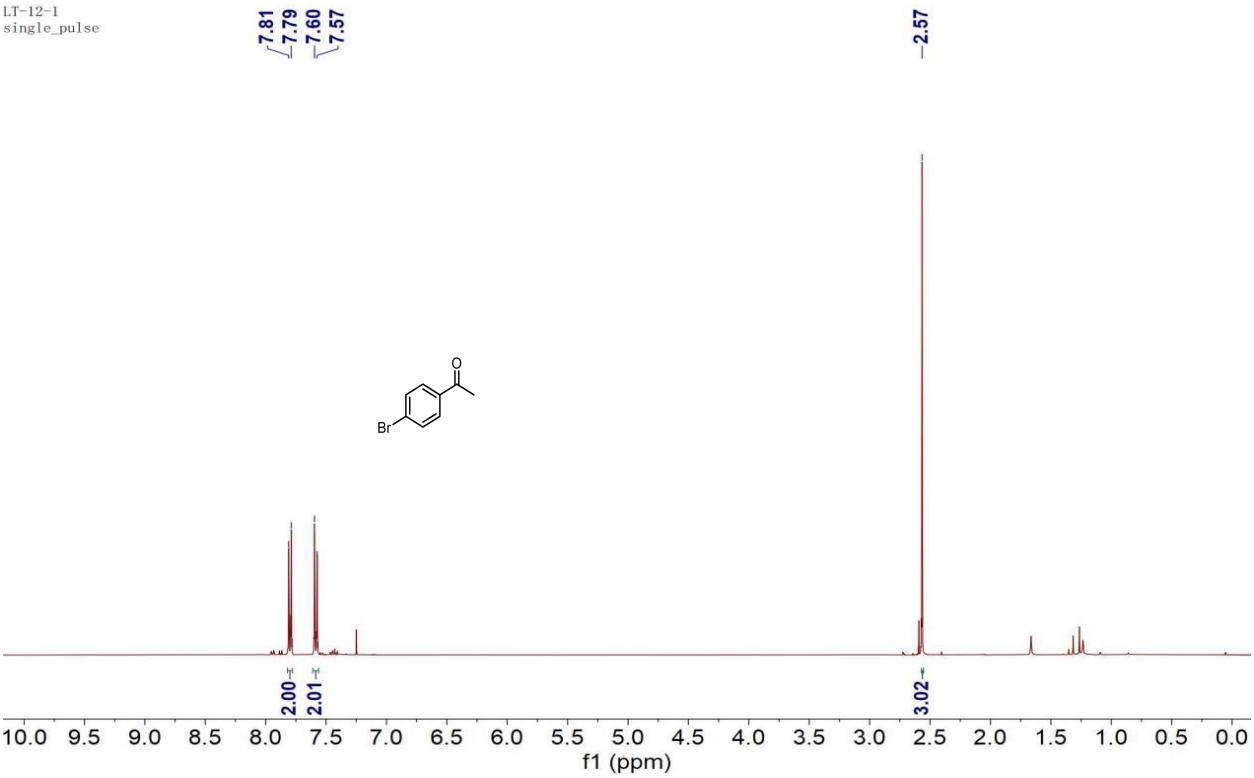

Figure S94. ^{1}H NMR spectrum of **6e** (400 MHz, Chloroform-d).

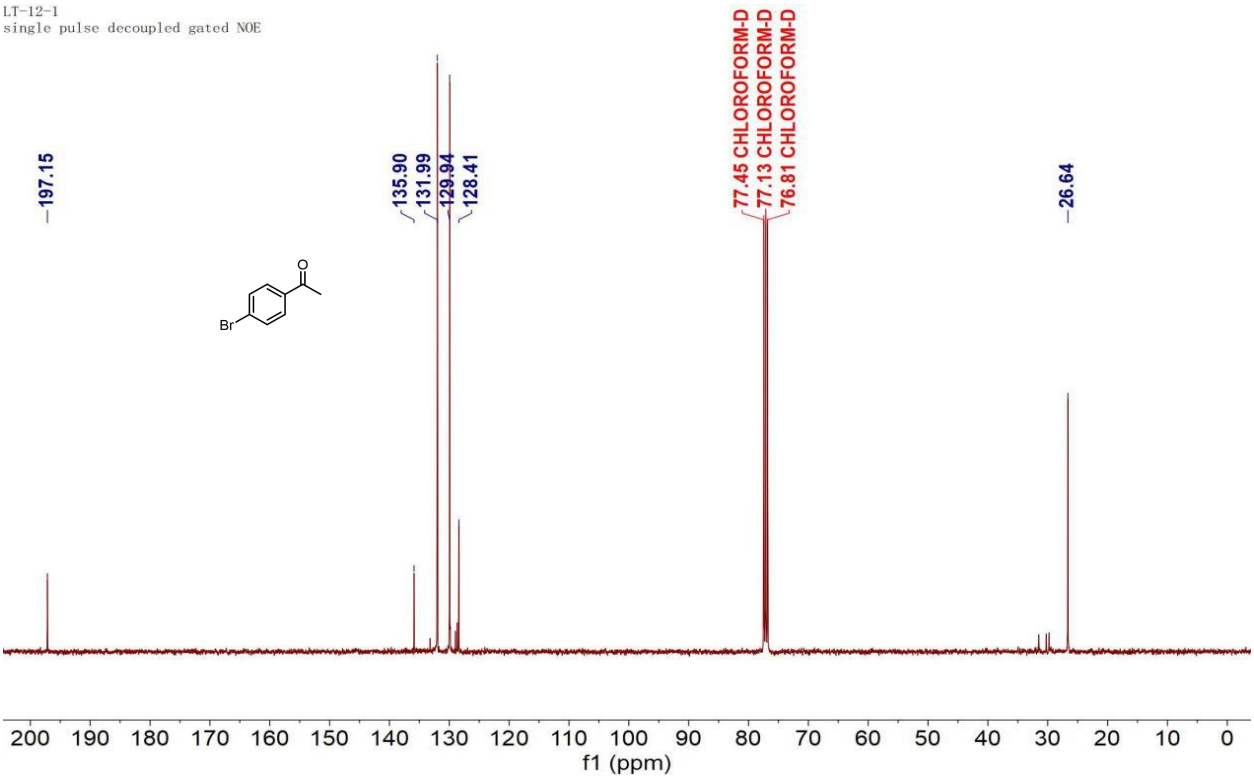

Figure S95. ^{13}C NMR spectrum of **6e** (101 MHz, Chloroform-d).

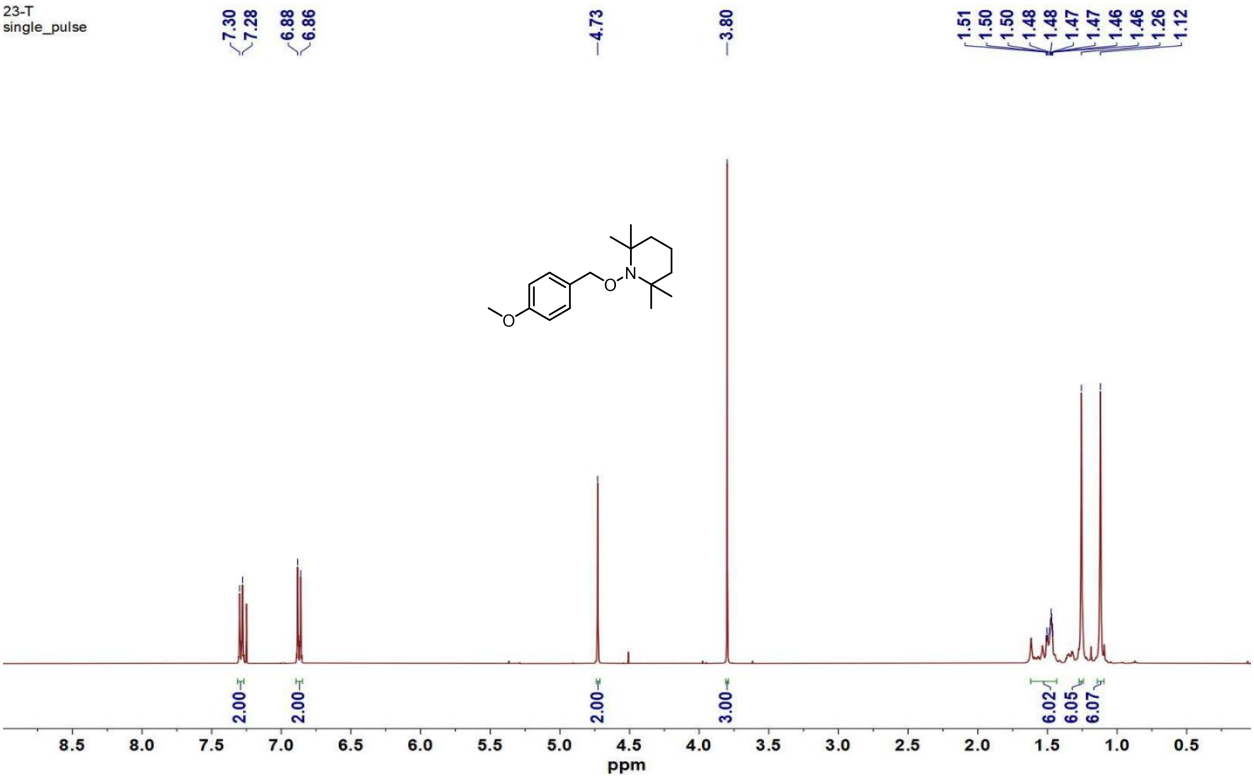

Figure S96. ^{1}H NMR spectrum of **2b-TEMPO** (400 MHz, Chloroform-d).

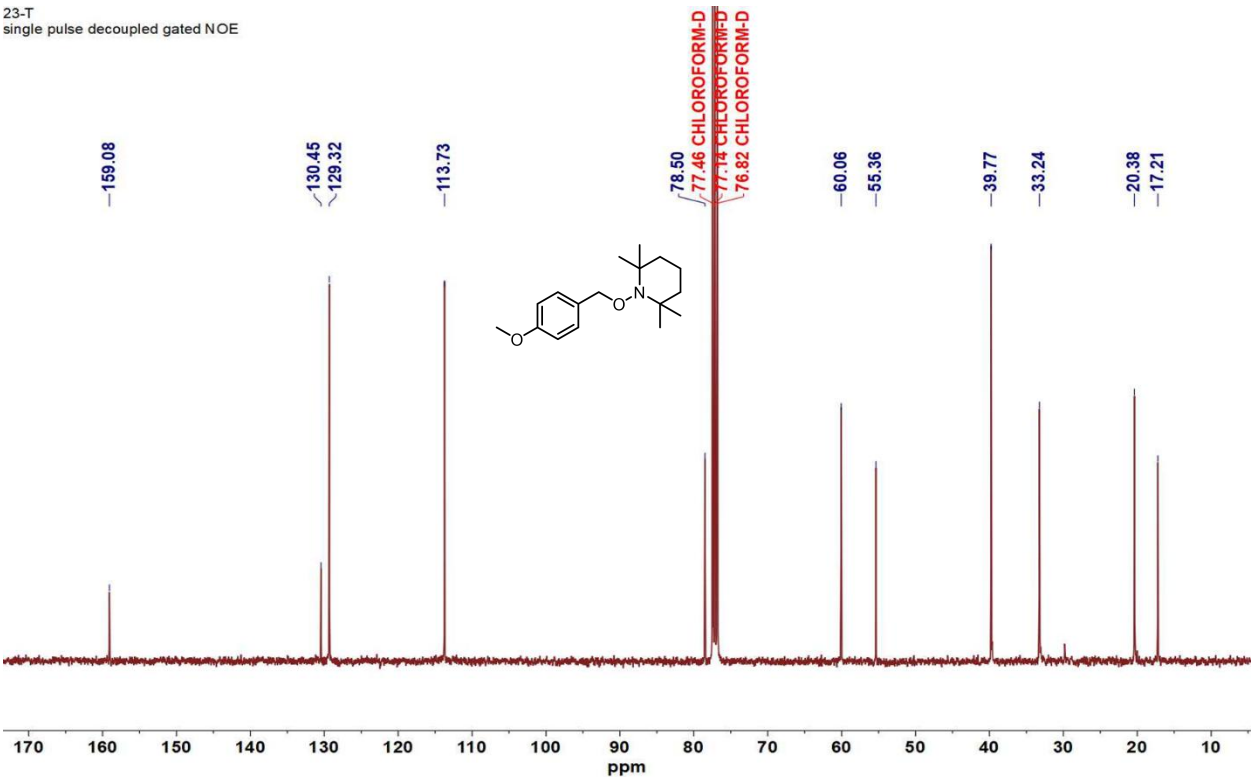

Figure S97. ^{13}C NMR spectrum of **2b-TEMPO** (101 MHz, Chloroform-d).

11. References

1. Dmitry V. Peryshkov and Richard R. Schrock*, Synthesis of Tungsten Oxo Alkylidene Complexes, *Organometallics*. **2012**, *31*, 7278-7286.

2. Xue, T.; Zhang, Z.; Zeng, R., Photoinduced Ligand-to-Metal Charge Transfer (LMCT) of Fe Alkoxide Enabled C–C Bond Cleavage and Amination of Unstrained Cyclic Alcohols. *Org. Lett.*

2022, *24*, 977-982.

3. Xu, Y.; Wang, J.; Zhang, Q.; Hu, X.; Lv, C.; Yang, H.; Sun, B.; Jin, C., Photo- and Cerium-Mediated C─C Bond Cleavage for the Deconstructive Diversification of Cyclic Acids. *Angew. Chem. Int. Ed.* **2025,** *64* (19).

4. a) P. J. Stephens, F. J. Devlin, C. F. Chabalowski and M. J. Frisch, J. *Phys. Chem.* **1994**, *98*, 11623–11627; b) S. H. Vosko, L. Wilk and M. Nusair, Can. J. *Phys.* **1980**, *58*, 1200 1211; c) Lee, Yang and Parr, Phys. Rev. B, 1988, 37, 785–789; d) A. D. Becke, J. *Chem. Phys.* **1993**, *98*, 5648-5652.

5. Bodiuzzaman, M.; Murugesan, K.; Yuan, P.; Maity, B.; Sagadevan, A.; Malenahalli H, N.; Wang, S.; Maity, P.; Alotaibi, M. F.; Jiang, D.-e.; Abulikemu, M.; Mohammed, O. F.; Cavallo, L.; Rueping, M.; Bakr, O. M., Modulating Decarboxylative Oxidation Photocatalysis by Ligand Engineering of Atomically Precise Copper Nanoclusters. *J. Am. Chem. Soc.* **2024,** *146*, 26994-27005.

6. Liu, Y.; Yin, Y.; Zhang, Z.; Li, C. J.; Zhang, H.; Zhang, D.; Jiang, C.; Nomie, K.; Zhang, L.; Wang, M. L.; Zhao, G. Eur. J. Med. *Chem.* **2017**, *138*, 543-551.

7. Tng, J.; Lim, J.; Wu, K.-C.; Lucke, A. J.; Xu, W.; Reid, R. C. J. Med. *Chem.* **2020**, *63*, 5956-5971.

9.Kweon, J.; Park, B.; Kim, D.; Chang, S. Decarboxylative stereoretentive C–N coupling by harnessing aminating reagent. *Nat. Commun.* **2024,** *15*, 3788.

8. Chai, Z.; Zeng, T.-T.; Li, Q.; Lu, L.-Q.; Xiao, W.-J.; Xu, D. *J. Am. Chem. Soc.* **2016**, *138*, 10128-10131.

9. Schoenebeck, F.; Murphy, J. A.; Zhou, S.-Z.; Uenoyama, Y.; Miclo, Y.; Tuttle, T., *J. Am. Chem. Soc.* **2007**, *129*, 13368-13369.